論文 / 著書情報
Article / Book Information

題目(和文)	リミットサイクル振動系の次元縮約理論： 拡張と応用
Title(English)	Dimension reduction theories of limit-cycling systems: some extensions and applications
著者(和文)	白坂将
Author(English)	Sho Shirasaka
出典(和文)	学位:博士(工学), 学位授与機関:東京工業大学, 報告番号:甲第10555号, 授与年月日:2017年3月26日, 学位の種別:課程博士, 審査員:中尾 裕也,木村 康治,井村 順一,早川 朋久,宮﨑 祐介
Citation(English)	Degree:Doctor (Engineering), Conferring organization: Tokyo Institute of Technology, Report number:甲第10555号, Conferred date:2017/3/26, Degree Type:Course doctor, Examiner:,,,,
学位種別(和文)	博士論文
Type(English)	Doctoral Thesis

Dimension reduction theories of limit-cycling systems: some extensions and applications

Sho Shirasaka

Department of Mechanical and Environmental Informatics
Graduate School of Information Science and Engineering
Tokyo Institute of Technology

Declaration

I hereby declare that this thesis contains no material which has been accepted for the award of any other degree or diploma at any university or equivalent institution and that, to the best of my knowledge and belief, this thesis contains no material previously published or written by another person, except where due reference is made in the text of the thesis.

This thesis includes one original paper (Sho Shirasaka, Wataru, Kurebayashi and Hiroya Nakao, "Phase reduction theory for hybrid nonlinear oscillators", Physical Review E, **95**, 012212, 2017) and one (Sho Shirasaka, Wataru Kurebayashi and Hiroya Nakao, "Phase-amplitude reduction of transient dynamics far from attractors for limit-cycling systems") to be published in Chaos. The ideas, development and writing up of all the papers in the thesis were the principal responsibility of myself, the student, working within the Department of Mechanical and Environmental Informatics under the supervision of Prof. Hiroya Nakao.

Sho Shirasaka

Acknowledgements

Firstly, I thank my supervisor Prof. Hiroya Nakao, who advised and guided my Ph.D study. I really enjoyed the inspiring and interdisciplinary atmosphere in the laboratory cultivated by his dedication. I owe him to open my mind on many interesting aspects of dynamical systems theory and its related areas, which deserve limitless enthusiastic studies.

I also thank to Prof. Wataru Kurebayashi, who always gave exceptionally deep insight into the subjects which we worked with collaboratively.

Many thanks to the rest of the laboratory members for stimulating and enriching group meetings.

I would like to give my gratitude to the faculty; Prof. Kenji Amaya, Prof. Junichi Imura, Prof. Koji Kimura, Prof. Tomohisa Hayakawa, Prof. Yusuke Miyazaki, Prof. Kazuhiro Nakadai and Prof. Yuki Onishi, who supported my graduate education.

I am grateful to brilliant researchers; Prof. Jaap Eldering, Prof. Naoya Fujiwara, Prof. Shigefumi Hata, Prof. Yuki Izumida, Prof. Hiroshi Kokubu, Prof. Hiroshi Kori, Prof. Kiyoshi Kotani, Prof. Oleg Makarenkov, Dr. Yutaro Ogawa, Prof. Hiromichi Suetani, Prof. Hisa-aki Tanaka, Mr. Yu Terada, Prof. Ikuhiro Yamaguchi and Prof. Yoshiyuki Yamaguchi, who gave me useful suggestions and comments.

I would like to thank the Japan Society for the Promotion of Science (JSPS) for the financial support.

Finally, I wish to acknowledge my family for their continuous support.

Abstract

Dimension reduction theories have played important roles in analyzing complex nonlinear dynamics in high-dimensional systems. In this thesis, dimension reduction theories of limit-cycling systems are extended to the cases where the conventional framework cannot be applied. The extension is two-fold. First, we develop a phase reduction theory for weakly perturbed limit cycles in hybrid dynamical systems and analyze their synchronization properties. Second, a phase-amplitude reduction framework using isochrons and isostables for transient dynamics far from limit-cycle attractors are proposed. Using this framework, we optimize injection timing of weak external signals to the oscillator so that deviations from the limit-cycle attractor are efficiently suppressed.

Table of contents

Chapter 1

Introduction

Many real world systems are considered to be dynamically interacting with the environment and/or with others. When we hope to understand such kind of systems, we might have to consider how a system responds to influences and/or how it influences others. Conversely, there arise problems which start from given response and influence properties to dynamic patterns. Tackling these problems is practically important because it might develop knowledge on how to accomplish useful complex functions in engineered systems as simply as possible, by leaving some difficulties to autonomy of the systems. However, in general high-dimensional nonlinear settings, their theoretical treatments seem to be hopeless, especially when we work with dynamic patterns with spatio-temporal heterogeneities. Nevertheless, the world of a class of nonlinear systems, limit-cycling oscillators and their large populations, has long been an active area of research for these forward/inverse problems in complex setup of such kind [1–10].

1.1 Background and theoretical developments of the theory of oscillators

The study of the coupled oscillator systems can be traced back to the C. Huygens's discovery of the synchronization of coupled pendulum clocks [11]. The analysis of the limit-cycling oscillator systems are limited to a small population of electric circuits [12] including models of the heartbeat [13] or musical instruments [14] until brain waves are conjectured [15, 16] to be a self-organizing phenomenon by the synchronization of the oscillatory behavior of neurons. A. T. Winfree was the first to consider a biological oscillator as a reduced phase oscillator evolving on a circle [17] and he demonstrated that a self-organizing coherent behavior of a large population of oscillators such as the

brain waves can be produced using the phase model. Y. Kuramoto made a significant theoretical development [18] by introducing an analytically tractable model of a large population of the phase oscillators. He predicted the transition point where the coherent behavior arises quantitatively and derived a critical scaling property near the transition. Thus the framework to analyze complex self-organizing behavior of limit-cycling oscillators, called *phase reduction theory*, is established. Collective and coherent self-organizing order has been experimentally observed in various physical. chemical, biological and engineered system [1–10], hence, the theoretical development of the phase reduction theory is significantly important.

The further developments of the reduction theories of limit-cycling oscillators and its applications has been done in considerably wide context. The above mentioned Kuramoto's analysis was done in a situation where the oscillators were all-to-all purely sinusoidally coupled. The general interaction functions which contain higher harmonics become to be considered [19–22]. In addition, the dynamics of oscillators on complex network substrates [23–25] and their continuous counterparts called graphons [26–28] are studied. Further dimension reduction techniques for a large population of coupled phase oscillators using Watanabe-Strogatz ansatz [29] or Ott-Antonsen ansatz [30] are developed. Methods for optimizing, controlling and designing synchronization of limit-cycle oscillators have been developed on the basis of the phase reduction theory [25, 31–33]. Various methods to obtain the phase models from experimental data are also developed [34–37]. A diverse set of phenomena such as rotating spiral waves, target patterns, standing waves, defect turbulence, oscillation quenching, clustering, chimera states and noise induced synchronization [2–5, 38–45] is studied using the standard phase reduction theory and its extensions together with the center manifold reduction theory [46]. The phase reduction theory has been extended to a wide class of systems such as stochastic [47–49], delay-induced [50, 51], collective [52, 53], spatially extended [54, 55], strongly modulated [56] oscillations. As in the last part, in this thesis, we extend the phase reduction theory to non-conventional cases.

1.2 Extension of the reduction theories

In phase reduction theory [1, 2, 8, 57], we often limit our interest to limit-cycle oscillators subjected to weak perturbation, described by

$$\dot{\boldsymbol{X}}(t) = \boldsymbol{F}(\boldsymbol{X}(t)) + \epsilon \boldsymbol{p}(\boldsymbol{X}(t), t), \tag{1.1}$$

where $\boldsymbol{X}(t) \in \mathbb{R}^N$ is the oscillator state, $\boldsymbol{F}(\boldsymbol{X}) : \mathbb{R}^N \to \mathbb{R}^N$ is a vector field representing the dynamics of the oscillator, $\boldsymbol{p}(\boldsymbol{X}, t) : \mathbb{R}^N \times \mathbb{R} \to \mathbb{R}^N$ denotes external perturbation applied to the oscillator, and $\epsilon \in \mathbb{R}$ is a small parameter representing the intensity of the perturbation. A system without perturbation ($\epsilon = 0$) is assumed to possess a stable limit-cycle solution $\chi : \boldsymbol{X}_0(t) = \boldsymbol{X}_0(t + T)$ of period $T \in \mathbb{R}$, and a phase θ of the oscillator state is introduced, which increases with a constant frequency.

When the perturbation is sufficiently small, phase reduction theory enables us to systematically approximate the original multidimensional system using a simple one-dimensional reduced phase equation of the form

$$\dot{\theta}(t) = 1 + \epsilon \boldsymbol{Z}(\theta) \cdot \boldsymbol{p}(\theta, t), \tag{1.2}$$

where $\theta(t) = \Theta(\boldsymbol{X}(t))$ is the oscillator phase and $\Theta(\boldsymbol{X}) : \mathbb{R}^N \to [0, T)$ gives the phase of the oscillator state $\boldsymbol{X}$. The function $\boldsymbol{Z}(\theta)$ quantifies the linear response of the oscillator phase to perturbations given at phase θ on χ. The phase reduction theory has been extended to a wide class of dynamical systems as mentioned above [47–56]. However, application of the phase reduction theory to oscillatory *hybrid dynamical systems*, which is continuous-time dynamical process involving some discontinuities, has so far been limited to specific cases [58–60], though their significance in many areas of science and engineering [61, 62].

In the phase reduction theory, the degrees of freedom corresponding to deviations from the limit-cycle orbit, which we call *amplitudes* in this thesis, are completely eliminated. Roles of amplitudes in systems of oscillators have also been extensively studied because they are rich sources of intriguing phenomena/properties of dynamics of oscillators at individual level [4, 47, 49, 63–65] and ensemble level [2–4, 38–40, 65, 66]. It is highly desirable to establish a method which provides us a reduced description of transient dynamics toward a limit-cycle attractor involving amplitudes. This would facilitate elaborate studies of roles of amplitudes in more complicated and realistic settings than many of those in the above studies, where only very simple characterization of amplitudes is considered using a canonical form of the oscillators.

1.3 Our contributions

Chapter 2

We formulated a phase reduction theory for a general class of hybrid limit-cycle oscillators and derived the adjoint equation for the phase response function. On the basis of the proposed theory, injection locking phenomena of hybrid limit-cycle oscillators by periodic forcing is analyzed, Some peculiar synchronization properties characteristic to hybrid dynamical systems are well predicted by the proposed theory, such as ultrafast and robust entrainment to the periodic forcing and logarithmic scaling at the synchronization transition. The synchronization dynamics of a simple physical model of biped locomotion is analyzed as an illustration.

Chapter 3

We formulated a phase-amplitude reduction theory for stable limit-cycle oscillators, which can be applied to high-dimensional systems and transient regimes far from attractors. A convenient systematic biorthogonalization method to obtain the response property of the reduced transient dynamics is proposed. We illustrated the utility of the proposed reduction framework by estimating optimal injection timing of external forcing signals which efficiently suppress deviations from a limit-cycle. The result is verified in numerical simulations using a chemical kinetic model of an oscillatory genetic circuit.

Chapter 2

Phase reduction theory for hybrid nonlinear oscillators

Abstract

Hybrid dynamical systems characterized by discrete switching of smooth dynamics have been used to model various rhythmic phenomena. However, the phase reduction theory, a fundamental framework for analyzing the synchronization of limit-cycle oscillations in rhythmic systems, has mostly been restricted to smooth dynamical systems. Here, we develop a general phase reduction theory for weakly perturbed limit cycles in hybrid dynamical systems that facilitates analysis, control, and optimization of nonlinear oscillators whose smooth models are unavailable or intractable. On the basis of the generalized theory, we analyze injection locking of hybrid limit-cycle oscillators by periodic forcing and reveal their characteristic synchronization properties, such as ultrafast and robust entrainment to the periodic forcing and logarithmic scaling at the synchronization transition. We also illustrate the theory by analyzing the synchronization dynamics of a simple physical model of biped locomotion.

2.1 Introduction

Hybrid dynamical systems have been used to describe physical processes that exhibit sudden qualitative changes or abrupt jumps during otherwise continuous evolution. Some examples are the collision of particles, refraction and reflection of waves, spiking of neurons, switching of gene expression, limb-substrate impacts in legged robots and animals, human-structure interaction, switching of elements in electric circuits, and

breakdown of nodes or links in networked systems [67–75]. Because such discontinuous events are found in many areas of science and engineering [61, 62], it is important to develop theoretical frameworks to analyze hybrid dynamical systems.

Many hybrid dynamical systems exhibit stable rhythmic activities, for example, periodic spiking of neurons, rhythmic locomotion of robots, oscillations in power electric circuits, and business cycles in economic models [58, 76–79], which are typically modeled as nonlinear limit-cycle oscillations. Synchronization of such rhythmic activities may play important functional roles in biological and engineered systems, e.g., in locomotor rhythms, vibro-impact energy harvesters, and wireless sensor networks [80–84].

One of the fundamental mathematical frameworks for analyzing limit-cycle oscillations is the phase reduction theory [1, 2, 57], which gives approximate reduced description of the dynamics of a weakly perturbed limit-cycle oscillator using a simple one-dimensional phase equation. The phase reduction theory is well established for stable limit-cycle oscillations of smooth dynamical systems and has successfully been applied to the analysis of rhythmic spatiotemporal dynamics in chemical and biological systems [1, 2]. Methods for optimizing and controlling synchronization of limit-cycle oscillators have also been developed on the basis of the phase reduction theory [25, 31–33].

In phase reduction theory for smooth dynamical systems, a weakly perturbed limit-cycle oscillator described by $\dot{\boldsymbol{X}}(t) = \boldsymbol{F}(\boldsymbol{X}(t)) + \epsilon \boldsymbol{p}(\boldsymbol{X}(t), t)$ is considered, where $\boldsymbol{X}(t) \in \mathbb{R}^N$ is the oscillator state, $\boldsymbol{F}(\boldsymbol{X}) : \mathbb{R}^N \to \mathbb{R}^N$ is a smooth vector field representing the dynamics of the oscillator, $\boldsymbol{p}(\boldsymbol{X}, t) : \mathbb{R}^N \times \mathbb{R} \to \mathbb{R}^N$ denotes external perturbation applied to the oscillator, and $\epsilon \in \mathbb{R}$ is a small parameter representing the intensity of the perturbation. A system without perturbation ($\epsilon = 0$) is assumed to possess a stable limit-cycle solution $\chi : \boldsymbol{X}_0(t) = \boldsymbol{X}_0(t + T)$ of period $T \in \mathbb{R}$, and a phase θ of the oscillator state is introduced, which increases with a constant frequency and takes the same value on the *isochron* [1, 85, 86], i.e., a codimension-one manifold of the oscillator states that share the same asymptotic behavior.

When the perturbation is sufficiently small, phase reduction theory enables us to systematically approximate the original multidimensional system using a simple one-dimensional reduced phase equation of the form $\dot{\theta}(t) = 1 + \epsilon \boldsymbol{Z}(\theta) \cdot \boldsymbol{p}(\theta, t)$, where $\theta(t) = \Theta(\boldsymbol{X}(t))$ is the oscillator phase and $\Theta(\boldsymbol{X}) : \mathbb{R}^N \to [0, T)$ gives the phase of the oscillator state $\boldsymbol{X}$. The range $[0, T)$ of the phase is identified with a one-dimensional torus $\mathbb{T}^1$. The function $\boldsymbol{Z}(\theta) : \mathbb{T}^1 \to \mathbb{R}^n$, which is the gradient of the isochron and is called the *phase sensitivity function* in this chapter, quantifies the linear response of the oscillator phase to perturbations given at phase θ on χ. It is known that $\boldsymbol{Z}(\theta)$

can be obtained as a T-periodic solution to the adjoint linear problem of the system, $\dot{\boldsymbol{Z}}(t) = -\left(D\boldsymbol{F}(\boldsymbol{X}_0(t))\right)^{\dagger} \cdot \boldsymbol{Z}(t)$ with a normalization condition $\boldsymbol{Z}(0) \cdot \boldsymbol{F}(\boldsymbol{X}_0(0)) = 1$, where $D\boldsymbol{F}$ denotes the Jacobi matrix of $\boldsymbol{F}$ and $\dagger$ its transpose [87, 57, 8].

Recently, the phase reduction theory has been extended to non-conventional cases such as stochastic [47–49], delay-induced [50, 51], collective [52, 53], spatially extended [54, 55], and strongly modulated [56] oscillations. Similar reduction methods that rely on sets of initial conditions characterized by the same long-term behavior have also been developed for heteroclinic orbits [88], limit tori [89–91] and stable fixed points [92–94]. However, application of the phase reduction theory to oscillatory hybrid dynamical systems has so far been limited to low-dimensional systems, or to a specific class of systems whose phase sensitivity function is obtained from adiabatic approximation [58–60]. To the best of our knowledge, no systematic phase reduction theory for oscillators of high-dimensional ($N \geq 3$) systems with discontinuity in χ has been developed. This is mainly because the non-smoothness of the vector fields at the jumps prevents straightforward utilization of the adjoint equation.

In this chapter, we develop a systematic phase reduction theory for a general class of autonomous limit-cycle oscillators in hybrid dynamical systems. This chapter is organized as follows: in Sec. 2.2, limit-cycle oscillations in hybrid dynamical systems are introduced. In Sec. 2.3, the phase reduction theory for hybrid limit cycles is developed. In Sec. 2.4, the theory is illustrated by analyzing synchronization dynamics of two examples of hybrid limit-cycle oscillators, that is, an analytically tractable Stuart-Landau-type oscillator and a physical model of biped locomotion. Section 2.5 summarizes the results, and Appendices A-I provide mathematical details of the main results presented in Sec. 2.2-2.4.

2.2 Hybrid limit cycles

The state of a hybrid dynamical system that we consider in this study is represented by a pair $\boldsymbol{s} = (I, \boldsymbol{X})$ of the discrete state $I \in \{1, 2, \cdots, m\} = \mathcal{M}$ for some $m \in \mathbb{N}$ ($m = +\infty$ is allowed) and the continuous state $\boldsymbol{X} \in \mathbb{R}^N$. We denote the set of ordered pairs (i, j) as $\mathcal{G} \subset \mathcal{M} \times \mathcal{M}$, which is a collection of all possible transitions from discrete state i to j. As in Ref. [95], we describe a hybrid dynamical system by the following hybrid automaton:

$$\dot{\boldsymbol{X}}(t) = \boldsymbol{F}(I(t), \boldsymbol{X}(t)), \quad \text{if} \quad I(t) = i \text{ and } \boldsymbol{X}(t) \notin \boldsymbol{\Pi}_{ij} \text{ for any } j, \tag{2.1}$$

$$\begin{aligned} \boldsymbol{X}(t+0) &= \boldsymbol{\Phi}((i,j),\boldsymbol{X}(t)),\ I(t+0)=j, \\ &\text{if}\ \ I(t)=i \text{ and } \boldsymbol{X}(t)\in\boldsymbol{\Pi}_{ij} \text{ for some } j, \end{aligned} \tag{2.2}$$

$$\boldsymbol{\Pi}_{ij} = \begin{cases} \{\boldsymbol{X} \mid L((i,j),\boldsymbol{X})=0\}, & \text{if}\ \ (i,j)\in\mathcal{G}. \\ \text{empty set}, & \text{otherwise.} \end{cases} \tag{2.3}$$

Here, Eq. (2.1) describes the smooth dynamics of the continuous state $\boldsymbol{X}(t)$ when the discrete state is $I(t)=i$, Eq. (2.2) the jump of $\boldsymbol{X}(t)$ when the discrete state switches from i to j, and Eq. (2.3) represents a plane in the space of continuous state on which the switching from i to j takes place. In Eq. (2.1), $\boldsymbol{F}(I,\boldsymbol{X}):\mathcal{M}\times\mathbb{R}^N\to\mathbb{R}^N$ is the vector field of the system. In Eq. (2.2), "$t+0$" indicates the moment just after the switching of the discrete state at t, the transition function $\boldsymbol{\Phi}((i,j),\boldsymbol{X}):\mathcal{G}\times\mathbb{R}^N\to\mathbb{R}^N$ gives the new continuous state after the switching of the discrete state from i to j, and $\boldsymbol{\Pi}_{ij}$ is an $(N-1)$ dimensional zero-level surface (or its subset) of the function $L((i,j),\boldsymbol{X}):\mathcal{G}\times\mathbb{R}^N\to\mathbb{R}$ on which the switching takes place. It is assumed that the functions $\boldsymbol{F}(I,\boldsymbol{X})$, $\boldsymbol{\Phi}((i,j),\boldsymbol{X})$, and $L\left((i,j),\boldsymbol{X}\right)$ are twice continuously differentiable with respect to $\boldsymbol{X}\in\mathbb{R}^N$ and do not depend explicitly on time.

Suppose there exists a periodic solution $\chi:\boldsymbol{s}_0(t)=(I_0(t),\boldsymbol{X}_0(t))$ of period T of Eqs. (2.1-2.3). As in Ref. [96, 97], we make several assumptions on the system (see Appendix A for details) so that the continuous part of the solution $\boldsymbol{X}_0(t)$ is piecewise continuously differentiable with respect to the initial continuous state $\boldsymbol{X}_0(0)$ on χ and linear stability analysis of the solution can be performed. Let $\boldsymbol{s}^*=(I(0),\boldsymbol{X}(0))$ be an initial condition of Eqs. (2.1-2.3) and $t=\tau_k(\boldsymbol{s}^*)$, $k\in\mathbb{N}$ be the moments of switching of the discrete state, where $0\le\tau_1(\boldsymbol{s}^*)<\tau_2(\boldsymbol{s}^*)<\cdots<\tau_k(\boldsymbol{s}^*)<\cdots<+\infty$. For convenience of notation, we also define $\tau_0(\boldsymbol{s}^*)=0$.

To simplify the expression of the periodic orbit χ, we hereafter use the following notation. By distinguishing the discrete states visited more than once in one period, and by renumbering the state indices, we introduce a set of discrete states $\mathcal{M}_0=\{1,2,\cdots,m_0\}$ where $m_0<+\infty$, such that the discrete state $I_0(t)$ is switched in numerical order as $1\to2\to\cdots\to m_0\to m_0+1=1$ at $t=\tau_1(\boldsymbol{s}^*),\tau_2(\boldsymbol{s}^*),\cdots,\tau_{m_0}(\boldsymbol{s}^*)$ (see Fig. 2.1). Here, m_0 is finite because the period T is finite and the assumption (C2) in Appendix A assures that the system stays in each discrete state for some nonzero duration. We also introduce the following simplified notations for the discrete state

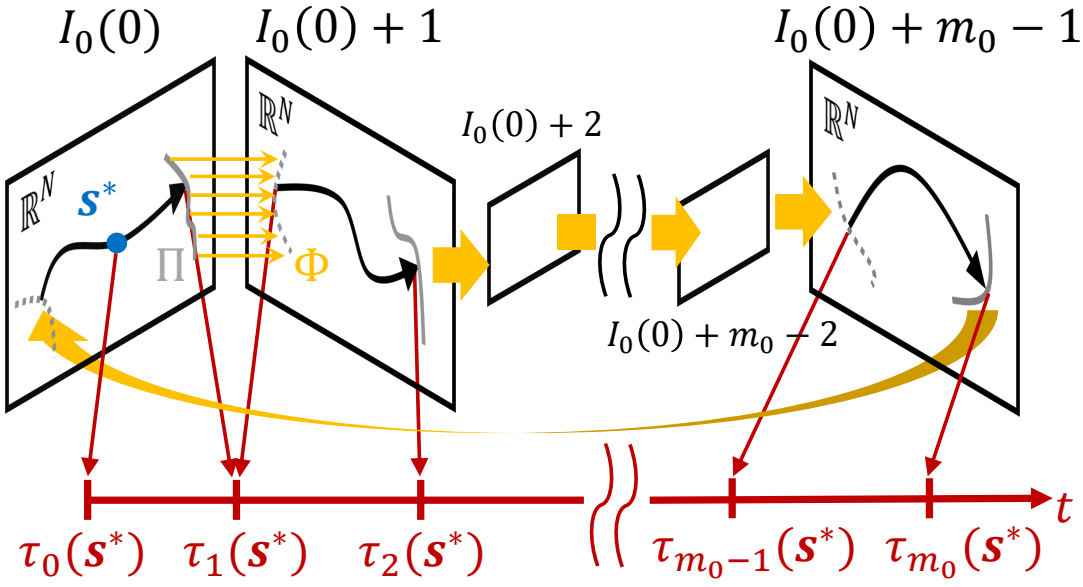

Fig. 2.1 Schematic representation of the dynamics of the hybrid limit cycles.

transitions on the periodic orbit χ:

$$\begin{aligned} L_k(\boldsymbol{X}_0(t)) &= L((k,k+1),\boldsymbol{X}_0(t)), \\ \boldsymbol{\Phi}_k(\boldsymbol{X}_0(t)) &= \boldsymbol{\Phi}((k,k+1),\boldsymbol{X}_0(t)). \end{aligned} \tag{2.4}$$

We call the periodic solution χ a hybrid limit cycle if it is linearly stable (see Appendix B for the linear stability analysis of the periodic solution).

2.3 Phase reduction

The aim of phase reduction is to describe the dynamics of the system state around the hybrid limit cycle χ by using a scalar phase θ. We first introduce the phase function $\Theta : \mathcal{M}_0 \times \mathbb{R}^N \to \mathbb{T}^1 (= [0,T))$ on χ, which gives the phase value of the state $\boldsymbol{s}_0 = (I_0, \boldsymbol{X}_0)$ on χ as

$$\Theta(\boldsymbol{s}_0(t+nT)) = \Theta(I_0(t+nT), \boldsymbol{X}_0(t+nT)) = t \ (\mathrm{mod}\ T), \tag{2.5}$$

where $n \in \mathbb{Z}_{\geq 0}$ is an arbitrary positive integer. Namely, we identify the time t (mod T) as the oscillator phase θ, which increases with a constant frequency 1 on χ, i.e.,

$$\dot{\theta}(t) = \dot{\Theta}(I_0(t), \boldsymbol{X}_0(t)) \equiv 1. \tag{2.6}$$

In the following, we will denote a system state with phase θ on χ also as $\boldsymbol{s}_0(\theta) = (I_0(\theta), \boldsymbol{X}_0(\theta))$ as a function of θ.

Phase θ can also be introduced in a neighborhood U containing χ within its basin of attraction by introducing an equivalence relation to initial conditions in U whose asymptotic behaviors are the same. Namely, we introduce the *isochron* of χ by assigning the same phase value to the set of states in U that eventually converge to the same state on χ. Suppose that $\boldsymbol{s}_1$ and $\boldsymbol{s}_2$ are taken from U, where $\boldsymbol{s}_2$ is on χ at phase θ, i.e., $\boldsymbol{s}_2 = \boldsymbol{s}_0(\theta)$. If $\boldsymbol{s}_1$ and $\boldsymbol{s}_2$ are asymptotically equivalent, we define the phase of $\boldsymbol{s}_1$ as

$$\Theta(\boldsymbol{s}_1) = \Theta(\boldsymbol{s}_2) = \theta. \tag{2.7}$$

Note that the convergence concept of the solutions in hybrid dynamical systems demands somewhat careful attention (see Appendix C for details). Some properties of the isochron and the phase function on U are discussed in Appendix D.

The above definition of the phase guarantees that the following relation holds for almost all t (excluding the Lebesgue measure zero set of the moments of switching) for an unperturbed oscillator:

$$\dot{\theta}(t) = \dot{\Theta}(I(t), \boldsymbol{X}(t)) = \nabla\Theta(I(t), \boldsymbol{X}(t)) \cdot \boldsymbol{F}(I(t), \boldsymbol{X}(t)) = 1, \tag{2.8}$$

where $\nabla\Theta$ represents the gradient of Θ with respect to $\boldsymbol{X}$. Namely, the phase θ rotates on a circle $\mathbb{T}^1$ at a constant frequency 1.

When a sufficiently small perturbation $\epsilon \boldsymbol{p}(I(t), \boldsymbol{X}(t), t)$ with $|\epsilon| \ll 1$ is introduced to the oscillator as

$$\dot{\boldsymbol{X}}(t) = \boldsymbol{F}(I(t), \boldsymbol{X}(t)) + \epsilon \boldsymbol{p}(I(t), \boldsymbol{X}(t), t), \tag{2.9}$$

we can obtain the following approximate phase equation closed in θ at the lowest order:

$$\begin{aligned}
\dot{\theta}(t) &= \dot{\Theta}(I(t), \boldsymbol{X}(t)) \\
&= 1 + \epsilon \nabla\Theta(I_0(\theta), \boldsymbol{X}_0(\theta)) \cdot \boldsymbol{p}(I_0(\theta), \boldsymbol{X}_0(\theta), t) + O(\epsilon^2) \\
&= 1 + \epsilon \boldsymbol{Z}(\theta) \cdot \boldsymbol{p}(I_0(\theta), \boldsymbol{X}_0(\theta), t) + O(\epsilon^2),
\end{aligned} \tag{2.10}$$

where we defined the phase sensitivity function

$$\boldsymbol{Z}(\theta) = \nabla\Theta(I_0(\theta), \boldsymbol{X}_0(\theta)) \tag{2.11}$$

characterizing the linear response property of the oscillator phase to perturbations. We consider that the phase evolves as a solution of a suitably regularized, multivalued system of Eq. (2.10), such as the Filippov system [98, 99]. (We do not consider impulsive perturbation at the moment of switching in this study, which requires special treatment.) The ideas underlying the phase approximation Eq. (2.10) and some notes on the notion of the solution of it are given in Appendix E.

Thus, once we obtain the phase sensitivity function $\boldsymbol{Z}(\theta)$, the dynamics of a weakly perturbed hybrid limit cycle described by Eq. (2.9) can be reduced to a single phase equation (2.10). Using the reduced phase equation, we can analyze various synchronization dynamics of hybrid limit cycles in detail. As we derive in Appendix F, $\boldsymbol{Z}(\theta)$ is given by a periodic solution to the following adjoint system:

$$\dot{\boldsymbol{Z}}(t) = -\mathbf{A}^\dagger(k,t)\boldsymbol{Z}(t) \quad \text{for} \quad t \ (\mathrm{mod}\ T) \in (\tau_{k-1}(\boldsymbol{s}^*), \tau_k(\boldsymbol{s}^*)), \tag{2.12}$$

$$\boldsymbol{Z}(t) = (\mathbf{C}_k)^\dagger \boldsymbol{Z}(t+0) \quad \text{at} \quad t \ (\mathrm{mod}\ T) = \tau_k(\boldsymbol{s}^*), \tag{2.13}$$

which is normalized to satisfy Eq. (2.8) on χ, that is,

$$\boldsymbol{Z}(t) \cdot \boldsymbol{F}(I_0(t), \boldsymbol{X}_0(t)) = 1. \tag{2.14}$$

Here, $\mathbf{A}(k,t) = D\boldsymbol{F}(k, \boldsymbol{X}_0(t))$ is the Jacobi matrix of $\boldsymbol{F}(k, \boldsymbol{X})$ estimated on χ, and $\mathbf{C}_k$ is a "saltation matrix" [62] given by

$$\begin{aligned}\mathbf{C}_k = {} & D\boldsymbol{\Phi}_k(\boldsymbol{X}_0(\tau_k(\boldsymbol{s}^*))) \\ & - \left[D\boldsymbol{\Phi}_k(\boldsymbol{X}_0(\tau_k(\boldsymbol{s}^*)))\dot{\boldsymbol{X}}_0(\tau_k(\boldsymbol{s}^*)) - \dot{\boldsymbol{X}}_0(\tau_k(\boldsymbol{s}^*)+0)\right] \\ & \otimes \left(\frac{\nabla L_k(\boldsymbol{X}_0(\tau_k(\boldsymbol{s}^*)))}{\nabla L_k(\boldsymbol{X}_0(\tau_k(\boldsymbol{s}^*))) \cdot \dot{\boldsymbol{X}}_0(\tau_k(\boldsymbol{s}^*))}\right),\end{aligned} \tag{2.15}$$

where $D\boldsymbol{\Phi}_k$ is the Jacobi matrix of $\boldsymbol{\Phi}_k$ and $\otimes$ represents a tensor product of two vectors. $\mathbf{C}_k$ represents expansion or contraction of small deviations from χ by the mapping $\boldsymbol{\Phi}_k$ at the switching $t = \tau_k(\boldsymbol{s}^*)$, where the second term on the right-hand side takes into account the shift in the switching time caused by the perturbation. In general,

the above adjoint system can be integrated only backward in time because $\mathbf{C}_k$ can be singular.

In numerical calculations, we integrate these adjoint equations backward in time with occasional renormalization of $\boldsymbol{Z}(t)$ so that Eq. (2.14) is satisfied. Then, reflecting the linear stability of χ, all modes except the neutrally stable periodic solution decay and $\boldsymbol{Z}(\theta)$ is eventually obtained. This is a standard procedure for calculating $\boldsymbol{Z}(\theta)$ of ordinary limit cycles and is called the adjoint method after Ermentrout [8].

2.4 Examples

As an application of the phase reduction theory for hybrid limit cycles that we developed, we analyze injection locking of hybrid limit-cycle oscillators, i.e., synchronization of the oscillator to a periodic external signal [2]. We apply a weak periodic signal $\boldsymbol{p}(t) = \boldsymbol{p}(t + T_{\text{ext}})$ to the hybrid limit cycle described by Eqs. (2.1) and (2.2). Using the phase reduction theory, the state of the perturbed oscillator, described by Eq. (2.9), can be approximately represented by its phase θ, which obeys the reduced phase equation (2.10).

To analyze the synchronization dynamics, we consider the phase difference ψ between the oscillator and the periodic signal,

$$\psi = \theta - \frac{T}{T_{\text{ext}}} t, \tag{2.16}$$

where θ is the phase of the hybrid limit cycle, T is the natural period of the hybrid limit cycle, and T_{ext} is the period of the external periodic signal. The frequency mismatch between the oscillator and the signal is given by $\epsilon\Delta = 1 - T/T_{\text{ext}}$. As shown in Appendix G, using the standard averaging approximation for weakly perturbed oscillators [2, 57, 8], the dynamics of ψ can be derived from the reduced phase equation (2.10) as

$$\dot{\psi} = \epsilon[\Delta + \Gamma(\psi)] \tag{2.17}$$

where the T-periodic phase coupling function $\Gamma(\psi)$ is given by

$$\Gamma(\psi) = \frac{1}{T_{\text{ext}}} \int_0^{T_{\text{ext}}} \boldsymbol{Z}\left(\frac{T}{T_{\text{ext}}} t + \psi\right) \cdot \boldsymbol{p}(t) dt. \tag{2.18}$$

As mentioned previously for the phase equation, we consider that the phase difference evolves as a solution of Eq. (2.17) in a regularized sense, if necessary. See [100–102] for

the averaging approximation in non-autonomous systems with jumps and multivalued righthand sides.

Synchronization dynamics of the oscillator can easily be understood from the phase coupling function $\Gamma(\psi)$. If Eq. (2.17) has a stable fixed point, the phase difference ψ converges to this point and the oscillator is phase-locked to the periodic signal. If there exist multiple stable fixed points, the oscillator can be phase-locked to the periodic signal at multiple phase differences depending on the initial condition. If Eq. (2.17) does not have a fixed point, ψ continues to increase or decrease and phase locking does not occur.

2.4.1 Glued Stuart-Landau oscillator

As the first example, we introduce an analytically tractable model of a hybrid limit-cycle oscillator, which is constructed by gluing two Stuart-Landau oscillators (normal forms of the supercritical Hopf bifurcation [103]) of different amplitudes. The glued Stuart-Landau oscillator has two discrete states $I \in \{1, 2\}$ and a two-dimensional continuous state variable $\boldsymbol{X}(t) = (x(t), y(t))^\dagger$, where $\dagger$ denotes the transpose of a matrix. The dynamics is described by

$$\boldsymbol{F}(1, \boldsymbol{X}) = \begin{pmatrix} x - ay - (x^2 + y^2)(x - by) \\ ax + y - (x^2 + y^2)(bx + y) \end{pmatrix},$$

$$\boldsymbol{F}(2, \boldsymbol{X}) = \begin{pmatrix} x - ay - \alpha^2(x^2 + y^2)(x - by) \\ ax + y - \alpha^2(x^2 + y^2)(bx + y) \end{pmatrix},$$

$$\boldsymbol{\Phi}_1(\boldsymbol{X}) = \begin{pmatrix} x \\ \alpha \\ y \end{pmatrix}, \ \boldsymbol{\Phi}_2(\boldsymbol{X}) = \begin{pmatrix} \alpha x \\ y \end{pmatrix},$$

$$\boldsymbol{\Pi}_{1,2} = \{\boldsymbol{X} \mid (L_1(\boldsymbol{X}) = 0) \ \cap \ (x \leq 0)\}, \quad \boldsymbol{\Pi}_{2,1} = \{\boldsymbol{X} \mid (L_2(\boldsymbol{X}) = 0) \ \cap \ (x \geq 0)\},$$
$$L_1(\boldsymbol{X}) = y, \ L_2(\boldsymbol{X}) = -y,$$

and the parameters are set as $a = 2\pi + 1, b = 1$ and $\alpha = 2$. With these parameter values, this system has a stable limit cycle of period $T = 1$. We take the origin of the phase $\theta = 0$ at $I = 1$ and $\boldsymbol{X} = (0, 1)^\dagger$, i.e., $\boldsymbol{\Theta}(1, (0, 1)^\dagger) = 0$.

The periodic orbit χ is depicted on $\mathbb{R}^2$ (Fig. 2.2(a)), which satisfies

$$(I_0(\theta), \boldsymbol{X}_0(\theta)) = (1, (-\sin(2\pi\theta), \cos(2\pi\theta))) \tag{2.19}$$

for $\theta \in \mathrm{D}_1$, and

$$(I_0(\theta), \boldsymbol{X}_0(\theta)) = (2, (-0.5\sin(2\pi\theta), 0.5\cos(2\pi\theta))) \tag{2.20}$$

for $\theta \in \mathrm{D}_2$, where $\mathrm{D}_1 = [0, 0.25) \cup [0.75, 1)$ and $\mathrm{D}_2 = [0.25, 0.75)$ are domains of the phase.

The phase sensitivity function can be obtained by solving the adjoint linear problem analytically and is given by

$$\boldsymbol{Z}(\theta) = -\frac{1}{2\pi}(\cos 2\pi\theta - \sin 2\pi\theta, \sin 2\pi\theta + \cos 2\pi\theta)^\dagger \tag{2.21}$$

for $\theta \in \mathrm{D}_1$, and

$$\boldsymbol{Z}(\theta) = -\frac{1}{\pi}(\cos 2\pi\theta - \sin 2\pi\theta, \sin 2\pi\theta + \cos 2\pi\theta)^\dagger \tag{2.22}$$

for $\theta \in \mathrm{D}_2$.

For the waveform of the periodic injection signal $\boldsymbol{p}(t) = (p_1(t), p_2(t))^\dagger$, we consider rectangular waves:

$$p_1(t) = -c \text{ (if } t \bmod T_{\mathrm{ext}} \in \mathrm{D}), \quad 0 \text{ (otherwise)}, \tag{2.23}$$

and

$$p_2(t) = 0 \text{ for all } t, \tag{2.24}$$

where the constant $c > 0$ is set so that the squared mean of the injection signal becomes unity, i.e., $\langle \boldsymbol{p}^2 \rangle \equiv \frac{1}{T_{\mathrm{ext}}} \int_0^{T_{\mathrm{ext}}} \boldsymbol{p}^2(t)dt = 1$ unless otherwise specified, and D is the time domain where the forcing takes place.

In Figs. 2.2(b) and 2.2(c), the phase sensitivity function $\boldsymbol{Z}(\theta)$ obtained by analytically solving the proposed adjoint systems is compared with the result of the direct numerical simulation (see Appendix H for details). The results are in good agreement and show the validity of the proposed adjoint method. The discontinuities in $\boldsymbol{Z}(\theta)$ are characteristic of a hybrid limit-cycle oscillator.

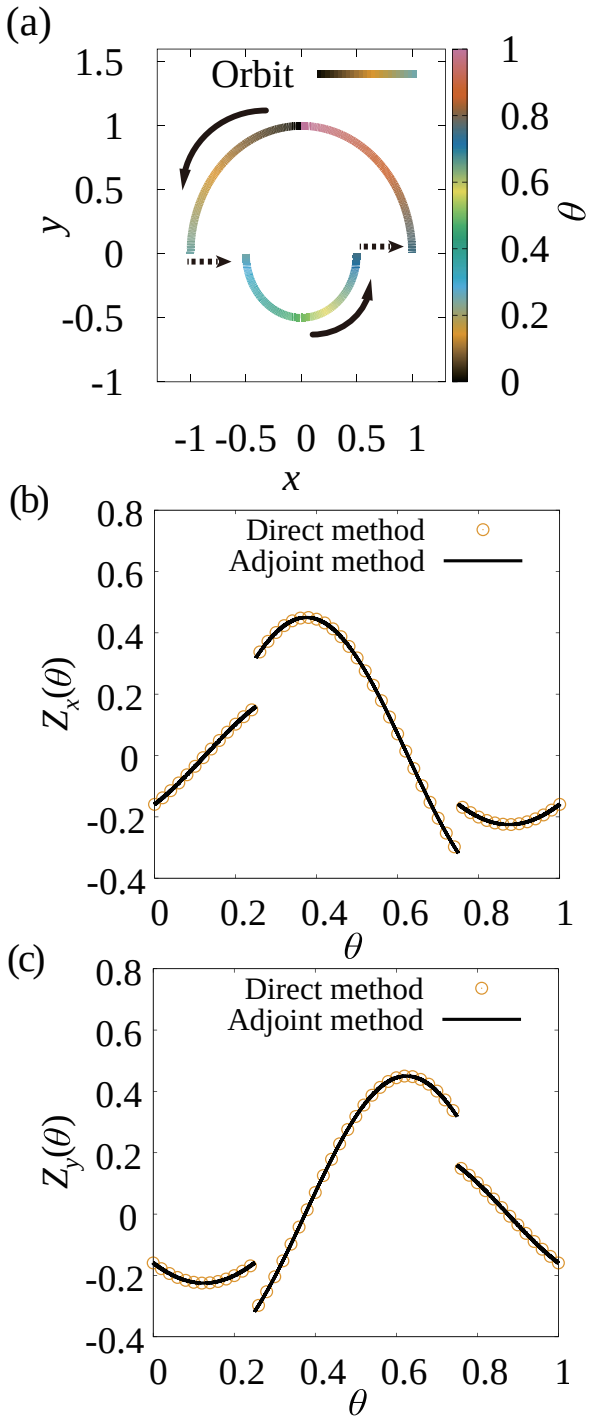

Fig. 2.2 The glued Stuart-Landau oscillator. (a) The periodic orbit of a glued Stuart-Landau oscillator. The phase of the oscillator is shown in color code. The arrows represent the direction of the time evolution of the continuous state. The broken arrows indicate jumps. (b),(c) The x and y components of the phase sensitivity function $\boldsymbol{Z}(\theta)$ obtained by the direct method (circles) and by the proposed adjoint method (lines).

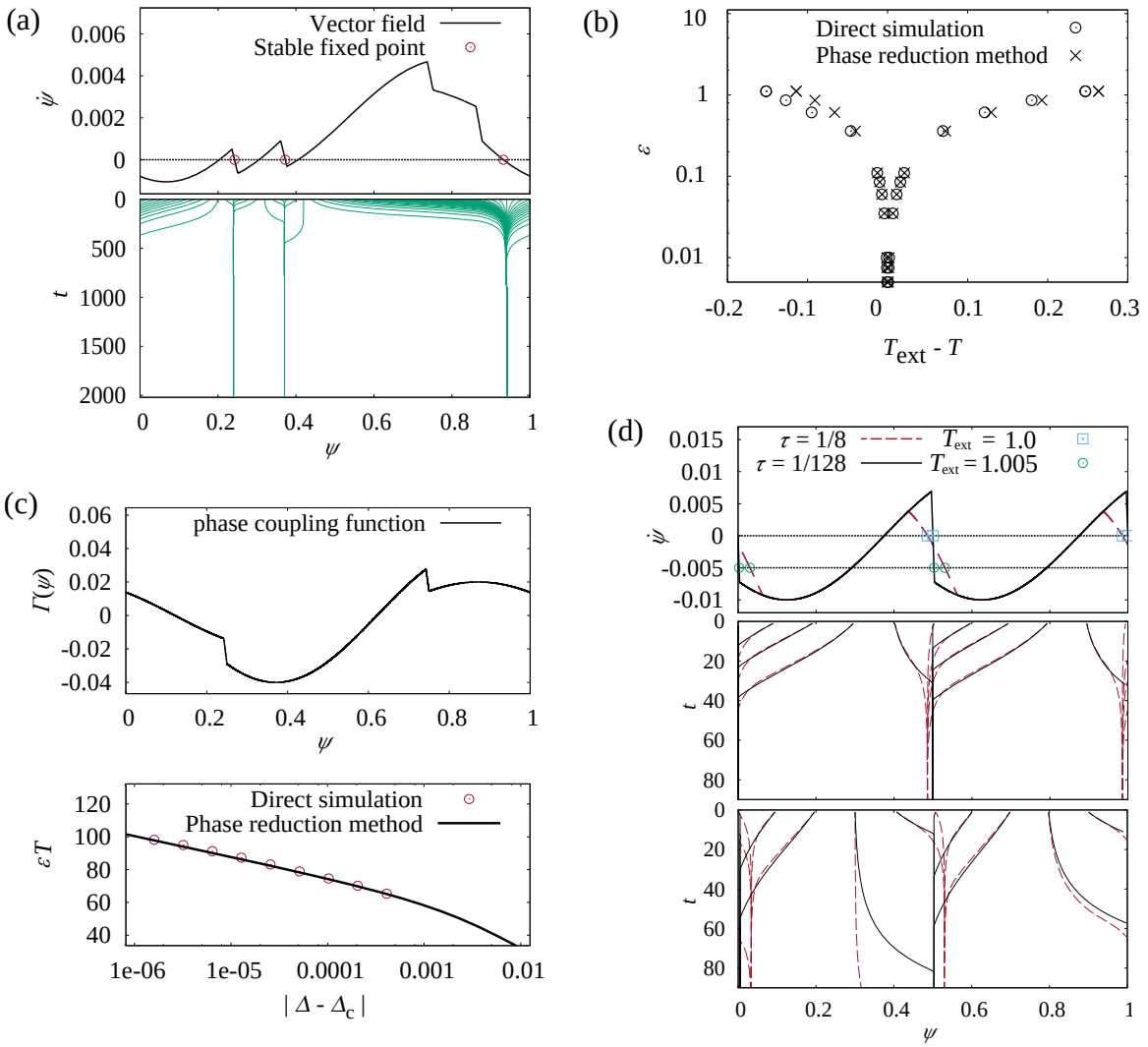

Fig. 2.3 Phase reduction analysis of the injection locking of a glued Stuart-Landau oscillator. (a) Dynamics of the phase difference ψ. Time derivative $\dot{\psi}$ plotted as a function of ψ, where three stable fixed points (circles) coexist (top panel). Trajectories of ψ from 50 different initial states obtained by direct numerical simulation of the original model, converging to the stable fixed points (bottom panel). The parameters are set as $\epsilon = 0.1$, $T_{\rm ext}/T = 1.002$, and the domain where $p_1(t)$ takes a non-zero value is $\mathrm{D} = \{t \mid 0 \le t \le T_{\rm ext}/64 \ \cup \ 3T_{\rm ext}/8 \le t \le 25T_{\rm ext}/64\}$. (b) The Arnold tongue showing the region where phase locking takes place. Here $\mathrm{D} = \{t \mid 0 \le t \le T_{\rm ext}/2\}$. (c) The phase coupling function with sharp corners (top panel) and the period of the phase slipping plotted in log-linear scales (bottom panel). Here $\epsilon = 0.01$ and $\mathrm{D} = \{t \mid 0 \le t \le T_{\rm ext}/128\}$. (d) Dynamics of the phase difference ψ for the mild, non-impulsive (yellow line) and impulsive (black line) signals. Time derivative $\dot{\psi}$ vs. ψ with stable fixed points (circles) for the different frequencies of the input for each case (top panel). Trajectories of ψ from 10 different initial states for $T_{\rm ext}/T = 1.0$ (middle panel) and for $T_{\rm ext}/T = 1.005$ (bottom panel). The parameters are set as follows: $\epsilon = 0.01$, and $\mathrm{D} = \{t \mid |t - T_{\rm ext}/4| \le \tau T_{\rm ext}/2 \ \cup \ |t - 3T_{\rm ext}/4| \le \tau T_{\rm ext}/2\}$.

Figure 2.3(a) displays the averaged dynamics of the phase difference ψ for several initial values, where the result of phase reduction is compared with direct numerical simulations. It can be seen that the asymptotic phase differences and their dependence on initial conditions are well predicted from the phase coupling function $\Gamma(\psi)$. Figure 2.3(b) shows the boundaries of the region where the injection locking takes place, called the Arnold tongue [57]. Results of the numerical simulation also agree well with the analytical prediction by the phase reduction theory. Thus, the injection locking of hybrid limit-cycle oscillators by weak periodic input can be theoretically predicted by using $\boldsymbol{Z}(\theta)$ obtained by the adjoint method.

Here, we emphasize one peculiar property of the hybrid oscillator. For smooth oscillators, the period of the phase slipping near the critical point generally obeys the inverse square-root scaling law, $\epsilon T_{\mathrm{slip}} \sim |\Delta - \Delta_c|^{-1/2}$, where Δ_c is the critical value of Δ [2, 104], because the phase coupling function $\Gamma(\psi)$ generally has quadratic maximum and minimum. In contrast, as shown in Fig. 2.3(c), the hybrid oscillator with discontinuous $\boldsymbol{Z}(\theta)$ can possess non-smooth $\Gamma(\psi)$ with sharp non-quadratic maximum or minimum when subjected to impulsive signals. For such $\Gamma(\psi)$, we can show that the period of phase slipping T_{slip} obeys

$$\epsilon T_{\mathrm{slip}} \sim -\ln|\Delta - \Delta_c| \tag{2.25}$$

at the leading order in the vicinity of the critical value Δ_c, where $\Delta_c + \Gamma(\psi^*) = 0$ and $\Gamma(\psi^*)$ is the extremum at the corner of $\Gamma(\psi)$, and the semiderivatives $\Gamma'(\psi^* - 0)$ and $\Gamma'(\psi^* + 0)$ are nonzero (see Appendix I for the derivation). Since non-smooth corners in $\Gamma(\psi)$ cannot exist in smooth systems, singular scaling law of this kind is characteristic of hybrid oscillators.

In Fig. 2.3(d), the transient dynamics of ψ for two different types of rectangular wave input, one with a low-duty ratio (impulsive) $\tau = 1/128$ and the other with a mediate one (mild, non-impulsive) $\tau = 1/8$, is compared. Here the magnitude c of the input signal is normalized so that the uniform norm of Γ becomes unity, i.e., $\max_\psi |\Gamma(\psi)| = 1$, for each case. For the impulsive case, ψ approaches the stable phase difference ψ_0 with a nonzero angle, while in the non-impulsive case, the approach is tangential. This implies that the decay of the deviation from ψ_0 is faster than exponential in the impulsive case and the time required to establish entrainment is drastically shorter. Moreover, variations in the input period only slightly changes ψ_0 for the impulsive input, while ψ_0 shows significant change for the non-impulsive input. This ultrafast entrainment and robustness of the stable phase difference can be attributed to the existence of the region $\mathrm{D_s}$ where $\Gamma(\psi)$ is extremely steep.

Note that the discontinuity in $\boldsymbol{Z}(\theta)$ is necessary for the existence of such a region $\mathrm{D_s}$, because $\Gamma(\psi)$ is given by the convolution (2.18) of $\boldsymbol{Z}(\theta)$ and $\boldsymbol{p}(t)$; when the input is an ideal impulse, the slope of $\Gamma(\psi)$ in $\mathrm{D_s}$ can be infinite. Therefore, these interesting synchronization properties are distinctive feature of the hybrid oscillators driven by impulsive periodic input. Such a type of very fast (or finite-time) synchronization has been studied for simple neuron models with discontinuity whose $\boldsymbol{Z}(\theta)$ can be obtained analytically, as well as in some fast-slow models in the fast-relaxation limit [59, 105–107]. Our argument based on the phase reduction theory for hybrid limit cycles is general and can be applied to high-dimensional systems where the non-smoothness is not the result of adiabatic approximation.

2.4.2 Passive bipedal walker

Next, we analyze a physical example of hybrid limit-cycle oscillator, namely, a two-link model of a passive walker walking down a slope [108], proposed as a simple model of biped locomotion. Figure 2.4(a) shows a schematic diagram of the model, where g is the gravitational acceleration, l is the length of the legs, M and m are the masses of the hip and the foot, respectively, ϕ_1 and ϕ_2 specify the angles of the swing and support legs, γ is the angle of the slope, and τ is a periodic torque applied to the ankle of the support leg. It is assumed that $m/M = 0$, i.e., the hip mass is much larger than the foot mass, the tip of the support leg does not slip along the ground, and the collision of the foot with the ground is perfectly inelastic (no slip and no bounce). This model exhibits a stable limit-cycle oscillation for appropriate parameter values that corresponds to periodic movements of the legs. This is a four dimensional hybrid dynamical system with impacts, hence it cannot be dealt with by the conventional methods [58–60] mentioned above.

The model has a one discrete state $I \in \{1\}$ and a continuous state variable $\boldsymbol{X}(t) = (\phi_1(t), \dot{\phi}_1(t), \phi_2(t), \dot{\phi}_2(t))^\dagger$. The dynamics is described by

$$\boldsymbol{F}(1, \boldsymbol{X}) = \begin{pmatrix} \dot{\phi}_1 \\ \sin(\phi_1 - \gamma) \\ \dot{\phi}_2 \\ \sin(\phi_1 - \gamma) + \dot{\phi}_1^2 \sin\phi_2 - \cos(\phi_1 - \gamma)\sin\phi_2 \end{pmatrix}, \tag{2.26}$$

$$\boldsymbol{\Phi}_1(\boldsymbol{X}) = \begin{pmatrix} -\phi_1 \\ \dot{\phi}_1 \cos 2\phi_1 \\ -2\phi_1 \\ \dot{\phi}_1 \cos 2\phi_1 (1 - \cos 2\phi_1) \end{pmatrix}, \tag{2.27}$$

$$\begin{aligned} &\boldsymbol{\Pi}_{1,1} = \{\boldsymbol{X} \mid (L((1,1), \boldsymbol{X}) = 0) \cap (\phi_2 < -\delta)\}, \\ &L_1(\boldsymbol{X}) = 2\phi_1 - \phi_2, \end{aligned} \tag{2.28}$$

where we have rescaled time by $\sqrt{l/g}$, and $\delta > 0$ is a small positive constant (we set $\delta = 0.1$), which is introduced to avoid foot scuffing (contact of the swing leg with the ground in the middle of the swing). The parameter γ is set as $\gamma = 0.009$. Note that Eq. (2.26) is an equation of motion representing continuous dynamics of the walker during the single-leg support phase, in which the walker stands on the support leg and moves the swing leg, where ϕ_1 and ϕ_2 are the angular coordinates of the swing and support legs. See Ref. [109] for a detailed derivation of the above type of equations in nearly the same setting. Note also that the main effect of the inclined ground to the walking dynamics, i.e., the ground reaction force, is already included in the dynamical model. This effect is not considered a perturbation and therefore needs not be weak, as long as the model exhibits stable rhythmic walking. If there exist additional small effects from the flat inclined ground, such as slight up and down, they can be incorporated into the reduced phase model perturbatively. Finally, although the motion of Eq. (2.26) during the single-leg support phase appears to be conservative, the collision of the leg with the ground, described Eq. (2.27) and Eq. (2.28), is perfectly inelastic (plastic), so that the impact of the leg with nonzero velocity relative to the ground causes energy dissipation. This energy loss is compensated by the gravitational potential energy, which is supplied to the system at each moment of the collision of the leg with the ground. Thus, a stable limit cycle can arise in this hybrid dynamical system.

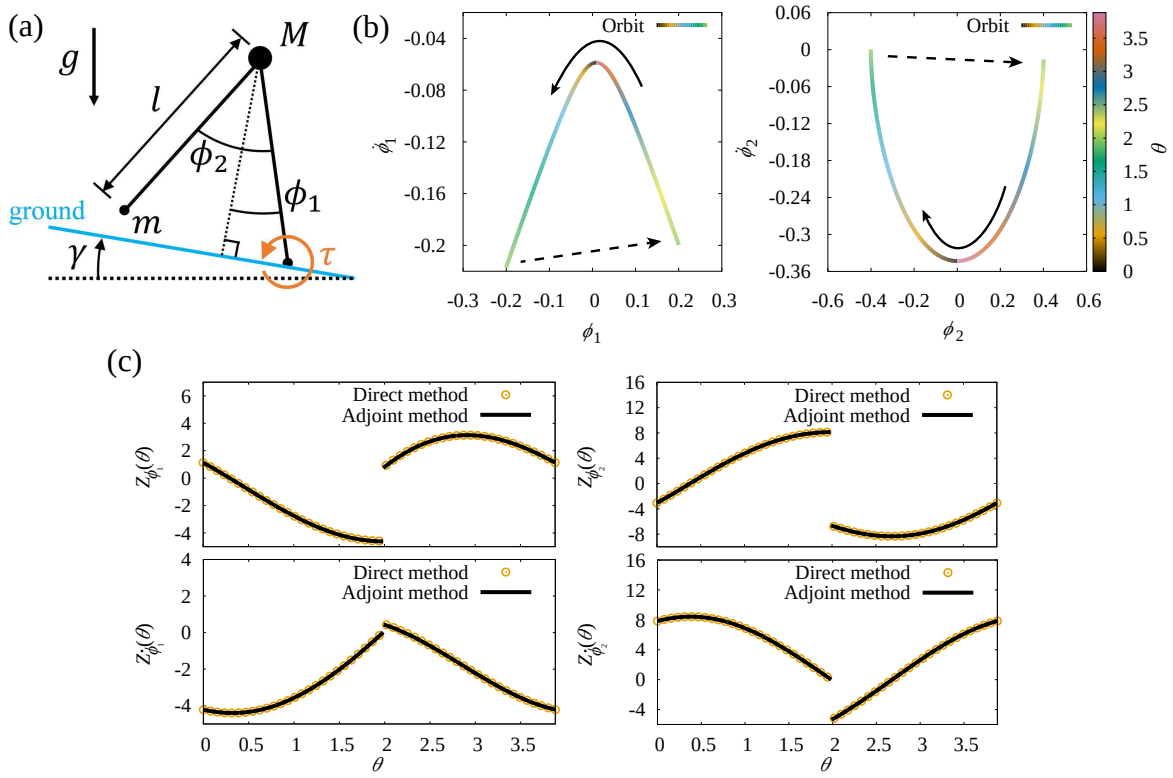

Fig. 2.4 Two-link model of a passive walker walking down a slope. (a) Schematic of the model. (b) The periodic orbit of the model. The orbit discontinuously jumps when the swing and support leg alternate with each other. The arrows represent the direction of the time evolution of the continuous state. The broken arrows indicate jumps. The phase is shown in color code. (c) Four components of the phase sensitivity function $\boldsymbol{Z}(\theta) = (Z_{\phi_1}(\theta), Z_{\dot{\phi}_1}(\theta), Z_{\phi_2}(\theta), Z_{\dot{\phi}_2}(\theta))^\dagger$ obtained by the direct method (circles) and by the proposed adjoint method (lines).

Figure 2.4(b) shows the stable periodic orbit of the model. Using the shooting method developed in [95], a point on χ, which we define as the origin of the phase, and the period T of the orbit can be obtained as

$$\boldsymbol{s}^* = (1, (0.009000, -0.05869, -0.0009629, -0.3432)^\dagger), \quad T = 3.882. \tag{2.29}$$

Figure 2.4(c) shows the phase sensitivity function $\boldsymbol{Z}(\theta) = (Z_{\phi_1}(\theta), Z_{\dot{\phi}_1}(\theta), Z_{\phi_2}(\theta), Z_{\dot{\phi}_2}(\theta))^\dagger$ with discontinuity in the middle, which is obtained numerically by the proposed adjoint method. The result agrees well with the one obtained by the direct method, thus the proposed adjoint method also works nicely for this model.

Using the reduced phase equation, we study the injection locking of the passive walker to the periodic ankle torque actuation. That is, we apply a weak periodic

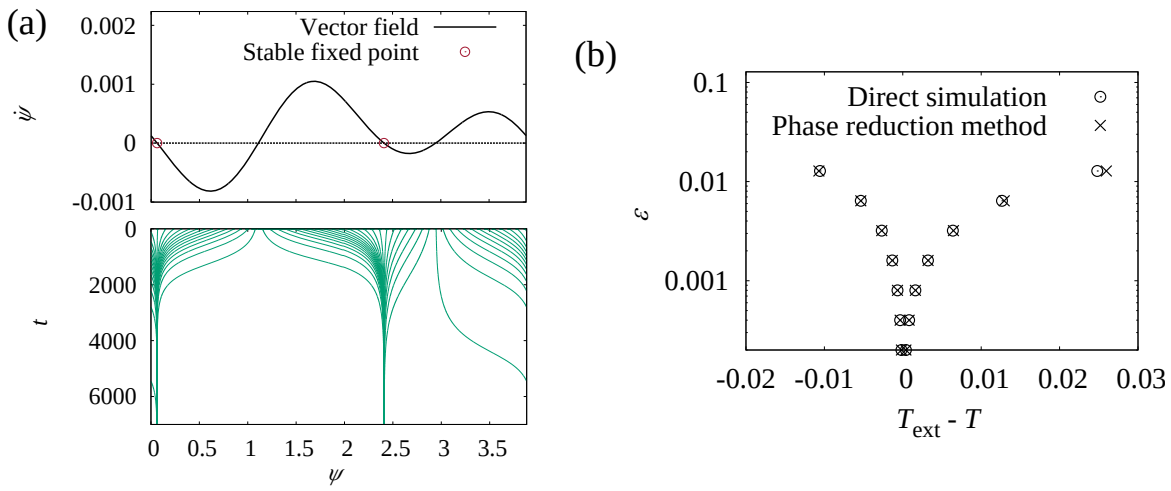

Fig. 2.5 Phase reduction analysis of the injection locking of the two-link model of the passive walker. (a) Dynamics of the phase difference ψ (line). $\dot{\psi}$ vs. ψ, where stable fixed points are represented by circles (top panel). Trajectories of ψ from 50 different initial states obtained by direct numerical simulation of the original model (bottom panel). The parameters are set as $\epsilon = 0.00253$ and $T_{\rm ext}/T = 1.0005$. (b) The Arnold tongue obtained by the phase reduction and by direct numerical simulation of the original model.

torque to the walker, where the frequency of the torque is close to that of the natural frequency of the walker, and analyze whether the walker synchronizes with the applied weak torque. We introduce periodic actuation of the ankle torque as the injection signal $\boldsymbol{p}(t) = (0, \tau(t), 0, 0)^{\dagger}$, where

$$\tau(t) = ce^{-0.5[t \pmod{T_{\rm ext}}]/T_{\rm ext}} \sin(4\pi t/T_{\rm ext}). \tag{2.30}$$

The magnitude c of the waveform is determined to satisfy the normalization condition $\langle \boldsymbol{p}^2 \rangle = 1$. As in the case of the glued Stuart-Landau oscillator, we can obtain the phase coupling function $\Gamma(\psi)$ from the phase sensitivity function $\boldsymbol{Z}(\theta)$ and the injected periodic signal $\boldsymbol{p}(t)$, and predict the dynamics of the phase difference ψ between the oscillator and the signal.

Figure 2.5(a) shows the dynamics of ψ. The reduced phase equation predicts that there are two stable fixed points of ψ, and direct numerical simulations of the original model from different initial conditions confirm that the phase difference of the passive walker is actually attracted to either of the stable fixed points. Figure 2.5(b) plots the Arnold tongue showing the region where the phase locking of the passive walker to the injected signal takes place. The results obtained by the phase reduction theory agree well with the results obtained by direct numerical simulations of the original model.

Thus, the proposed phase reduction theory is also useful in analyzing realistic physical systems, even when the hybrid limit-cycle oscillator has a high-dimensional continuous state.

2.5 Summary

We formulated a phase reduction theory for a general class of hybrid limit-cycle oscillators and derived the adjoint equation for the phase sensitivity function. The proposed theory provides precise phase sensitivity functions and the derived phase equation accurately predicts the injection locking properties of hybrid oscillators. We illustrated synchronization properties characteristic to hybrid oscillators, such as ultrafast entrainment to periodic signal and negative logarithmic scaling at the synchronization transition, and explained them by using the reduced phase equation with discontinuous phase sensitivity functions.

The phase reduction theory developed in this study would serve as a powerful tool for investigating synchronization phenomena in complex non-smooth systems and for finding various applications in controlling distributed interacting nonlinear oscillators [80–84].

Chapter 3

Phase-amplitude reduction theory of transient dynamics far from attractors for limit-cycling systems

Abstract

Phase reduction framework for limit-cycling systems based on isochrons has been used as a powerful tool for analyzing rhythmic phenomena. Recently, the notion of isostables, which complements the isochrons by characterizing amplitudes of the system state, i.e., deviations from the limit-cycle attractor, has been introduced to describe transient dynamics around the limit cycle [Wilson and Moehlis, Phys. Rev. E **94**, 052213 (2016)]. In this study, we introduce a framework for a reduced phase-amplitude description of transient dynamics of stable limit-cycling systems. In contrast to the preceding study, the isostables are treated in a fully consistent way with the Koopman operator analysis, which enables us to avoid discontinuities of the isostables and to apply the framework to system states far from the limit cycle. We also propose a new, convenient bi-orthogonalization method to obtain the response functions of the amplitudes, which can be interpreted as an extension of the adjoint covariant Lyapunov vector to transient dynamics in limit-cycling systems. We illustrate the utility of the proposed reduction framework by estimating optimal injection timing of external input that efficiently suppresses deviations of the system state from the limit cycle in a model of a biochemical oscillator.

3.1 Introduction

The phase reduction theory provides a general framework to simplify a complex, multi-dimensional limit-cycling system describing a stable rhythmic activity to a one-dimensional phase equation evolving on a circle [1, 2, 8, 57, 65, 110]. It has been successfully used to understand synchronization phenomena of weakly interacting rhythmic elements in physical, chemical, biological and engineered systems [1, 2, 4, 7–9, 25, 57, 65, 81, 110, 111]. Methods to optimize and control synchronization of rhythmic elements have also been developed by using the phase reduction framework [6, 31–33, 112]. However, to describe the system dynamics far from the limit cycle, amplitude degrees of freedom should be taken into account. In this study, by extending preceding studies, we propose a phase-amplitude reduction framework that is applicable to transient dynamics far from the limit cycle.

The roles of amplitude degrees of freedom in limit-cycling systems, which represent deviations of the system states from the limit-cycle attractor and are eliminated in the phase-reduction framework, have been extensively studied because they are rich sources of intriguing oscillator dynamics at individual [4, 47, 49, 63–65, 113] and ensemble [2–4, 38–40, 65, 66] levels. In most studies, however, the analysis is restricted to the vicinity of a supercritical Hopf bifurcation, where a simple normal form (Stuart-Landau equation) of the oscillator dynamics is available [103, 114]. Some other studies use moving orthonormal frames along the limit cycle to define the amplitudes of the oscillator [63, 65, 113], which allows quantitative study of the amplitude dynamics of oscillators far from bifurcation points. However, in general, those amplitude variables interact nonlinearly with each other, which hinders simplification of the system description. Thus, it is highly desirable to establish a framework for a quantitative reduced description of limit-cycling systems applicable to transient dynamics far from the limit cycle. Such a framework would facilitate in-depth studies of the roles of amplitude degrees of freedom of limit-cycling systems in realistic settings.

The key idea in the phase reduction is assigning the same phase value to the set of initial conditions that share the same asymptotic behavior. These sets of identical phase values are called *isochrons* [1, 2, 4, 8, 57, 110]. Analogously, in a recent work [94], the notion of *isostables* is introduced by identifying the initial conditions that share the same relaxation property, i.e., the same decay rate toward the attractor. It has also been shown [94] that the isochrons and isostables can be understood from a unified point of view of the spectral properties of the *Koopman* (*composition*) *operator* [115]. For each characteristic decay rate of the system state toward the attractor, a set of isostables representing an amplitude degree of freedom can be introduced, which is

independent from the phase and the other amplitude degrees of freedom. By retaining a small number of amplitude variables representing dominant (slowly-decaying) part of the transient dynamics, reduced description of the system dynamics can be derived. The Koopman operator has attracted broad interest recently, because it is closely related to a rapidly developing data-driven approach to complex nonlinear systems, called the dynamic mode decomposition [115–121].

Amplitude reduction frameworks for a system near a stable equilibrium based on isostables have been established for multi-dimensional [94, 122, 123] and infinite-dimensional systems [124] and have been used to formulate optimal control problems of moving the system state toward the equilibrium [94, 123, 124]. Recently, Wilson and Moehlis [125] have extended the isostable reduction framework to limit-cycling systems. However, the isostables introduced in their work have discontinuities on one leaf of the isochrons. To avoid this problem, it is assumed in Ref. [125] that the system evolves in a close-enough neighborhood of the limit cycle so that the discontinuities are negligible, and the amplitude response to perturbation in their reduced system involves the first order response evaluated only on the limit cycle. Therefore, their analysis is essentially equivalent to deriving a decoupled linear system preserving spectral properties of the original system in a vicinity of the limit-cycle attractor (called *kinematically similar* system in terms of *Lyapunov transformations* [126–128]) by making use of covariant properties of *adjoint covariant Lyapunov vectors* [129] (also called adjoint Floquet vectors [130] or dual Lyapunov vectors [131]). A method to analyze response functions of decoupled phase and amplitude variables in limit-cycling systems, which is based on the *Lie symmetries* formalism and is valid far from the attractors, has also been proposed [132, 133]. However, the latter analysis is limited to two-dimensional dynamical systems and naive application of the method proposed in Ref. [133], that is, solving *adjoint equations* to calculate the response functions, can yield flawed results numerically, as we discuss in this paper.

In this study, we introduce a phase-amplitude reduction framework to describe transient dynamics of stable limit-cycle oscillators, which is applicable to high-dimensional dynamics far from the limit-cycle attractor. We propose a systematic bi-orthogonalization method to numerically estimate the fundamental quantities for the reduction accurately, i.e., the first order response functions of the phase and amplitudes to perturbations along a given trajectory, which is not necessarily the limit cycle itself. These response functions can be interpreted as an extension of the adjoint covariant Lyapunov vectors to transient dynamics. We illustrate the utility of the proposed framework by estimat-

ing optimal injection timing of external input that realizes maximal suppression of the most persistent (least decaying) amplitude degree of freedom.

This paper is organized as follows: in Sec. 3.2, phase and amplitudes in limit-cycling systems are introduced using the Koopman operator theory. In Sec. 3.3, the phase-amplitude reduction framework for limit-cycling systems is introduced and the bi-orthogonalization method to obtain their response properties is developed. In Sec. 3.4, the theory is illustrated by analyzing the phase-amplitude response properties of a minimal chemical kinetic model of an oscillatory genetic circuit. Also, the optimal injection timing problem is introduced and analyzed. Section 3.5 summarizes the results.

3.2 Phase, amplitudes and the Koopman operator

We consider a N-dimensional autonomous dynamical system

$$\dot{\boldsymbol{X}} = \boldsymbol{F}(\boldsymbol{X}), \qquad \boldsymbol{X} \in \mathbb{R}^N, \tag{3.1}$$

where $\boldsymbol{X}(t)$ is a system state and $\boldsymbol{F}(\boldsymbol{X})$ is a vector field. Suppose the system (3.1) has a periodic orbit $\chi : \boldsymbol{X}_0(t)$ with period T. Let $\phi : \mathbb{R} \times \mathbb{R}^N \to \mathbb{R}^N$ denote the flow induced by Eq. (3.1), i.e., $\phi(t, \boldsymbol{X})$ is the solution of Eq. (3.1) at the time t with the initial condition $\boldsymbol{X}$ at $t = 0$.

The stability of the periodic orbit χ is characterized by the *characteristic multipliers* [103] Λ_i $(i = 1, \cdots, N)$, which are the eigenvalues of the time-T flow linearized around a point $\boldsymbol{X}_0(t_*)$ on the orbit χ (also called the *monodromy matrix*): $\mathbf{M}(\boldsymbol{X}_0(t_*)) = \partial\phi(T, \boldsymbol{X})/\partial\boldsymbol{X}|_{\boldsymbol{X}=\boldsymbol{X}_0(t_*)}$. When the relation $1 = \Lambda_1 > |\Lambda_2| \geq \cdots \geq |\Lambda_N|$ holds, the periodic orbit χ is a stable limit cycle. For simplicity, we hereafter assume that the Floquet multipliers Λ_i are positive, real, and simple. Extension to the case with complex conjugate multipliers can be performed in a parallel way to the analysis of stable equilibria [94, 124]. We consider dynamics of the system in the basin of attraction $\mathcal{B} \subset \mathbb{R}^N$ of the stable limit cycle χ.

The Koopman operator U^t is a linear operator that describes the evolution of a function defined on the phase space, called an observable $f : \mathbb{R}^N \to \mathbb{C}$. It is defined as $U^t f(\boldsymbol{X}) = f \circ \phi(t, \boldsymbol{X})$, where $\circ$ represents composition of functions. The operator U^t has eigenfunctions [134, 135] $s_i(\boldsymbol{X})$ $(i = 1, \cdots, N)$ associated with eigenvalues λ_i $(i = 1, \cdots, N)$, that is,

$$U^t s_i(\boldsymbol{X}) = e^{\lambda_i t} s_i(\boldsymbol{X}), \tag{3.2}$$

where $\lambda_1 = \sqrt{-1}\omega$, $\omega \equiv 2\pi/T$, and $\lambda_i = \log(\Lambda_i)/T$ $(i = 2, \cdots, N)$. The eigenvalues correspond to the *characteristic exponents* of the limit cycle χ [103], hence they reflect the spectral property of the limit-cycling system.

We hereafter assume that the vector field $\boldsymbol{F}$ is twice continuously differentiable so that the continuously differentiable eigenfunctions s_i exist on the whole basin of attraction [135], and we further assume the gradients of s_i are *Lipschitz continuous* on $\mathcal{B}$, which is required for the perturbative analysis. Note that a *non-resonant* analyticity of $\boldsymbol{F}$, which holds generically in practical situations, is sufficient for the Lipschitz continuity, because this assures that s_i is analytic.

Let us introduce amplitudes of the system state $\boldsymbol{X}$ by $r_i(\boldsymbol{X}) \equiv \mathrm{Re}(s_i(\boldsymbol{X}))$ $(i = 2, \cdots, N)$, where $\mathrm{Re}(z)$ is the real part of a complex number z. Because

$$U^{\Delta t} r_i(\boldsymbol{X}) = \mathrm{Re}(s_i(\phi(\Delta t, \boldsymbol{X}))) = e^{\lambda_i \Delta t} r_i(\boldsymbol{X}), \tag{3.3}$$

each r_i obeys

$$\dot{r_i}(\boldsymbol{X}) = \lim_{\Delta t \to 0} \frac{U^{\Delta t} r_i(\boldsymbol{X}) - r_i(\boldsymbol{X})}{\Delta t} = \lambda_i r_i. \tag{3.4}$$

We can also introduce a phase of $\boldsymbol{X}$ by $\theta(\boldsymbol{X}) \equiv \arg(s_1(\boldsymbol{X}))$, where $\arg(z)$ is the argument of z, whose range is defined as the interval $[0, 2\pi)$. Because $\lambda_1 = \sqrt{-1}\omega$, θ obeys

$$\dot{\theta}(\boldsymbol{X}) = \omega. \tag{3.5}$$

This definition of the phase coincides with that of the *asymptotic phase* used in the conventional phase reduction theory [1, 2, 8, 57, 65, 110]. Therefore, level sets of θ provide isochrons. Analogously, isostables are defined as level sets of $|r_i|$. Note that the linear form (3.4,3.5), which is valid in the entire basin of attraction [135], is not necessarily derived by the perturbative power-series approach based on the *Poincaré-Dulac normal form theory* and its extensions [103, 136–139]. Hence we do not assume the non-resonance condition usually required for a complete linearization in the Poincaré-Dulac type scheme. See Sec. 3.2 of Lan and Mezić's work [135] for an example with resonance that can be linearized by using Koopman eigenfunctions including non-analytic (trans)monomials.

Because the sign of r_i is neglected, each isostable is composed of two connected components corresponding to $+r_i$ and $-r_i$. These connected components of isostables, associated with one of the exponents λ_i, foliate the basin of attraction of the limit cycle, and each leaf of this foliation provides a level set of the amplitude associated with the exponent. From Eq. (3.4), we can see that initial conditions on the same isostable

share the same decay rate toward the limit cycle. These phase and amplitudes defined above evolve independently under linear time invariant dynamics and thus provide simple description of the dynamics around the limit cycle.

Here, we note that the amplitudes can also be defined as $\tilde{r}_i(\boldsymbol{X}) \equiv |s_i(\boldsymbol{X})|$, as in the preceding study [94]. However, this definition makes a coordinate transformation $\boldsymbol{X} \mapsto (\theta, \tilde{r}_2, \cdots, \tilde{r}_N)^\dagger$ ($\dagger$ denotes transpose) non-invertible, i.e., its inversion can be multi-valued in some region. The phase-amplitude expression may suffer from this ambiguity, particularly when we apply perturbations to the system. Therefore, we adopt the definition $r_i(\boldsymbol{X}) \equiv \mathrm{Re}(s_i(\boldsymbol{X}))$ in this study.

3.3 Reduction framework and a method to calculate the response functions of the phase and amplitudes

Suppose that perturbation $\epsilon \boldsymbol{p}(t)$, where $\epsilon > 0$ characterizes its magnitude, is introduced to the oscillator (3.1) as

$$\dot{\boldsymbol{X}} = \boldsymbol{F}(\boldsymbol{X}) + \epsilon \boldsymbol{p}(t). \tag{3.6}$$

We denote a coordinate transformation $\boldsymbol{X} \mapsto \Theta$ by $\boldsymbol{X} = \boldsymbol{h}(\Theta)$, where $\Theta = (\theta, r_2, \cdots, r_N)^\dagger$. In this phase-amplitudes coordinate, the perturbed system (3.6) takes the following form:

$$\dot{\theta} = \omega + \epsilon \nabla \theta(\boldsymbol{h}(\Theta)) \cdot \boldsymbol{p}(t), \tag{3.7}$$

$$\dot{r_i} = \lambda_i r_i + \epsilon \nabla r_i(\boldsymbol{h}(\Theta)) \cdot \boldsymbol{p}(t), \quad (i = 2, \cdots, N), \tag{3.8}$$

where ∇ represents gradient and $\cdot$ is a dot product.

Consider a solution $\chi^* : \boldsymbol{X}^*(t)$ of the unperturbed system (3.1) with an initial condition $\boldsymbol{X}^*(0)$ taken arbitrarily in the basin of attraction $\mathcal{B}$, and let $\chi_p^* : \boldsymbol{X}_p^*(t)$ be a solution of the perturbed system (3.6) with the same initial condition $\boldsymbol{X}_p^*(0) = \boldsymbol{X}^*(0)$ as the unperturbed system. As is known in a regular perturbation theory [139–143], we can show by the *Grönwall-Bellman inequality* that the magnitude of the error $||\boldsymbol{X}_p^*(t) - \boldsymbol{X}^*(t)||$, where $||\cdot||$ denotes the Euclidean norm, is bounded by $b\epsilon(e^{at} - 1)/a$, where a and b are positive constants. This means that $\boldsymbol{X}_p^*(t)$ is in a neighborhood of radius ϵ of $\boldsymbol{X}^*(t)$ within a finite time interval of length $O(1)$. We here emphasize that this does not imply the breakdown of the continuous dependence of the solutions on ϵ within a specific, fixed finite time interval (as long as the unperturbed solution

exists on an entire half line, which is the case here). In fact, once we fix an arbitrary large finite length interval $[0, T_{\mathrm{f}}]$, we can consider $\boldsymbol{X}_p^*(t)$ is in a neighborhood of radius ϵ of $\boldsymbol{X}^*(t)$ on this interval by taking appropriately small ϵ, because T_{f} is independent of ϵ, and this is sufficient for our argument. The fact that the length of this interval is $O(1)$ means that the convergence of $\boldsymbol{X}_p^*(t)$ to $\boldsymbol{X}^*(t)$ is *non-uniform* on an ϵ-dependent interval $[0, \epsilon^\beta)$ for any $\beta < 0$, i.e., the limiting passages $t \to \epsilon^\beta$ and $\epsilon \to +0$ cannot be interchanged. This does not affect our analysis in this study, because no asymptotic properties of the perturbed dynamics are discussed. In this interval, we can expand the gradients using the Lipschitz continuity as $\nabla\theta(\boldsymbol{h}(\Theta)) = \nabla\theta(\boldsymbol{X}^*(t)) + O(\epsilon)$ and $\nabla r_i(\boldsymbol{h}(\Theta)) = \nabla r_i(\boldsymbol{X}^*(t)) + O(\epsilon)$ in Eqs. (3.7,3.8). Thus, we can approximate Eqs. (3.7,3.8) as

$$\dot{\theta} = \omega + \epsilon\nabla\theta(\boldsymbol{X}^*(t)) \cdot \boldsymbol{p}(t), \tag{3.9}$$

$$\dot{r_i} = \lambda_i r_i + \epsilon\nabla r_i(\boldsymbol{X}^*(t)) \cdot \boldsymbol{p}(t), \quad (i = 2, \cdots, N), \tag{3.10}$$

by neglecting the terms of order ϵ^2.

These equations are completely decoupled from each other and we can adopt combinations of these N equations (3.9,3.10) as a reduced form of the system dynamics in the close-enough neighborhood of the transient trajectory χ_*. In most cases, the first K equations of (3.9,3.10) for some $K(\ll N)$ are of interest, because they describe relatively persistent, slowly decaying modes. Hereafter, we discuss a method to obtain the reduced K equations. The phase and amplitude response functions to perturbation, $\nabla\theta(\boldsymbol{X}^*(t))$ and $\nabla r_i(\boldsymbol{X}^*(t))$, are the fundamental quantities for the proposed reduction framework.

First, we evaluate the gradients on the periodic orbit χ. Consider an initial condition slightly deviated from the periodic orbit, $\boldsymbol{h}_p \equiv \boldsymbol{h}(\Theta_1) + \delta\boldsymbol{x}$, where we defined $\Theta_1 = (\theta, 0, \cdots, 0)^\dagger$. Then

$$U^T r_i(\boldsymbol{h}_p) = e^{\lambda_i T} r_i(\boldsymbol{h}(\Theta_1) + \delta\boldsymbol{x}). \tag{3.11}$$

Using the time-T flow, we can also express $U^T r_i(\boldsymbol{h}_p)$ as

$$U^T r_i(\boldsymbol{h}_p) = r_i(\boldsymbol{h}(\Theta_1) + \mathbf{M}(\boldsymbol{h}(\Theta_1))\delta\boldsymbol{x} + O(||\delta\boldsymbol{x}||^2)). \tag{3.12}$$

Equating the RHSs of Eqs. (3.11,3.12), Taylor expanding r_i around $\boldsymbol{h}(\Theta_1)$, considering that $r_i(\boldsymbol{h}(\Theta_1)) = 0$ and that the direction of $\delta\boldsymbol{x}$ is arbitrary and taking the limit

$||\delta \boldsymbol{x}|| \to 0$, we can show that

$$\nabla r_i^\dagger(\boldsymbol{h}(\Theta_1))\mathbf{M}(\boldsymbol{h}(\Theta_1)) = e^{\lambda_i T}\nabla r_i^\dagger(\boldsymbol{h}(\Theta_1)). \tag{3.13}$$

Similarly, we obtain

$$\nabla \theta^\dagger(\boldsymbol{h}(\Theta_1))\mathbf{M}(\boldsymbol{h}(\Theta_1)) = \nabla \theta^\dagger(\boldsymbol{h}(\Theta_1)). \tag{3.14}$$

Thus, the gradient vectors of the phase and amplitudes evaluated on χ are left eigenvectors of the monodromy matrix, which are called the adjoint covariant Lyapunov vectors [129–131]. These vectors can be numerically obtained by the *QR-decomposition* based methods [129, 131] or by the *spectral dichotomy* approaches [144, 145].

Next, we seek the equations for the gradients of the phase and amplitudes on the transient trajectory $\chi^* : \boldsymbol{X}^*(t)$. Here, we introduce logarithmic amplitudes $\psi_i(\boldsymbol{X}) \equiv \log(|r_i(\boldsymbol{X})|)$ $(i = 2, \cdots, N)$ in order to make the following treatment of the gradients of the amplitudes simple and parallel with the standard arguments in the conventional phase reduction theory. For convenience of notation, let $\psi_1(\boldsymbol{X}) = \theta(\boldsymbol{X})$. In the following, we evaluate the gradient vectors of ψ_i, whose directions coincide with those of θ and r_i. The gradients $\nabla\theta$ and ∇r_i can be calculated from $\nabla\psi_i$ by rescaling, where the following normalization conditions should be satisfied:

$$\nabla r_i(\boldsymbol{X}^*(t)) \cdot \boldsymbol{F}(\boldsymbol{X}^*(t)) = \lambda_i r_i, \tag{3.15}$$

$$\nabla \theta(\boldsymbol{X}^*(t)) \cdot \boldsymbol{F}(\boldsymbol{X}^*(t)) = \omega. \tag{3.16}$$

These normalization conditions are equivalent to Eqs. (3.4,3.5).

We can derive adjoint equations for the gradients by using the same argument as the conventional derivation of the adjoint equation for the phase response curves, given by Brown et al. [146]. It is well known that an infinitesimal error $\delta\boldsymbol{x}(0)$ introduced at $t = 0$ between two unperturbed solutions $\boldsymbol{X}^*(t) + \delta\boldsymbol{x}(t)$ and $\boldsymbol{X}^*(t)$ satisfies the *variational equation* [103, 136, 139, 140, 142, 143] $\mathrm{d}(\delta\boldsymbol{x}(t))/\mathrm{d}t = \mathrm{D}\boldsymbol{F}(\boldsymbol{X}^*(t))\delta\boldsymbol{x}(t)$. Because each logarithmic amplitude ψ_i increases constantly as $\dot{\psi}_i(\boldsymbol{X}(t)) = \nabla\psi_i(\boldsymbol{X}(t)) \cdot \dot{\boldsymbol{X}}(t) = \lambda_i$ in the absence of perturbation, the error in the logarithmic amplitude coordinate $\psi_i(\boldsymbol{X}^*(t) + \delta\boldsymbol{x}(t)) - \psi_i(\boldsymbol{X}^*(t)) = \nabla\psi_i(\boldsymbol{X}^*(t)) \cdot \delta\boldsymbol{x}(t)$ should be independent of time,

i.e., $\mathrm{d}(\nabla\psi_i(\boldsymbol{X}^*(t))\cdot\delta\boldsymbol{x}(t))/\mathrm{d}t = 0$. This yields

$$\begin{aligned}\frac{\mathrm{d}\nabla\psi_i(\boldsymbol{X}^*(t))}{\mathrm{d}t}\cdot\delta\boldsymbol{x}(t) &= -\nabla\psi_i(\boldsymbol{X}^*(t))\cdot\frac{\mathrm{d}(\delta\boldsymbol{x}(t))}{\mathrm{d}t}\\ &= -\nabla\psi_i(\boldsymbol{X}^*(t))\cdot\mathrm{D}\boldsymbol{F}(\boldsymbol{X}^*(t))\delta\boldsymbol{x}(t)\\ &= -\mathrm{D}\boldsymbol{F}^\dagger(\boldsymbol{X}^*(t))\nabla\psi_i(\boldsymbol{X}^*(t))\cdot\delta\boldsymbol{x}(t). \end{aligned} \tag{3.17}$$

Here we used the variational equation and the definition of the adjoint matrix. We can take N linearly independent initial errors $\delta\boldsymbol{x}_i(0) = \epsilon'\boldsymbol{e}_i$, where $0 < \epsilon' \ll 1$ and $\boldsymbol{e}_i$ is the ith unit vector and define the *fundamental solution matrix* $\mathbf{L}(t)$ of the variational equation as $\mathbf{L}(t) = (\delta\boldsymbol{x}_1(t), \delta\boldsymbol{x}_2(t), \cdots, \delta\boldsymbol{x}_N(t))$. The sign of the determinant of the fundamental solution matrix, called the *Wronskian*, is time-invariant due to *Liouville's trace formula* [127, 128, 138, 140, 142, 143]. Because $\det(\mathbf{L}(0)) = (\epsilon')^N > 0$, we obtain $\det(\mathbf{L}(t)) > 0$ for all t, and thus the fundamental solution matrix is always invertible. Consider a matrix form of the Eq. (3.17), $(\mathrm{d}(\nabla\psi_i(\boldsymbol{X}^*(t))/\mathrm{d}t)\mathbf{L}(t) = -\mathrm{D}\boldsymbol{F}^\dagger(\boldsymbol{X}^*(t))\nabla\psi_i(\boldsymbol{X}^*(t))\mathbf{L}(t)$. We can eliminate $\mathbf{L}(t)$ by multiplying its inverse from the right side on both sides of this equation. Therefore,

$$\frac{\mathrm{d}\nabla\psi_i(\boldsymbol{X}^*(t))}{\mathrm{d}t} = -\mathrm{D}\boldsymbol{F}^\dagger(\boldsymbol{X}^*(t))\nabla\psi_i(\boldsymbol{X}^*(t)) \tag{3.18}$$

should hold. Note that this equation should be solved with an appropriate end condition. Here, we can approximately take the end condition of Eq. (3.18) as $\nabla\psi_i(\boldsymbol{X}^*(\tau)) \parallel \nabla r_i(\boldsymbol{h}(\Theta_1))|_{\theta=\theta_*}$ for some $t = \tau$ and $\theta = \theta_*$, because the gradient field $\nabla r_i(\boldsymbol{X})$ is continuous and the transient trajectory eventually converges to the limit cycle. The adjoint tangent *propagator* $\mathcal{G}(t_1, t_2) \equiv \mathbf{N}(t_2)\mathbf{N}^{-1}(t_1)$, where $\mathbf{N}(t)$ is a fundamental solution matrix of the linear system given by Eq. (3.18), maps $\nabla\psi_i(\boldsymbol{X}^*(t_1))$ to $\nabla\psi_i(\boldsymbol{X}^*(t_2))$. Thus, $\nabla\theta(\boldsymbol{X}^*(t_2)) \parallel \mathcal{G}(t_1, t_2)\nabla\theta(\boldsymbol{X}^*(t_1))$ and $\nabla r_i(\boldsymbol{X}^*(t_2)) \parallel \mathcal{G}(t_1, t_2)\nabla r_i(\boldsymbol{X}^*(t_1))$ hold. Therefore, the gradient vectors of the phase and amplitudes are covariant with respect to the action of the propagator $\mathcal{G}$ and they can be interpreted as an extension of the adjoint covariant Lyapunov vectors to transient regimes (note that the adjoint covariant Lyapunov vectors evaluated on the limit cycle, given by Eqs. (3.13,3.14), are covariant w.r.t. the action of the adjoint of the monodromy matrix, which is the one period (time-T) propagator).

In the numerical estimation of $\nabla\theta$ (or $\nabla\psi_1$), a standard method is to integrate the adjoint equation backward in time, while renormalizing $\nabla\theta$ occasionally so that the normalization condition (3.16) is satisfied [8]. This is because $\nabla\theta$ corresponds to the neutrally stable component ($\mathrm{Re}(\lambda_1) = 0$) while other components have negative growth

rates ($\lambda_{2,\dots,N} < 0$). However, in the present case, naive backward integration does not provide correct results for the amplitudes, $\psi_{2,\dots,N}$, because vector components caused by numerical errors in the relatively (backward-in-time) unstable covariant subspaces accumulate. Therefore, we have to develop a method to subtract them off. Note that the standard QR-decomposition based methods [129, 131] to obtain the covariant subspace require the ergodicity of the underlying dynamical process, hence they cannot be directly applied to the process far from attractors, and that the spectral dichotomy techniques [144, 145] to evaluate them may not work well near the left boundary of the time evolution (See Secs. 2.6 and Sec. 2.7 of Hüls's work [145]).

To develop a numerical method, we introduce dual vectors $\boldsymbol{\gamma}_i$ of $\nabla\psi_i$ that are bi-orthogonal to $\nabla\psi_j$ as

$$\boldsymbol{\gamma}_i(\boldsymbol{X}^*(t)) \cdot \nabla\psi_j(\boldsymbol{X}^*(t)) = \delta_{ij}, \tag{3.19}$$

where δ_{ij} is the Kronecker delta. By using $\boldsymbol{\gamma}_i(\boldsymbol{X}^*(t))$, we can subtract the vector component in the covariant subspace $\nabla\psi_i(\boldsymbol{X}^*(t))$ from the solution $\boldsymbol{z}(t)$ of Eq. (3.18), which is given by projecting $\boldsymbol{z}(t)$ onto this subspace as

$$(\boldsymbol{\gamma}_i(\boldsymbol{X}^*(t)) \cdot \boldsymbol{z}(t))\nabla\psi_i(\boldsymbol{X}^*(t)). \tag{3.20}$$

Differentiating Eq. (3.19) by t, we obtain $(\dot{\boldsymbol{\gamma}}_i(\boldsymbol{X}^*(t)) - D\boldsymbol{F}(\boldsymbol{X}^*(t))\boldsymbol{\gamma}_i(\boldsymbol{X}^*(t)))$
$\cdot \nabla\psi_j(\boldsymbol{X}^*(t)) = 0$. The sign of the Wronskian of Eq. (3.18) is time-invariant due to Liouville's trace formula. By using this fact and linear independence of the left eigenvectors of the monodromy matrix, we can show linear independence of $\{\nabla\psi_i(\boldsymbol{X})\}_{i=1}^N$ for every point $\boldsymbol{X}$ in the whole basin of attraction $\mathcal{B}$. Thus, we obtain

$$\dot{\boldsymbol{\gamma}}_i(\boldsymbol{X}^*(t)) = D\boldsymbol{F}(\boldsymbol{X}^*(t))\boldsymbol{\gamma}_i(\boldsymbol{X}^*(t)). \tag{3.21}$$

The vectors $\boldsymbol{\gamma}_i$ are covariant w.r.t. the action of the propagator $\mathcal{F}(= (\mathcal{G}^\dagger)^{-1})$ of the linear system (3.21), hence they can be seen as covariant Lyapunov vectors extended to transient regimes. The relative stability relation of covariant subspace of Eq. (3.21) forward-in-time coincides with that of Eq. (3.18) backward-in-time. In order to subtract unstable components using the projection (3.20), the system (3.21) should be solved forward-in-time with an approximate initial condition $\boldsymbol{\gamma}_i(\boldsymbol{X}^*(0))$. The vectors $\{\nabla\psi_i(\boldsymbol{X}^*(0))\}_{i=1}^N$ can be approximated by direct numerical simulation of the dynamics, using the *Fourier averages* and the *generalized Laplace averages* [91, 134] (See

Appendix J for details). Then, $\boldsymbol{\gamma}_i(\boldsymbol{X}^*(0))$ can be obtained by using the bi-orthogonality relation (3.19).

Now, we introduce a bi-orthogonalization method to obtain the response functions of the phase and amplitudes up to the Kth unstable mode. The procedure is as follows: (a) evaluate the adjoint Lyapunov vectors on the limit cycle χ and the characteristic exponents, (b) calculate $\{\boldsymbol{\gamma}_i(\boldsymbol{X}^*(0))\}_{i=1}^K$ from $\{\nabla\psi_i(\boldsymbol{X}^*(0))\}_{i=1}^N$ obtained by direct numerical simulation using the bi-orthogonality relation (3.19), (c) obtain $\nabla\psi_1(\boldsymbol{X}^*(t))$ by backward integration of Eq. (3.18), (d) obtain $\boldsymbol{\gamma}_1(\boldsymbol{X}^*(t))$ by forward integration of Eq. (3.21), (e) obtain $\nabla\psi_2(\boldsymbol{X}^*(t))$ by backward integration of Eq. (3.18) while subtracting relatively unstable mode $\nabla\psi_1(\boldsymbol{X}^*(t))$ by the projection (3.20), (f) obtain $\boldsymbol{\gamma}_2(\boldsymbol{X}^*(t))$ by the forward integration of Eq. (3.21) while subtracting relatively unstable mode $\boldsymbol{\gamma}_1(\boldsymbol{X}^*(t))$ by the projection

$$(\nabla\psi_i(\boldsymbol{X}^*(t))\cdot\boldsymbol{y}(t))\boldsymbol{\gamma}_i(\boldsymbol{X}^*(t)), \tag{3.22}$$

where $\boldsymbol{y}(t)$ is a solution of Eq. (3.21), (g) perform (e) and (f) consecutively to obtain $\{\nabla\psi_i(\boldsymbol{X}^*(t))\}_{i=3}^K$ and $\{\boldsymbol{\gamma}_i(\boldsymbol{X}^*(t))\}_{i=3}^K$ (note that all relatively unstable modes should be subtracted during integration), (h) obtain $\nabla\theta$ and ∇r_i $(i=2,\cdots,K)$ using the normalization conditions (3.15,3.16), where $r_i(\boldsymbol{X}^*(t))$ on the transient orbit χ^* is evaluated using Eq. (3.4) with the initial condition $r_i(\boldsymbol{X}^*(0))$, which is calculated in (b) by the direct numerical simulation.

This method has a significant computational advantages in evaluating the response functions. To calculate response functions $\{\nabla\psi_i\}_{i=1}^K$ at m points on the transient orbit χ^*, it is necessary to repeat long-time evolution $mK(N+1)$ times if we evaluate them directly by the direct numerical simulation. In contrast, we need only $K(N+1)+2K$ times long-time evolution in the proposed bi-orthogonalization method.

3.4 Examples

As an example, we analyze the Goodwin model, a minimal chemical kinetic model of an oscillatory genetic circuit [147, 148]. The Goodwin model has a three-dimensional state $\boldsymbol{X}=(x,y,z)^\dagger\in\mathbb{R}^3$. The state variables x, y, and z can be interpreted as concentrations of a given clock mRNA, the corresponding protein, and a transcriptional

inhibitor, respectively. We use a simple dimensionless form of the Goodwin model [149],

$$\begin{aligned}\dot{x} &= \frac{\alpha}{1+z^n} - x,\\ \dot{y} &= x - y,\\ \dot{z} &= y - z.\end{aligned}$$

The parameters are set as $\alpha = 1.8$ and $n = 20$. Figure 3.1 shows the stable periodic solution of the model. The period and Lyapunov exponents are estimated as $T = 3.63$, $\lambda_2 = -0.0766$, and $\lambda_3 = -2.92$. We consider a transient solution $\boldsymbol{X}^*(t)$ with an initial condition $\boldsymbol{X}^*(0) = (1.30, 0.900, 0.800)^\dagger$. Figure 3.1 shows the transient solution. We set the end time $\tau = 63.0$ for the backward integration in the following calculation.

In Fig. 3.2, the phase response function $\nabla\theta(\boldsymbol{X}^*(t))$ obtained by the backward integration of the adjoint equation (3.18) is compared with the result of the direct numerical simulations. The results agree well, hence, along this transient solution $\boldsymbol{X}^*(t)$, $\nabla\theta(\boldsymbol{X}^*(t))$ can always be considered as the most unstable covariant subspace.

Figure 3.3 shows the amplitude response functions $\nabla r_2(\boldsymbol{X}^*(t))$, which is obtained by the proposed bi-orthogonalization method, by naive backward integration method, and by direct numerical simulations. All results are normalized using the condition (3.15). Note here that, in the close-enough neighborhood of the limit cycle orbit χ, the vectors $\nabla r_2(\boldsymbol{X}^*(t))$ and $\boldsymbol{F}(\boldsymbol{X}^*(t))$ are nearly normal. Hence, the normalization procedure using (3.15) is very sensitive to tiny change in their directions. Therefore, not only the normalization condition (3.15) but the duality relation (3.19) must be carefully imposed on the results of the direct numerical simulation in order to make a reasonable comparison with those of the other methods. The results obtained by the naive backward integration considerably deviates from those obtained by direct numerical simulations, while those obtained by the proposed bi-orthogonalization method are in good agreement.

Next, we illustrate the utility of the reduced amplitude equation (3.10) by estimating the optimal injection timing of weak external input to suppress the most persistent component r_2 of the amplitudes. We apply a transient control input $\epsilon\boldsymbol{p}(t)$ of a fixed waveform $\boldsymbol{w}$ and a fixed duration τ_*, i.e., $\boldsymbol{p}(t) = \boldsymbol{w}(t-s)$ where $\boldsymbol{w}(\cdot)$ is nonzero only on $[0, \tau_*]$ and the time s determines the injection timing of the input. In the spirit of Mauroy's preceding study [122], we introduce a finite-horizon optimal control problem of minimizing the amplitude $|r_2|$ at a given time T_e. This control problem can be

formulated as follows: find the injection timing s_* such that

$$s_* = \mathrm{argmin}_{s\in\mathcal{I}_\sigma}|r_2(\boldsymbol{X}_p^*(T_e))|, \tag{3.23}$$

where $\mathcal{I}_\sigma \equiv [0, T_e - \tau_*]$ and $\boldsymbol{X}_p^*(t)$ is the solution of Eq. (3.6). When the magnitude of the input ϵ is sufficiently small, the evolution of the amplitude r_2 is approximated by the reduced equation (3.10). Then, using an analytical solution of the linear one-dimensional non-homogeneous differential equation (3.10) of r_2, the optimal control problem (3.23) can be approximated to the problem of finding s_* such that

$$\mathrm{sgn}(r_2(\boldsymbol{X}^*(0)))\int_0^{T_e}\boldsymbol{p}(t)\cdot\nabla r_2(\boldsymbol{X}^*(t))e^{\lambda_2(T_e-t)}\mathrm{d}t \tag{3.24}$$

is minimized.

Figure 3.4 shows the effect of the control input on the amplitude $r_2(\boldsymbol{X}_p^*(T_e))$ at time $T_e = 5$. The control input is assumed as $\boldsymbol{w}(t) = (0, 0, -1)^\dagger$ and $\tau_* = 0.25$. The results obtained by the analytical solution of the reduced amplitude equation (3.10) is compared with the result of direct numerical simulations, showing good agreement for sufficiently weak input ($\epsilon = 0.01, 0.1$). This verifies the validity of the approximate amplitude equation in the present situation. Thus, the optimal injection timing of sufficiently weak input can be theoretically predicted using the formula (3.24), because it is essentially equivalent to solving the approximate amplitude equation (3.10) directly. In this case, the initial value of the amplitude is negative, i.e., $r_2(\boldsymbol{X}^*(0)) < 0$. Hence, the optimal injection timing s_* of the sufficiently weak input can be estimated by finding the maximum of the waveform in Fig. 3.4, which gives $s_* = 2.08$ in this particular case. Finally, we note that when the magnitude becomes large ($\epsilon = 1.0$), the approximation (3.10) fails and then the results considerably deviate from each other.

3.5 Summary

We formulated a phase-amplitude reduction framework for stable limit-cycling systems, which can be applied to transient dynamical regimes far from attractors in high-dimensional systems. We also developed a bi-orthogonalization method for numerical estimation of the response function of the phase and amplitudes, which provides accurate phase-amplitude response functions. As an application, we illustrated that the response functions accurately predicts the optimal injection timing of external input which efficiently suppress deviations from attractors. The proposed theory would be

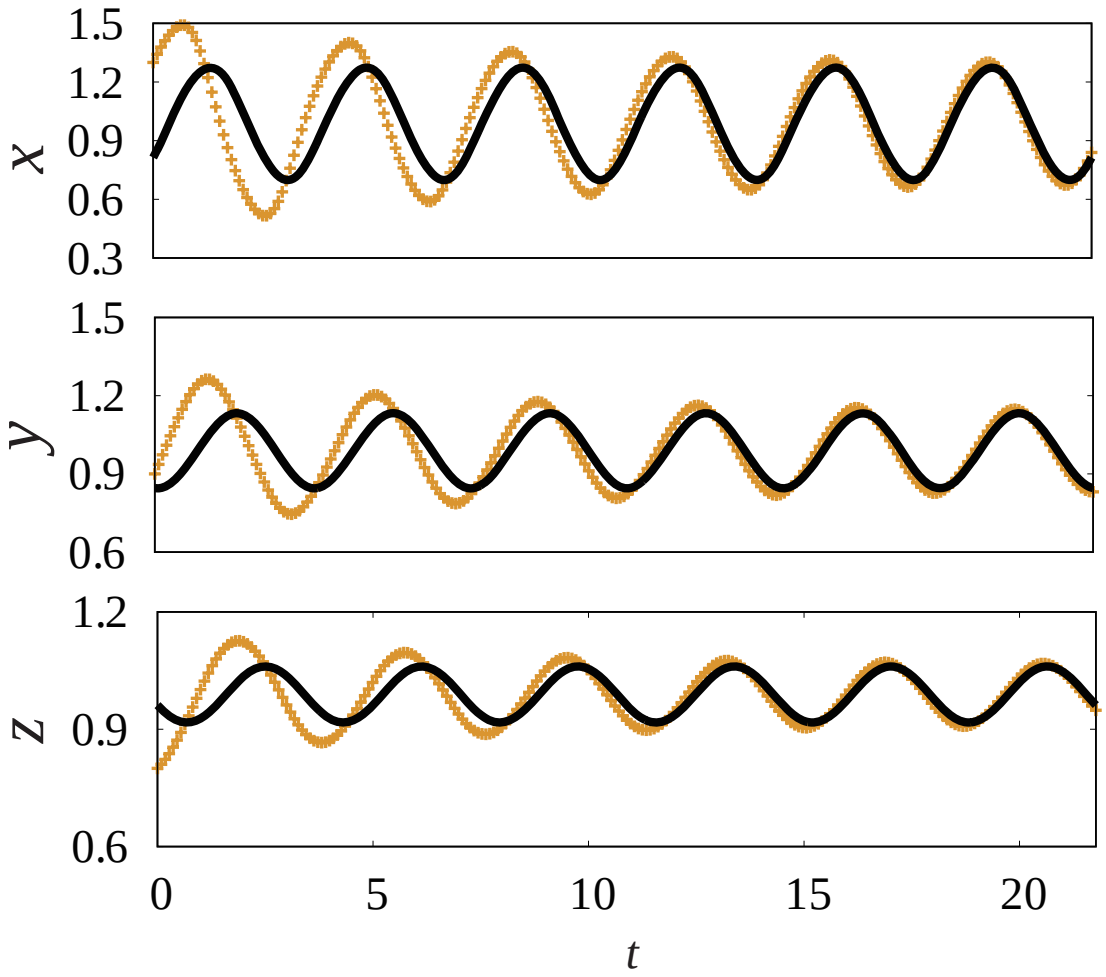

Fig. 3.1 The Goodwin model. The stable periodic solution of the model (lines) and the transient solution $\boldsymbol{X}^*(t)$ (plus signs).

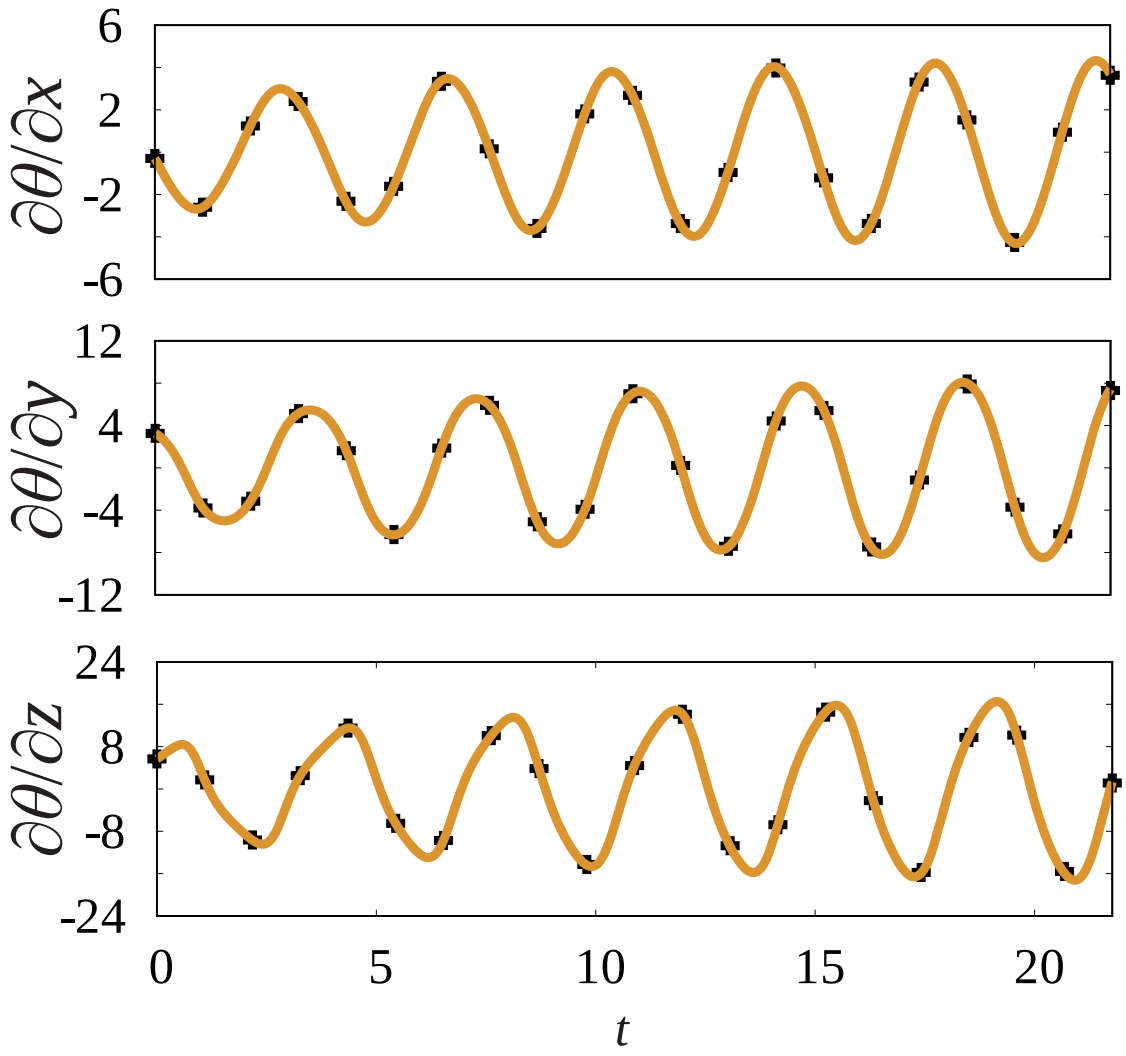

Fig. 3.2 Phase response function of the Goodwin model. Three components of the phase response function $\nabla\theta(\boldsymbol{X}^*(t))$ obtained by the direct numerical simulation (plus signs) and by the backward integration of the adjoint equation (lines).

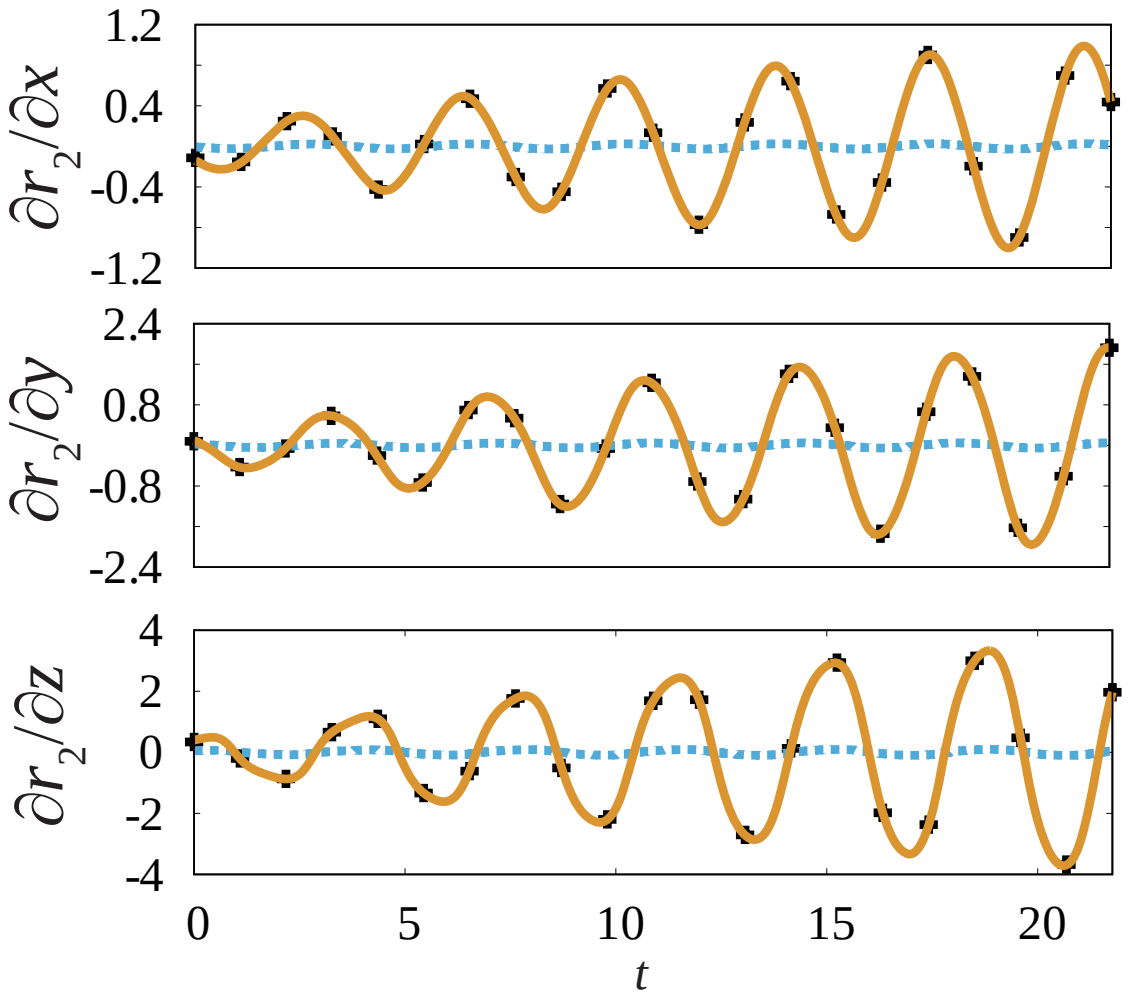

Fig. 3.3 Amplitude response function of the Goodwin model. Three components of the second amplitude response function $\nabla r_2(\boldsymbol{X}^*(t))$ obtained by the direct numerical simulation (plus signs), the naive backward integration method (blue dashed lines) and by the proposed bi-orthogonalization method (yellow lines). They are all normalized using the condition (3.15), and the results obtained by the direct numerical simulation are appropriately bi-orthogonalized to satisfy the duality relation (3.19).

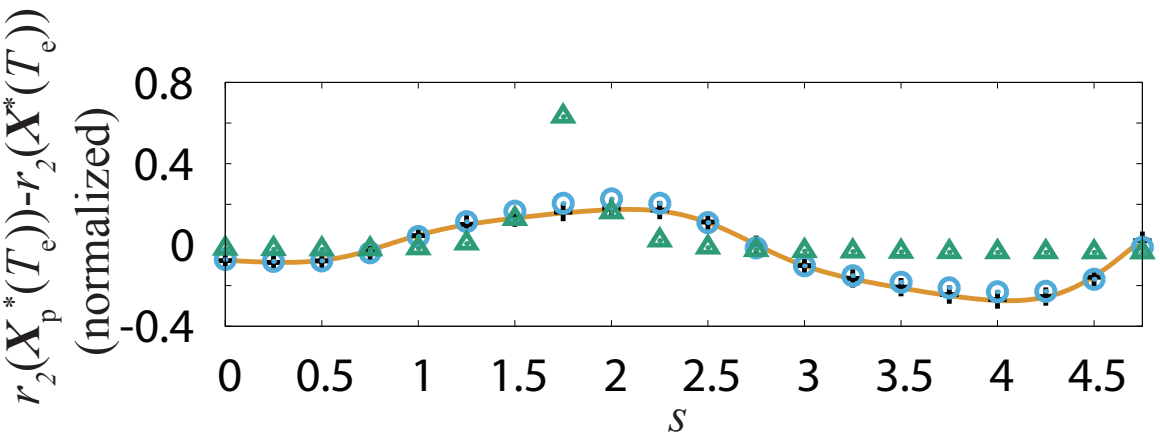

Fig. 3.4 Optimal control problem for the Goodwin model. Effect of the control input on the amplitude at a given time $r_2(\boldsymbol{X}_p^*(T_e))$, obtained by an analytical solution of the reduced amplitude equation (line) and by the direct numerical simulations for 20 different injection timings for three different magnitudes of the input: $\epsilon = 0.01$ (black plus signs), $\epsilon = 0.1$ (blue circles) and $\epsilon = 1.0$ (green triangles). The results are normalized so that the l_2 norms of the waveforms evaluated using the 20 discrete time points are the same.

useful in analyzing and controlling response properties of high-dimensional rhythmic systems.

Chapter 4

Conclusion

In Chapter. 2, we formulated a phase reduction theory for a general class of hybrid limit-cycle oscillators and derived the adjoint equation for the phase sensitivity function. The proposed theory provides precise phase sensitivity functions and the derived phase equation accurately predicts the injection locking properties of hybrid oscillators. We illustrated synchronization properties characteristic to hybrid oscillators, such as ultrafast entrainment to periodic signal and negative logarithmic scaling at the synchronization transition, and explained them by using the reduced phase equation with discontinuous phase sensitivity functions.

The phase reduction theory developed in this study would serve as a powerful tool for investigating synchronization phenomena in complex systems whose smooth models are unavailable or intractable and for finding various applications in controlling distributed interacting nonlinear oscillators [80–84].

In Chapter. 3, we formulated a phase-amplitude reduction theory for stable limit-cycle oscillators, which can be applied to high-dimensional systems and transient regimes far from attractors. We also developed a convenient biorthogonalization method for the response function of the phase and amplitudes. It is illustrated that the proposed method provides precise phase-amplitude response functions and that the response functions accurately predicts the optimal injection timing of external forcing signals which efficiently suppress deviations from attractors.

Future directions

This thesis contributes to the dimension reduction theories in a fundamental way by extending classes of rhythmic behavior that can be studied systematically in these

kinds of frameworks. The proposed theories in this thesis may find fruitful applications in various situations where nonsmoothness or transients arise.

Based on the phase reduction theory for hybrid nonlinear oscillators, studies of coupled homogeneous rhythmic elements functioning nonsmoothly such as networked distributive sensors and a relatively homogeneous population of neurons in a specific domains of the brain such as the hippocampus may be done in a similar way as in the conventional smooth case. Moreover, it may make studies of interacting heterogeneous structures such as the neural system and the musculo-skeletal system somewhat tractable by simplifying the system's description. This kind of study may provide a unified and integrated view of the interacting heterogeneous structures where each of the subsystems is studied in a corresponding specific discipline and facilitate intriguing interdisciplinary research.

Evaluation of the amplitude response properties of transient dynamics in real-world systems might make our mind open to novel perspectives on the notion of adaptivity. A system can make use of the very amplitude-sensitive region to suppress deviations from the desired behavior efficiently and to adjust its behavior rapidly and adaptively to change in environment by escaping from an attractor. Though the physical and biological relevance is unclear, this might be a possible mechanism for adaptive behavior of animals and can be a design principle for intelligent systems. Thus, the consideration of the amplitude degrees of freedom can provide an insight into understanding the adaptivity.

References

[1] A. T. Winfree. *The Geometry of Biological Time*. Springer, New York, 2001.

[2] Y. Kuramoto. *Chemical Oscillations, Waves, and Turbulence*. Springer, Berlin, 1984.

[3] M. C. Cross and P. C. Hohenberg. *Reviews of Modern Physics*, 65:851, 1993.

[4] A. Pikovsky, M. Rosenblum, and J. Kurths. *Synchronization: A Universal Concept in Nonlinear Sciences*. Cambridge university press, Cambridge, 2003.

[5] A. S. Mikhailov and K. Showalter. *Physics Reports*, 425:79, 2006.

[6] I. Z. Kiss, C. G. Rusin, H. Kori, and J. L. Hudson. *Science*, 316:1886, 2007.

[7] P. A. Tass. *Phase Resetting in Medicine and Biology: Stochastic Modelling and Data Analysis*. Springer, Berlin, 2007.

[8] G. B. Ermentrout and D. H. Terman. *Mathematical Foundations of Neuroscience*. Springer, New York, 2010.

[9] N. W. Schultheiss, A. A. Prinz, and R. J. Butera, editors. *Phase Response Curves Neuroscience: Theory, Experiment, and Analysis*. Springer, New York, 2011.

[10] F. Dörfler, M. Chertkov, and F. Bullo. *Proceedings of the National Academy of Sciences*, 110:2005, 2013.

[11] C. Huygens. Letter to de Sluse. In *Oeuveres Completes de Christian Huygens*. Societe Hollandaise Des Sciences, La Haye, 1893.

[12] B. van der Pol. *The London, Edinburgh, and Dublin Philosophical Magazine and Journal of Science*, 3:65, 1927.

[13] B. van der Pol and J. van der Mark. *The London, Edinburgh, and Dublin Philosophical Magazine and Journal of Science*, 6:763, 1928.

[14] J. W. S. B. Rayleigh. *The Theory of Sound*. Macmillan, London, 1894.

[15] N. Wiener. *Cybernetics or Control and Communication in the Animal and the Machine*. MIT Press, Cambridge, 1961.

[16] N. Wiener. *Nonlinear Problems in Random Theory*. MIT Press, Cambridge, 1966.

[17] A. T. Winfree. *Journal of Theoretical Biology*, 16:15, 1967.

[18] Y. Kuramoto. Self-entrainment of a population of coupled non-linear oscillators. In *International Symposium on Mathematical Problems in Theoretical Physics*, pages 420–422. Springer, Berlin, 1975.

[19] H. Daido. *Progress of Theoretical Physics*, 88:1213, 1992.

[20] H. Daido. *Progress of Theoretical Physics*, 89:929, 1993.

[21] J. D. Crawford and K. T. R. Davies. *Physica D: Nonlinear Phenomena*, 125:1, 1999.

[22] S. H. Strogatz. *Physica D: Nonlinear Phenomena*, 143:1, 2000.

[23] S. H. Strogatz. *Nature*, 410:268, 2001.

[24] A. Arenas, A. Díaz-Guilera, J. Kurths, Y. Moreno, and C. Zhou. *Physics Reports*, 469:93, 2008.

[25] F. Dörfler and F. Bullo. *Automatica*, 50:1539, 2014.

[26] G. S. Medvedev. *SIAM Journal on Mathematical Analysis*, 46:2743, 2014.

[27] D. Kaliuzhnyi-Verbovetskyi and G. S. Medvedev. The semilinear heat equation on sparse random graphs. *arXiv:1605.02114*, 2016.

[28] H. Chiba and G. S. Medvedev. The mean field analysis for the kuramoto model on graphs i. the mean field equation and transition point formulas. *arXiv:1612.06493*, 2016.

[29] S. Watanabe and S. H. Strogatz. *Physica D: Nonlinear Phenomena*, 74:197, 1994.

[30] E. Ott and T. M. Antonsen. *Chaos: An Interdisciplinary Journal of Nonlinear Science*, 19:023117, 2009.

[31] T. Harada, H-A. Tanaka, M. J. Hankins, and I. Z. Kiss. *Physical Review Letters*, 105:088301, 2010.

[32] A. Zlotnik, Y. Chen, I. Z. Kiss, H-A. Tanaka, and J-S. Li. *Physical Review Letters*, 111:024102, 2013.

[33] A. Zlotnik, R. Nagao, I. Z. Kiss, and J-S. Li. *Nature Communications*, 7:10788, 2016.

[34] B. Kralemann, L. Cimponeriu, M. Rosenblum, A. Pikovsky, and R. Mrowka. *Physical Review E*, 77:066205, 2008.

[35] B. Kralemann, M. Frühwirth, A. Pikovsky, M. Rosenblum, T. Kenner, J. Schaefer, and M. Moser. *Nature Communications*, 4:2418, 2013.

[36] I. Tokuda, S. Jain, I. Z. Kiss, and J. L. Hudson. *Physical Review Letters*, 99:064101, 2007.

[37] T. Stankovski, A. Duggento, P. V. E. McClintock, and A. Stefanovska. *Physical Review Letters*, 109:024101, 2012.

[38] I. S. Aranson and L. Kramer. *Reviews of Modern Physics*, 74:99, 2002.

[39] H. Nakao and A. S. Mikhailov. *Physical Review E*, 79:036214, 2009.

[40] A. Koseska, E. Volkov, and J. Kurths. *Physics Reports*, 531:173, 2013.

[41] M. J. Panaggio and D. M. Abrams. *Nonlinearity*, 28:R67, 2015.

[42] J-N. Teramae and D. Tanaka. *Physical Review Letters*, 93:204103, 2004.

[43] H. Nakao, K. Arai, and Y. Kawamura. *Physical Review Letters*, 98:184101, 2007.

[44] K. H. Nagai and H. Kori. *Physical Review E*, 81:065202, 2010.

[45] Y. M. Lai and M. A. Porter. *Physical Review E*, 88:012905, 2013.

[46] H. Haken. *Synergetics: Introduction and Advanced Topics*. Springer, Berlin, 2004.

[47] K. Yoshimura and K. Arai. *Physical Review Letters*, 101:154101, 2008.

[48] J-N. Teramae, H. Nakao, and G. B. Ermentrout. *Physical Review Letters*, 102:194102, 2009.

[49] D. S. Goldobin, J-N. Teramae, H. Nakao, and G. B. Ermentrout. *Physical Review Letters*, 105:154101, 2010.

[50] V. Novičenko and K. Pyragas. *Physica D: Nonlinear Phenomena*, 241:1090, 2012.

[51] K. Kotani, I. Yamaguchi, Y. Ogawa, Y. Jimbo, H. Nakao, and G. B. Ermentrout. *Physical Review Letters*, 109:044101, 2012.

[52] Y. Kawamura, H. Nakao, K. Arai, H. Kori, and Y. Kuramoto. *Physical Review Letters*, 101:024101, 2008.

[53] H. Kori, Y. Kawamura, H. Nakao, K. Arai, and Y. Kuramoto. *Physical Review E*, 80:036207, 2009.

[54] Y. Kawamura and H. Nakao. *Chaos: An Interdisciplinary Journal of Nonlinear Science*, 23:043129, 2013.

[55] H. Nakao, T. Yanagita, and Y. Kawamura. *Physical Review X*, 4:021032, 2014.

[56] W. Kurebayashi, S. Shirasaka, and H. Nakao. *Physical Review Letters*, 111:214101, 2013.

[57] F. C. Hoppensteadt and E. M. Izhikevich. *Weakly Connected Neural Networks*. Springer, New York, 2012.

[58] S. Coombes, R. Thul, and K. C. A. Wedgwood. *Physica D: Nonlinear Phenomena*, 241:2042, 2012.

[59] E. M. Izhikevich. *SIAM Journal on Applied Mathematics*, 60:1789, 2000.

[60] Y. Park. Infinitesimal phase response curves for piecewise smooth dynamical systems. Master's thesis, Case Western Reserve University, Cleveland, 2013.

[61] O. Makarenkov and J. S. W. Lamb. *Physica D: Nonlinear Phenomena*, 241:1826, 2012.

[62] M. Bernardo, C. Budd, A. R. Champneys, and P. Kowalczyk. *Piecewise-Smooth Dynamical Systems: Theory and Applications*. Springer, London, 2008.

[63] K. C. A. Wedgwood, K. K. Lin, R. Thul, and S. Coombes. *The Journal of Mathematical Neuroscience*, 3:2, 2013.

[64] A. Mauroy, B. Rhoads, J. Moehlis, and I. Mezić. *SIAM Journal on Applied Dynamical Systems*, 13:306, 2014.

[65] P. Ashwin, S. Coombes, and R. Nicks. *The Journal of Mathematical Neuroscience*, 6:2, 2016.

[66] P. C. Matthews, R. E. Mirollo, and S. H. Strogatz. *Physica D: Nonlinear Phenomena*, 52:293, 1991.

[67] I. S. Aranson and L. S. Tsimring. *Reviews of Modern Physics*, 78:641, 2006.

[68] K. B. Wolf and G. Krotzsch. *European Journal of Physics*, 16:14, 1995.

[69] K. Aihara and H. Suzuki. *Philosophical Transactions of the Royal Society of London A: Mathematical, Physical and Engineering Sciences*, 368:4893, 2010.

[70] P. Holmes, R. J. Full, D. Koditschek, and J. Guckenheimer. *SIAM Review*, 48:207, 2006.

[71] J. H. G. Macdonald. *Proceedings of the Royal Society of London A: Mathematical, Physical and Engineering Sciences*, page 1055, 2008.

[72] A. A. Andronov, A. A. Vitt, and S. E. Khaikin. *Theory of Oscillators*. Dover Publications, New York, 2011.

[73] D. Helbing. *New Journal of Physics*, 5:90, 2003.

[74] J. P. Hespanha, S. Bohacek, K. Obraczka, and J. Lee. Hybrid modeling of tcp congestion control. In *Proceedings of the 4th International Workshop on Hybrid Systems: Computation and Control*, pages 291–304. Springer, 2001.

[75] Y. Susuki, Y. Takatsuji, and T. Hikihara. *IEICE Transactions on Fundamentals of Electronics, Communications and Computer Sciences*, 92:871, 2009.

[76] T. McGeer. *The International Journal of Robotics Research*, 9:62, 1990.

[77] K. Zimmermann and I. Zeidis. *Journal of Theoretical and Applied Mechanics*, 45:179, 2007.

[78] S. Banerjee and G. C. Verghese. *Nonlinear Phenomena in Power Electronics: Bifurcations, Chaos, Control, and Applications*. Wiley-IEEE press, New York, 2001.

[79] A. Jenkins. *Physics Reports*, 525:167, 2013.

[80] A. J. Ijspeert. *Neural Networks*, 21:642, 2008.

[81] S. H. Strogatz, D. M. Abrams, A. McRobie, B. Eckhardt, and E. Ott. *Nature*, 438:43, 2005.

[82] J. A. Dunnmon, S. C. Stanton, B. P. Mann, and E. H. Dowell. *Journal of Fluids and Structures*, 27:1182, 2011.

[83] S. Moss, A. Barry, I. Powlesland, S. Galea, and G. P. Carman. *Applied Physics Letters*, 97:234101, 2010.

[84] H-A. Tanaka, H. Nakao, and K. Shinohara. *IEICE Electronics Express*, 6:1562, 2009.

[85] J. K. Hale. *Ordinary Differential Equations*. Dover Publications, New York, 2009.

[86] J. Guckenheimer. *Journal of Mathematical Biology*, 1:259, 1975.

[87] I. G. Malkin. *The Methods of Lyapunov and Poincaré in the Theory of Non-Linear Oscillations*. Gostexizdat, Moscow, 1949.

[88] K. M. Shaw, Y. Park, H. J. Chiel, and P. J. Thomas. *SIAM Journal on Applied Dynamical Systems*, 11:350, 2012.

[89] A. Demir, C. Gu, and J. Roychowdhury. Phase equations for quasi-periodic oscillators. In *2010 IEEE/ACM International Conference on Computer-Aided Design (ICCAD)*, pages 292–297. IEEE, New Jersey, 2010.

[90] Y. Kawamura and H. Nakao. *Physica D: Nonlinear Phenomena*, 295:11, 2015.

[91] A. Mauroy and I. Mezić. *Chaos: An Interdisciplinary Journal of Nonlinear Science*, 22:033112, 2012.

[92] N. Ichinose, K. Aihara, and K. Judd. *International Journal of Bifurcation and Chaos*, 8:2375, 1998.

[93] A. Rabinovich and I. Rogachevskii. *Chaos: An Interdisciplinary Journal of Nonlinear Science*, 9:880, 1999.

[94] A. Mauroy, I. Mezić, and J. Moehlis. *Physica D: Nonlinear Phenomena*, 261:19, 2013.

[95] K. A. Khan, V. P. Saxena, and P. I. Barton. *SIAM Journal on Scientific Computing*, 33:1475, 2011.

[96] M. U. Akhmet. *Nonlinear Analysis: Theory, Methods & Applications*, 60:311, 2005.

[97] M. Akhmet. *Principles of Discontinuous Dynamical Systems*. Springer, New York, 2010.

[98] A. F. Filippov. *Differential Equations with Discontinuous Righthand Sides: Control Systems*. Springer Netherlands, Dordrecht, 2013.

[99] J. Cortes. *IEEE Control Systems*, 28:36, 2008.

[100] S. Klymchuk, A. Plotnikov, and N. Skripnik. *Physica D: Nonlinear Phenomena*, 241:1932, 2012.

[101] N. A. Perestyuk and N. V. Skripnik. *Ukrainian Mathematical Journal*, 65:126, 2013.

[102] N. A. Perestyuk, V. A. Plotnikov, A. M. Samoilenko, and N. V. Skripnik. *Differential Equations with Impulse Effects: Multivalued Right-hand Sides With Discontinuities*. Walter De Gruyter, Berlin, 2011.

[103] J. Guckenheimer and P. J. Holmes. *Nonlinear Oscillations, Dynamical Systems, and Bifurcations of Vector Fields*. Springer, New York, 1983.

[104] E. M. Izhikevich. *Dynamical Systems in Neuroscience: The Geometry of Excitability and Bursting*. The MIT Press, Cambridge, 2006.

[105] Y. Kuramoto. *Physica D: Nonlinear Phenomena*, 50:15, 1991.

[106] A. Mauroy, P. Sacré, and R. Sepulchre. Kick synchronization versus diffusive synchronization. In *the 51st IEEE Conference on Decision and Control (CDC)*, pages 7171–7183. IEEE, New Jersey, 2012.

[107] D. Somers and N. Kopell. *Biological Cybernetics*, 68:393, 1993.

[108] M. Garcia, A. Chatterjee, A. Ruina, and M. Coleman. *Journal of Biomechanical Engineering*, 120:281, 1998.

[109] A. Goswami, B. Thuilot, and B. Espiau. Compass-like biped robot part i: Stability and bifurcation of passive gaits. 1996.

[110] H. Nakao. *Contemporary Physics*, 57:188, 2016.

[111] M. R. Tinsley, S. Nkomo, and K. Showalter. *Nature Physics*, 8:662, 2012.

[112] J. Moehlis, E. Shea-Brown, and H. Rabitz. *Journal of Computational and Nonlinear Dynamics*, 1:358, 2006.

[113] P. Hitczenko and G. S. Medvedev. *Journal of Nonlinear Science*, 23:835, 2013.

[114] S. H. Strogatz. *Nonlinear Dynamics and Chaos: with Applications to Physics, Biology, Chemistry, and Engineering*. Westview press, Boulder, 2014.

[115] M. Budišić, R. Mohr, and I. Mezić. *Chaos: An Interdisciplinary Journal of Nonlinear Science*, 22:047510, 2012.

[116] C. W. Rowley, I. Mezić, S. Bagheri, P. Schlatter, and D. S. Henningson. *Journal of Fluid Mechanics*, 641:115, 2009.

[117] P. J. Schmid. *Journal of Fluid Mechanics*, 656:5, 2010.

[118] M. O. Williams, I. G. Kevrekidis, and C. W. Rowley. *Journal of Nonlinear Science*, 25:1307, 2015.

[119] N. B. Erichson, S. L. Brunton, and J. N. Kutz. *Journal of Real-Time Image Processing*, 2016.

[120] J. Mann and J. N. Kutz. *Quantitative Finance*, 16:1643, 2016.

[121] J. L. Proctor, S. L. Brunton, and J. N. Kutz. *SIAM Journal on Applied Dynamical Systems*, 15:142, 2016.

[122] A. Mauroy. In *the 53rd IEEE Conference on Decision and Control*, pages 5888–5893. IEEE, New Jersey, 2014.

[123] D. Wilson and J. Moehlis. *SIAM Review*, 57:201, 2015.

[124] D. Wilson and J. Moehlis. *Physical Review E*, 94:012211, 2016.

[125] D. Wilson and J. Moehlis. *Physical Review E*, 94:052213, 2016.

[126] A. M. Lyapunov. *General Problem of the Stability of Motion*. Taylor & Francis, London, 1992.

[127] L. Adrianova. *Introduction to Linear Systems of Differential Equations*. American Mathematical Society, Providence, 1995.

[128] F. Colonius and W. Kliemann. *Dynamical systems and Linear Algebra*. American Mathematical Society, Providence, 2014.

[129] P. V. Kuptsov and U. Parlitz. *Journal of Nonlinear Science*, 22:727, 2012.

[130] F. L. Traversa, M. Bonnin, F. Corinto, and F. Bonani. *Journal of Computational Electronics*, 14:51, 2015.

[131] A. Pikovsky and A. Politi. *Lyapunov Exponents: A Tool to Explore Complex Dynamics*. Cambridge University Press, Cambridge, 2015.

[132] A. Guillamon and G. Huguet. *SIAM Journal on Applied Dynamical Systems*, 8:1005, 2009.

[133] O. Castejón, A. Guillamon, and G. Huguet. *The Journal of Mathematical Neuroscience*, 3:13, 2013.

[134] I. Mezić. *Annual Review of Fluid Mechanics*, 45:357, 2013.

[135] Y. Lan and I. Mezić. *Physica D: Nonlinear Phenomena*, 242:42, 2013.

[136] L. P. Shilnilov, A. L. Shilnilov, D. V. Turaev, and L. O. Chua. *Methods of Qualitative Theory in Nonlinear Dynamics. Part I.* World Scientific, Singapore, 1998.

[137] G. Gaeta. *Acta Applicandae Mathematica*, 70:113, 2002.

[138] S. Wiggins. *Introduction to Applied Nonlinear Dynamical Systems and Chaos.* Springer, New York, 2003.

[139] J. A. Sanders, F. Verhulst, and J. Murdock. *Averaging Methods in Nonlinear Dynamical Systems.* Springer, New York, 2007.

[140] A. Coddington and N. Levinson. *Theory of Ordinary Differential Equations.* McGraw-Hill, New York, 1955.

[141] F. C. Hoppensteadt. *Analysis and Simulation of Chaotic Systems.* Springer, New York, 2000.

[142] C. Chicone. *Ordinary Differential Equations with Applications.* Springer, New York, 2006.

[143] G. Teschl. *Ordinary Differential Equations and Dynamical Systems.* American Mathematical Society, Providence, 2012.

[144] G. Froyland, T. Hüls, G. P. Morriss, and T. M. Watson. *Physica D: Nonlinear Phenomena*, 247:18, 2013.

[145] T. Hüls. Computing stable hierarchies of fiber bundles. *Discrete and continuous dynamical systems. Series B.* To appear.

[146] E. Brown, J. Moehlis, and P. Holmes. *Neural Computation*, 16:673, 2004.

[147] B. C. Goodwin. *Advances in Enzyme Regulation*, 3:425, 1965.

[148] D. Gonze and W. Abou-Jaoudé. *PloS ONE*, 8:e69573, 2013.

[149] A. Woller, D. Gonze, and T. Erneux. *Physical Biology*, 11:045002, 2014.

[150] A. J. van der Schaft and H. Schumacher. *An Introduction to Hybrid Dynamical Systems.* Springer, Berlin, 2000.

[151] M. R. Jeffrey. *Physical Review Letters*, 106:254103, 2011.

[152] R. A. Horn and C. R. Johnson. *Matrix Analysis.* Cambridge university press, Cambridge, 2012.

[153] J. J. B. Biemond, N. van de Wouw, W. P. M. H. Heemels, and H. Nijmeijer. *IEEE Transactions on Automatic Control*, 58:876, 2013.

[154] M. Broucke and A. Arapostathis. *Systems & Control Letters*, 47:149, 2002.

[155] R. Goebel and A. R. Teel. *Automatica*, 42:573, 2006.

[156] S. N. Simic, K. H. Johansson, J. Lygeros, and S. Sastry. *Dynamics of Continuous, Discrete and Impulsive Systems Series B: Applications and Algorithms*, 12:649, 2005.

[157] S. A. Burden. *A Hybrid Dynamical Systems Theory for Legged Locomotion*. PhD thesis, University of California, Berkeley, 2014.

[158] J. M. Lee. *Introduction to Smooth Manifolds*. Springer, New York, 2003.

[159] P. Krbec. On nonparasite solutions. In *Equadiff 6*, pages 133–139. Springer, Berlin, 1986.

[160] J-P. Aubin, J. Lygeros, M. Quincampoix, S. Sastry, and N. Seube. *IEEE Transactions on Automatic Control*, 47:2, 2002.

[161] G. N. Silva and R. B. Vinter. *Journal of Mathematical Analysis and Applications*, 202:727, 1996.

[162] N. N. Bogolyubov and I. A. Mitropolsky. *Asymptotic Methods in the Theory of Nonlinear Oscillations*. Gordon and Breach, New York, 1945.

[163] I. A. Mitropolsky. *International Journal of Non-Linear Mechanics*, 2:69, 1967.

[164] A. M. Samoilenko and A. N. Stanzhitskii. *Differential Equations*, 42:505, 2006.

[165] R. J. Aumann. *Journal of Mathematical Analysis and Applications*, 12:1, 1965.

[166] V. S. Burd. *International Journal of Non-Linear Mechanics*, 32:1143, 1997.

[167] J. Newman and O. Makarenkov. *Nonlinear Dynamics*, 79:111, 2015.

Appendix A

Assumptions for the periodic solution in hybrid dynamical systems

In this section, we introduce the assumptions that are necessary for the periodic solution to be piecewise continuously differentiable with respect to the initial condition [96, 97]. Hybrid dynamical systems can exhibit pathological behaviors, which do not occur in smooth dynamical systems, such as the grazing, sliding, and Zeno phenomena owing to the effect of discrete switching [62, 150]. The grazing phenomenon [62] occurs when the orbit becomes tangent to the switching surface. This condition can be written as

$$\nabla L((i,j), \boldsymbol{X}_0(t))|_{L=0} \cdot \dot{\boldsymbol{X}}_0(t) = 0, \tag{A.1}$$

where $\nabla L : \mathcal{G} \times \mathbb{R}^N \to \mathbb{R}^N$ is the gradient of L with respect to $\boldsymbol{X}$ and $\cdot$ denotes inner product of vectors. The sliding and Zeno phenomena [150] can arise when the points $\boldsymbol{X}_0(\tau_k(\boldsymbol{s}^*)+0),\ k \in \mathbb{Z}_{\geq 0}$ are allowed to be accumulation points of the switching surfaces. These conditions can lead to infinite sensitivity to the initial conditions [151]. This can also be the case when the solution intersects a boundary of a switching surface (in the relative topology of its corresponding zero-level set of L induced by the Euclidean topology of $\mathbb{R}^N$). In this study, we do not consider such pathological situations, namely, we assume that (C1) the orbit is always transversal to the switching plane and that (C2) each continuous state right after the discrete state transition has a neighborhood that is disjoint from the switching surfaces and that (C3) the orbit does not intersect the boundaries of the switching surfaces.

Appendix B

Linear stability of the hybrid limit cycle

In this section, we formalize the linear stability of the periodic solution. Let $\boldsymbol{\xi}^\alpha$ ($\alpha = 1, ..., N$) be the αth initial-condition sensitivity vector [95] with respect to an initial state $\boldsymbol{s}^* = (I_0(0), \boldsymbol{X}_0(0))$ on χ at $t = 0$, defined as

$$\boldsymbol{\xi}^\alpha(t) = \lim_{\epsilon \to 0} \left(\frac{\boldsymbol{X}(t; (I_0(0), \boldsymbol{X}_0(0) + \epsilon \boldsymbol{e}^\alpha)) - \boldsymbol{X}_0(t)}{\epsilon} \right). \tag{B.1}$$

Here, the second argument of $\boldsymbol{X}(t; \cdot)$ represents an initial state that is slightly perturbed in the αth direction ($\boldsymbol{e}^\alpha$ is the αth unit vector) from $(I_0(0), \boldsymbol{X}_0(0))$ on χ. We introduce a *sensitivity matrix* $\boldsymbol{\Xi} = (\boldsymbol{\xi}^1, \boldsymbol{\xi}^2, \cdots, \boldsymbol{\xi}^N) \in \mathbb{R}^{N \times N}$ as the collection of sensitivity vectors in all directions. Note that

$$\boldsymbol{\Xi}(0) = (\boldsymbol{e}^1, ..., \boldsymbol{e}^N) = \mathbf{I} \tag{B.2}$$

where $\mathbf{I}$ is the identity matrix, because $\boldsymbol{X}(0; (I_0(0), \boldsymbol{X}_0(0) + \epsilon \boldsymbol{e}^\alpha)) = \boldsymbol{X}_0(0) + \epsilon \boldsymbol{e}^\alpha$.

In Refs. [96, 97, 95], the linear variational system for $\boldsymbol{\Xi}$ has been derived as

$$\dot{\boldsymbol{\Xi}}(t) = \mathbf{A}(k, t) \boldsymbol{\Xi}(t) \quad \text{for} \quad t \ (\text{mod } T) \in (\tau_{k-1}(\boldsymbol{s}^*), \tau_k(\boldsymbol{s}^*)), \tag{B.3}$$

$$\boldsymbol{\Xi}(t + 0) = \mathbf{C}_k \boldsymbol{\Xi}(t) \quad \text{at} \quad t \ (\text{mod } T) = \tau_k(\boldsymbol{s}^*), \tag{B.4}$$

where $\mathbf{A}(k, t) = D\boldsymbol{F}(k, \boldsymbol{X}_0(t))$ is the Jacobi matrix of $\boldsymbol{F}(k, \boldsymbol{X})$ estimated on χ, and $\mathbf{C}_k$ is the so-called *saltation matrix* [62] (Eq. (2.15) in the main part).

We define a *monodromy matrix* $\mathbf{M}$ from the sensitivity matrix $\mathbf{\Xi}(t)$ as $\mathbf{M} = \mathbf{\Xi}(T)$. If this $\mathbf{M}$ has one simple eigenvalue equal to 1 and all other eigenvalues lie strictly inside the unit circle on the complex plane, the periodic solution is linearly stable [95]. We call such a stable isolated periodic solution a hybrid limit cycle. It can be shown that the eigenvalues and their algebraic multiplicities of monodromy matrices do not depend on the choice of the initial state. We can also consider initial-condition sensitivity vectors with respect to the state $\boldsymbol{s}_0(\theta) = (I_0(\theta), \boldsymbol{X}_0(\theta))$ on the limit cycle χ, instead of $\boldsymbol{s}^* = (I_0(0), \boldsymbol{X}_0(0))$, as

$$\boldsymbol{\xi}^{\alpha}(t;\theta) = \lim_{\epsilon \to 0} \left(\frac{\boldsymbol{X}(t; (I_0(\theta), \boldsymbol{X}_0(\theta) + \epsilon \boldsymbol{e}^{\alpha})) - \boldsymbol{X}_0(t+\theta)}{\epsilon} \right). \tag{B.5}$$

We denote by a matrix $\mathbf{\Xi}(t;\theta) = (\boldsymbol{\xi}^1(t;\theta), \boldsymbol{\xi}^2(t;\theta), \cdots, \boldsymbol{\xi}^N(t;\theta)) \in \mathbb{R}^{N \times N}$ the collection of the sensitivity vectors in all directions, and introduce a monodromy matrix $\mathbf{M}(\theta) = \mathbf{\Xi}(T;\theta)$ of the linear variational system, which satisfies

$$\dot{\mathbf{\Xi}}(t;\theta) = \mathbf{A}(k, t+\theta)\mathbf{\Xi}(t;\theta) \quad \text{for} \quad t+\theta \ (\text{mod } T) \in (\tau_{k-1}(\boldsymbol{s}^*), \tau_k(\boldsymbol{s}^*)), \tag{B.6}$$

$$\mathbf{\Xi}(t+0;\theta) = \mathbf{C}_k \mathbf{\Xi}(t;\theta) \quad \text{at} \quad t+\theta \ (\text{mod } T) = \tau_k(\boldsymbol{s}^*), \tag{B.7}$$

$$\mathbf{\Xi}(0;\theta) = \mathbf{I}. \tag{B.8}$$

There exist a unique state transition matrix $\mathbf{H}_k(t,s)$ of the linear variational system (B.6) satisfying

$$\mathbf{\Xi}(t;\theta) = \mathbf{H}_k(t+\theta, s+\theta)\ \mathbf{\Xi}(s;\theta) \quad \text{for} \quad t+\theta, s+\theta \in [\tau_{k-1}(\boldsymbol{s}^*) + nT, \tau_k(\boldsymbol{s}^*) + nT), \tag{B.9}$$

which is a solution to

$$\dot{\mathbf{H}}_k(t,s) = \mathbf{A}(k,t)\ \mathbf{H}_k(t,s) \quad \text{for} \quad t, s \in [\tau_{k-1}(\boldsymbol{s}^*) + nT, \tau_k(\boldsymbol{s}^*) + nT], \tag{B.10}$$

with the initial condition $\mathbf{H}_k(s,s) = \mathbf{I}$.

Suppose that θ is in the interval $[\tau_{m^*-1}(\boldsymbol{s}^*), \tau_{m^*}(\boldsymbol{s}^*))$, where $m^* \in \mathcal{M}_0 \cup \{m_0+1\}$. Using $\mathbf{H}_k(t,s)$, the monodromy matrix can be expressed as $\mathbf{M}(0) = \mathbf{M}_1\mathbf{M}_2$, where

$$\mathbf{M}_1 = \mathbf{H}_1(T, \tau_{m_0}(\boldsymbol{s}^*)) \left(\prod_{l=m^*}^{m_0}{}^{+} \mathbf{H}_{l+1}(\tau_{l+1}(\boldsymbol{s}^*), \tau_l(\boldsymbol{s}^*))\mathbf{C}_l \right) \cdot \mathbf{H}_{m^*}(\tau_{m^*}(\boldsymbol{s}^*), \theta), \tag{B.11}$$

and

$$\mathbf{M}_2 = \mathbf{H}_{m^*}(\theta, \tau_{m^*-1}(\boldsymbol{s}^*)) \cdot \prod_{k=1}^{m^*-1}{}^{+} \mathbf{C}_k\mathbf{H}_k(\tau_k(\boldsymbol{s}^*), \tau_{k-1}(\boldsymbol{s}^*)). \tag{B.12}$$

Here, we denote by $\prod_{i=1}^{+n} \mathbf{Y}_i = \mathbf{Y}_n\mathbf{Y}_{n-1}\cdots\mathbf{Y}_2\mathbf{Y}_1$ the ordered product of matrices. With these matrices $\mathbf{M}_1$ and $\mathbf{M}_2$, one can also show that $\mathbf{M}(\theta) = \mathbf{M}_2\mathbf{M}_1$, where $\mathbf{H}_k(t,s) = \mathbf{H}_k(t+nT, s+nT)$, which follows from $\mathbf{A}(k,t) = \mathbf{A}(k,t+nT)$, is used. Therefore, $\mathbf{M}(0)$ and $\mathbf{M}(\theta)$ has the same set of eigenvalues with the same algebraic multiplicities, because the Jordan blocks with nonzero eigenvalues of the products of the matrices $\mathbf{AB}$ and $\mathbf{BA}$ are identical [152, Th. 3.2.11.1.].

Appendix C

Asymptotic equivalence of initial conditions in hybrid dynamical systems

In this section, we introduce an asymptotic equivalence of the initial conditions that we use for defining the isochrons, which is different from the one used in smooth systems. Suppose $\boldsymbol{X}_1(t)$ and $\boldsymbol{X}_2(t)$ are the continuous parts of the solutions to a system with initial conditions $\boldsymbol{s}_1$ and $\boldsymbol{s}_2$, respectively. In smooth systems, the asymptotic equivalence relation of the initial conditions $\boldsymbol{s}_1$ and $\boldsymbol{s}_2$ is defined as the convergence of the error $\boldsymbol{X}_1(t) - \boldsymbol{X}_2(t)$ in the Euclidean topology. That is, if $\lim_{t\to+\infty} |\boldsymbol{X}_1(t) - \boldsymbol{X}_2(t)| = 0$ where $|\cdot|$ is the Euclidean norm, then $\boldsymbol{s}_1$ and $\boldsymbol{s}_2$ are asymptotically equivalent. In hybrid dynamical systems, the moments of switching of the two solutions for these initial conditions generally do not coincide in a finite time. Hence, the Euclidean norm of the error of the continuous part $|\boldsymbol{X}_1(t)-\boldsymbol{X}_2(t)|$ causes some kind of "peaking behavior" [153]; $|\boldsymbol{X}_1(t) - \boldsymbol{X}_2(t)|$ can be larger than a constant $c > 0$ (of order $|\boldsymbol{\Phi}_k(\boldsymbol{X}) - \boldsymbol{X}|$) for some $t \in [t_*, \infty]$ for an arbitrarily large $t_* > 0$ owing to the continuous state jumps. This violates the definition of convergence in Euclidean topology. Therefore, we need to consider convergence in some other suitable topology to define the asymptotic equivalence notion in hybrid dynamical systems.

Various topologies suitable for hybrid dynamical systems have been proposed in the literature, such as the Skorohod topology [154] originally designed as a tool to analyze stochastic processes, the topology of graphical convergence that is based on set-valued analysis [155], and the quotient topology generated on the hybrifold [156], which is, roughly speaking, the manifold constructed by identifying the switching surface $\boldsymbol{\Pi}_{k,k+1}$ with its image of the transition function $\boldsymbol{\Phi}_k$.

In this study, we adopt an asymptotic equivalence that is based on convergence in B-topology [96, 97], which is defined as follows: if for any $\epsilon > 0$, there exists $T^* = T^*(\epsilon) > 0$ such that, in the time domain $[T^*, +\infty)$, every moment of switching of the solution $\boldsymbol{X}_2(t)$ lies in some ϵ-neighborhood of the moment of switching of the solution $\boldsymbol{X}_1(t)$, and for all $t \in [T^*, +\infty)$, which are outside the ϵ-neighborhoods of the moments of switching of $\boldsymbol{X}_1(t)$, $|\boldsymbol{X}_1(t) - \boldsymbol{X}_2(t)| < \epsilon$ holds, then we call the initial conditions $\boldsymbol{s}_1$ and $\boldsymbol{s}_2$ asymptotically equivalent. The benefit of this definition is intuitively clear; the error $|\boldsymbol{X}_1(t) - \boldsymbol{X}_2(t)|$ is evaluated outside of the neighborhoods of the points of discontinuity, and thus we can avoid the effect of the peaking behavior, and the error that occurs at the moment of switching is guaranteed to disappear.

Appendix D

Some properties of the isochron and the phase function of hybrid limit cycles

Using the following equivalence relation (Eq. (2.7) in the main part)

$$\Theta(\boldsymbol{s}_1) = \Theta(\boldsymbol{s}_2) = \theta, \tag{D.1}$$

we can introduce the "conditional" isochron $W_k(\theta) = \{\boldsymbol{X} \,|\, \Theta(k, \boldsymbol{X}) = \theta\}$, i.e., the set of continuous states sharing the same phase value θ for each discrete state $k \in \mathcal{M}_0$. We can then define the isochron of χ with phase θ as the union $W(\theta) = \bigcup_{k=1}^{m_0} (k, W_k(\theta))$. We note that the notion of the isochron in hybrid dynamical systems has been proposed in [157], but the phase dynamics of weakly perturbed hybrid oscillators has not been discussed so far.

We can show that, in a domain $\tilde{U} \equiv \mathcal{A} \setminus \bigcup_{k=1}^{m_0} (k, \boldsymbol{\Pi}_{k,k+1})$, where $\mathcal{A} \subset U$ is a neighborhood of χ such that the solution starting from the point in $\mathcal{A}$ is piecewise continuously diffentiable with respect to the initial condition, the phase function Θ is totally differentiable with respect to the continuous state and that it is one-sided differentiable on the switching surfaces as follows.

We consider two slightly different initial conditions, $\boldsymbol{s}_1$ and $\boldsymbol{s}_2 = \boldsymbol{s}_1 + (0, \epsilon \boldsymbol{h})$, where $\boldsymbol{s}_1, \boldsymbol{s}_2 \in \mathcal{A}$, $0 < \epsilon \ll 1$ and $\boldsymbol{h} \in \mathbb{R}^N$. Note that, when $\boldsymbol{s}_1 \in \bigcup_{k=1}^{m_0} (k, \boldsymbol{\Pi}_{k,k+1})$, $\boldsymbol{h}$ should be taken from the subset of $\mathbb{R}^N$ whose elements point in the opposite direction as $\boldsymbol{F}(\boldsymbol{s}_1)$ in the tangent space [158] of the switching boundary. From the differentiability with respect to initial conditions, the following relation holds for all t outside the

ϵ-neighborhoods of the moments of switching,

$$\boldsymbol{X}_2(t) = \boldsymbol{X}_1(t) + \epsilon \boldsymbol{\Xi}_{\boldsymbol{s}_1}(t)\boldsymbol{h} + O(\epsilon^2), \tag{D.2}$$

where $\boldsymbol{X}_1(t)$ and $\boldsymbol{X}_2(t)$ are the continuous part of the solutions with the initial conditions $\boldsymbol{s}_1$ and $\boldsymbol{s}_2$, respectively, and $\boldsymbol{\Xi}_{\boldsymbol{s}_1}(t) \in \mathbb{R}^{N\times N}$ denotes the initial condition sensitivity matrix with the initial state $\boldsymbol{s}_1$. Since $\boldsymbol{s}_1$ and $\boldsymbol{s}_2$ are taken from $\mathcal{A}$, which is a subset of the basin of attraction U of the hybrid limit cycle χ, the solutions $\boldsymbol{X}_1, \boldsymbol{X}_2$ relax to χ, which we denote as $\boldsymbol{X}_{0,1}, \boldsymbol{X}_{0,2}$ in this section. One can easily see that the following relation holds:

$$\boldsymbol{X}_{0,2}(t) = \boldsymbol{X}_{0,1}(t) + \int_0^{\theta(\boldsymbol{s}_2)-\theta(\boldsymbol{s}_1)} \boldsymbol{F}(k, \boldsymbol{X}_{0,1}(t+t'))dt'. \tag{D.3}$$

Since $\boldsymbol{X}_{0,1}(t)$ is not an equilibrium, we can assume that the first entry $F_1(k, \boldsymbol{X}_{0,1}(t))$ of $\boldsymbol{F}(k, \boldsymbol{X}_{0,1}(t))$ is nonzero without loss of generality and denote its absolute value as $|F_1(k, \boldsymbol{X}_{0,1}(t))| = d$. Considering the continuity of the continuous part of the solution with respect to the initial condition and the continuity of the vector field $\boldsymbol{F}(k, \boldsymbol{X})$ with respect to the continuous variable $\boldsymbol{X}$, there exists $\epsilon' > 0$ such that for any $\epsilon < \epsilon'$, the inequality $|F_1(k, \boldsymbol{X}_{0,1}(t+t'))| \geq d/2$ holds for $t' \in [0, \theta(\boldsymbol{s}_2) - \theta(\boldsymbol{s}_1)]$. Hence we can obtain the following inequality for $\epsilon < \epsilon'$:

$$\begin{aligned} |\boldsymbol{X}_{0,2}(t) - \boldsymbol{X}_{0,1}(t)| &= \left| \int_0^{\theta(\boldsymbol{s}_2)-\theta(\boldsymbol{s}_1)} \boldsymbol{F}(k, \boldsymbol{X}_{0,1}(t+t'))dt' \right| \\ &= |\boldsymbol{d}||\theta(\boldsymbol{s}_2) - \theta(\boldsymbol{s}_1)| \geq \frac{d}{2}|\theta(\boldsymbol{s}_2) - \theta(\boldsymbol{s}_1)| \end{aligned} \tag{D.4}$$

where $\boldsymbol{d}$ is a constant vector obtained by applying the mean value theorem to each entry of $\boldsymbol{F}(k, \boldsymbol{X})$. From Eqs. (D.2) and (D.4), we can show the continuity of θ as follows:

$$\lim_{\boldsymbol{s}_2 \to \boldsymbol{s}_1} |\theta(\boldsymbol{s}_2) - \theta(\boldsymbol{s}_1)| \leq \lim_{\epsilon \to 0} \left(\left| \frac{2\epsilon}{d} \boldsymbol{\Xi}_{\boldsymbol{s}_1}(t)\boldsymbol{h} \right| + O(\epsilon^2) \right) = 0. \tag{D.5}$$

The continuity assures that $\theta(\boldsymbol{s}_2) - \theta(\boldsymbol{s}_1)$ is $O(\epsilon)$. Therefore, we can restate Eq. (D.3) as

$$\boldsymbol{X}_{0,2}(t) = \boldsymbol{X}_{0,1}(t) + (\theta(\boldsymbol{s}_2) - \theta(\boldsymbol{s}_1))\boldsymbol{F}(k, \boldsymbol{X}_{0,1}(t)) + O(\epsilon^2). \tag{D.6}$$

From Eqs. (D.2) and (D.6), we can obtain

$$\theta(\boldsymbol{s}_2)-\theta(\boldsymbol{s}_1)=\frac{\epsilon \boldsymbol{F}^{\dagger}(k,\boldsymbol{X}_{0,1}(t))\boldsymbol{\Xi}_{\boldsymbol{s}_1}(t)\boldsymbol{h}}{\boldsymbol{F}^{\dagger}(k,\boldsymbol{X}_{0,1}(t))\boldsymbol{F}(k,\boldsymbol{X}_{0,1}(t))}+O(\epsilon^2). \tag{D.7}$$

Now we consider the asymptotic property of $\boldsymbol{\Xi}_{\boldsymbol{s}_1}(t)$. The assumption (C2) in Appendix A assures that for sufficiently small ϵ, there exists t_* such that the discrete states of $\boldsymbol{s}_1(t_*+nT)$ and $\boldsymbol{s}_2(t_*+nT)$ are the same and invariant for all $n\in\mathbb{Z}_{\geq 0}$ for any $\boldsymbol{h}$. We define a time-T map $\boldsymbol{P}:\mathbb{R}^N\to\mathbb{R}^N$ as

$$\boldsymbol{P}(\boldsymbol{X}(t))=\boldsymbol{X}(t+T), \tag{D.8}$$

and its n-fold composition as $\boldsymbol{P}^n$. By a similar argument to the proof of the Lemma in Appendix A in [86], we can show that the sequences $\{\boldsymbol{P}^n(\boldsymbol{X}_1(t_*))\}$ and $\{D\boldsymbol{P}^n(\boldsymbol{X}_1(t_*))\}$ are convergent and that $\lim_{n\to\infty}\boldsymbol{P}^n(\boldsymbol{X}_1(t_*))=\boldsymbol{X}_0(\theta_*)$ and
$\lim_{n\to\infty}(D\boldsymbol{P})\circ(\boldsymbol{P}^{n-1}(\boldsymbol{X}_1(t_*))=\mathbf{M}(\theta_*)$. Here, θ_* is a unique phase value that depends on $\boldsymbol{X}_1(t_*)$, and the monodromy matrix $\mathbf{M}(\theta_*)$ is defined in Appendix B.

Let us define $\boldsymbol{Q}(t_*)\equiv\lim_{n\to\infty}D\boldsymbol{P}^n(\boldsymbol{X}_1(t_*))$. One can easily see that $\mathbf{M}(\theta_*)\boldsymbol{Q}(t_*)=\boldsymbol{Q}(t_*)$. Using this relation and the fact shown in [95],

$$\lim_{n\to\infty}\mathbf{M}^n(\theta_*)=\boldsymbol{F}(I_0(\theta_*),\boldsymbol{X}_0(\theta_*))\otimes\boldsymbol{v}(\theta_*), \tag{D.9}$$

where $\boldsymbol{v}(\theta_*)\in\mathbb{R}^N$ is a left eigenvector of $\mathbf{M}(\theta_*)$ corresponding to the eigenvalue unity, one can obtain

$$\begin{aligned}
&\lim_{n\to\infty}\boldsymbol{\Xi}_{\boldsymbol{s}_1}(t_*+nT)=\boldsymbol{Q}(t_*)\boldsymbol{\Xi}_{\boldsymbol{s}_1}(t_*)\\
&=\lim_{n\to\infty}\mathbf{M}^n(\theta_*)\boldsymbol{Q}(t_*)\boldsymbol{\Xi}_{\boldsymbol{s}_1}(t_*)\\
&=\boldsymbol{F}(I_0(\theta_*),\boldsymbol{X}_0(\theta_*))\otimes\boldsymbol{v}(\theta_*)\boldsymbol{Q}(t_*)\boldsymbol{\Xi}_{\boldsymbol{s}_1}(t_*).
\end{aligned} \tag{D.10}$$

Note that $\boldsymbol{v}(\theta_*)$ also satisfies the condition $\boldsymbol{v}(\theta_*)\cdot\boldsymbol{F}(I_0(\theta_*),\boldsymbol{X}_0(\theta_*))=1$, hence, in fact, it is the phase sensitivity function evaluated at $\theta=\theta_*$ as shown in Appendix F.

Using $\boldsymbol{v}(\theta_*)$, $\boldsymbol{Q}(\theta_*)$ and $\boldsymbol{\Xi}_{\boldsymbol{s}_1}(\theta_*)$, we can rewrite Eq. (D.7) as

$$\theta(\boldsymbol{s}_2)-\theta(\boldsymbol{s}_1)=\epsilon\boldsymbol{v}^{\dagger}(\theta_*)\boldsymbol{Q}(t_*)\boldsymbol{\Xi}_{\boldsymbol{s}_1}(t_*)\boldsymbol{h}+O(\epsilon^2)=\epsilon\boldsymbol{v}^{\dagger}(\theta_*)\boldsymbol{R}(\theta_*;\boldsymbol{s}_1)\boldsymbol{h}+O(\epsilon^2), \tag{D.11}$$

where $\boldsymbol{R}(\theta_*;\boldsymbol{s}_1)\equiv\boldsymbol{Q}(t_*)\boldsymbol{\Xi}_{\boldsymbol{s}_1}(t_*)$ is introduced to emphasize that it depends only on θ_* and $\boldsymbol{s}_1$. As shown below, $\boldsymbol{v}^{\dagger}(\theta_*)\boldsymbol{R}(\theta_*;\boldsymbol{s}_1)$ on the right-hand side does not depend on the choice of θ_*. One can see that $\boldsymbol{R}(\theta+\theta';\boldsymbol{s}_1)=\boldsymbol{\Xi}(\theta';\theta)\boldsymbol{R}(\theta;\boldsymbol{s}_1)$ and that

$\boldsymbol{v}(\theta) = \boldsymbol{\Psi}(-\theta';\theta+\theta')\boldsymbol{v}(\theta+\theta')$, where $\boldsymbol{\Xi}(\cdot;\theta)$ and $\boldsymbol{\Psi}(\cdot;\theta)$ are defined in Appendix B and F, respectively. The latter equality follows from the fact shown in Appendix F that $\boldsymbol{v}(\theta)$ is a periodic solution of the adjoint linear system Eq. (F.13, F.14). Similarly to Eq. (F.7), we can show $\boldsymbol{\Xi}(\theta';\theta) = \boldsymbol{\Psi}^\dagger(-\theta';\theta+\theta')$. Thus,

$$\begin{aligned}
&\boldsymbol{v}^\dagger(\theta+\theta')\boldsymbol{R}(\theta+\theta';\boldsymbol{s}_1) = \boldsymbol{v}^\dagger(\theta+\theta')\boldsymbol{\Xi}(\theta';\theta)\boldsymbol{R}(\theta;\boldsymbol{s}_1)\\
&= \left(\boldsymbol{\Psi}(-\theta';\theta+\theta')\boldsymbol{v}(\theta+\theta')\right)^\dagger \boldsymbol{R}(\theta;\boldsymbol{s}_1)\\
&= \boldsymbol{v}^\dagger(\theta)\boldsymbol{R}(\theta;\boldsymbol{s}_1),
\end{aligned} \tag{D.12}$$

and we finally obtain

$$\lim_{\boldsymbol{s}_2\to\boldsymbol{s}_1} \frac{|\theta(\boldsymbol{s}_2)-\theta(\boldsymbol{s}_1)-\boldsymbol{S}^\dagger(\boldsymbol{s}_1)(\boldsymbol{X}_2(0)-\boldsymbol{X}_1(0))|}{|\boldsymbol{X}_2(0)-\boldsymbol{X}_1(0)|} = \lim_{\epsilon\to 0} O(\epsilon) = 0, \tag{D.13}$$

where we defined $\boldsymbol{S}^\dagger(\boldsymbol{s}_1) \equiv \boldsymbol{v}^\dagger(\theta_*)\boldsymbol{R}(\theta_*;\boldsymbol{s}_1)$. This concludes the proof of the total differentiability (and one-sided differentiability at switching boundaries) of the phase.

Next, we show a smoothness property of the isochrons. The assumption that $\boldsymbol{F}, \boldsymbol{\Phi}, L$ are twice continuously differentiable with respect to the continuous state assures the piecewise twice continuously differentiable dependence of the solution with respect to the initial condition on $\mathcal{A}$ [96]. This means that the initial condition sensitivity matrix $\boldsymbol{\Xi}_{\boldsymbol{s}}(t)$ depends on the continuous part of $\boldsymbol{s}$ smoothly. From this fact, we can easily show the piecewise continuous differentiability of the gradient of the phase $\boldsymbol{S}^\dagger(\boldsymbol{s})$. The definition of the phase guarantees that the relation (Eq. (2.8) in the main part)

$$\dot{\theta}(t) = \dot{\Theta}(I(t),\boldsymbol{X}(t)) = \nabla\Theta(I(t),\boldsymbol{X}(t))\cdot\boldsymbol{F}(I(t),\boldsymbol{X}(t)) = 1 \tag{D.14}$$

holds for an unperturbed oscillator for almost all t (excluding the set of the moments of switching, which has zero Lebesgue measure) and for $\boldsymbol{X}(t) \in \tilde{U}$. From this relation, $\nabla\Theta$ is nonzero everywhere on in $\tilde{U}$. Therefore, by using the implicit function theorem, we can show that each connected component of the subset of the conditional isochron $\tilde{W}_k(\theta) = \{\boldsymbol{X} \,|\, \boldsymbol{X} \in W_k(\theta) \cap (k,\boldsymbol{X}) \in \tilde{U}\}$ is an $(N-1)$-dimensional smooth submanifold embedded in $\mathbb{R}^N$.

Appendix E

Approximation of the phase dynamics of hybrid limit cycles

Using the chain rule, the phase dynamics of the weakly perturbed hybrid oscillator described by Eq. (2.8) in the main part is given by

$$\dot{\theta}(t) = \dot{\Theta}(I(t), \boldsymbol{X}(t)) = 1 + \epsilon \nabla \Theta(I(t), \boldsymbol{X}(t)) \cdot \boldsymbol{p}(I(t), \boldsymbol{X}(t), t). \tag{E.1}$$

This is still not a closed equation in the phase θ because the map $\Theta : U \to \mathbb{T}^1$ is not injective. To obtain a closed equation, we assume the magnitude ϵ of the perturbation to be sufficiently small and approximate $\nabla\Theta(I(t), \boldsymbol{X}(t))$ and $\boldsymbol{p}(I(t), \boldsymbol{X}(t), t)$ by replacing $I(t)$ with $I_0(\theta(t))$ and $\boldsymbol{X}(t)$ with $\boldsymbol{X}_0(\theta(t))$ [2]. We can then obtain the following approximate phase equation closed in θ at the lowest order:

$$\begin{aligned}
\dot{\theta}(t) &= \dot{\Theta}(I(t), \boldsymbol{X}(t)) \\
&= 1 + \epsilon \nabla \Theta(I_0(\theta), \boldsymbol{X}_0(\theta)) \cdot \boldsymbol{p}(I_0(\theta), \boldsymbol{X}_0(\theta), t) + O(\epsilon^2) \\
&= 1 + \epsilon \boldsymbol{Z}(\theta) \cdot \boldsymbol{p}(I_0(\theta), \boldsymbol{X}_0(\theta), t) + O(\epsilon^2),
\end{aligned} \tag{E.2}$$

where we defined the phase sensitivity function $\boldsymbol{Z}(\theta) = \nabla\Theta(I_0(\theta), \boldsymbol{X}_0(\theta))$ characterizing the linear response property of the oscillator phase to weak external perturbations.

We interpret Eq. (E.2) as a suitably regularized, multivalued system, such as the Filippov system [98, 99], since some important solutions can not be obtained in the classical Carathéodory sense [98]. For example, a stable stationary solution at the point of discontinuity of the RHS of Eq. (E.2) is, in general, not a Carathéodory solution, because it is required to satisfy Eq. (E.2) for almost all t by definition, but the desired stationary solution may not satisfy Eq. (E.2) for all t.

When the perturbation $\boldsymbol{p}$ is locally bounded, we can introduce the Filippov solution to Eq. (E.2) as an absolutely continuous map $\theta(t) : \mathbb{R} \to \mathbb{T}^1$, which satisfies the following differential inclusion:

$$\dot{\theta}(t) \in 1 + \epsilon \boldsymbol{G}(\theta, t) \tag{E.3}$$

for almost all t, where $\boldsymbol{G}(\theta, t)$ is a set of closed convex combinations of $\boldsymbol{Z}(\theta - 0) \cdot \boldsymbol{p}(I_0(\theta - 0), \boldsymbol{X}_0(\theta - 0), t)$ and $\boldsymbol{Z}(\theta + 0) \cdot \boldsymbol{p}(I_0(\theta + 0), \boldsymbol{X}_0(\theta + 0), t)$. Obviously, the Filippov system Eq. (E.3) allows stationary solutions at the point of discontinuity described above. Note that the above Filippov regularization of the system can also produce physically meaningless solutions. For example, the Filippov system admits an evidently unfeasible, unstable stationary solution staying at the point of discontinuity of the RHS of Eq. (E.2). This kind of solution, called a parasite solution [159], should be carefully omitted. See [98, 99] for sufficient conditions for the existence and uniqueness of solution to the Filippov system.

When the perturbation is not locally bounded, for instance, when it includes the Dirac delta function, we need to consider a physically relevant solution, which is generally not absolutely continuous, by employing suitable formulations such as impulse differential inclusions [160] or measure driven differential inclusions [161]. Though we do not consider such a special situation in this study, if an impulsive input is applied at the moment of switching of the discrete states, it requires a special attention because the choice of the value of the integrand at the atom of the driving measure crucially affects the solution.

Consider the case where an impulsive input $\boldsymbol{p}(\cdot, \cdot, t) = \boldsymbol{c}\delta(t - \tau)$, where $\delta(\cdot)$ is Dirac's delta function, is applied at the moment of switching $t = \tau$. If the impulsive input is applied when the state $(I_0(\theta(\tau)), \boldsymbol{X}_0(\theta(\tau)))$ is on the switching plane, there are two possible cases: (a) $(\nabla L_{I_0(\theta(\tau))}(\boldsymbol{X}_0(\theta(\tau))) \cdot \boldsymbol{c})(\nabla L_{I_0(\theta(\tau))}(\boldsymbol{X}_0(\theta(\tau))) \cdot \dot{\boldsymbol{X}}_0(\theta(\tau))) > 0$, i.e., the perturbation and the vector field point in the same direction in the tangent space [158] of the switching boundary or (b) otherwise. In the case (a), the one-sided derivative of the phase function $\boldsymbol{\Theta}$ in the direction of $\boldsymbol{c}$ is undefined. If we redefine the hybrid automaton Eq. (2.1-2.3) in the main part, for example, by replacing the switching surface with the switching region $\boldsymbol{\Pi}_{ij} = \{\boldsymbol{X} \mid L((i, j), \boldsymbol{X}) \leq 0\}$, we can introduce a one-sided derivative of $\boldsymbol{\Theta}$ in the direction of $\boldsymbol{c}$. However, in general, it does not coincide with the phase sensitivity function obtained from the proposed adjoint method. Hence, this situation requires special treatments beyond the scope of this study. In the case (b), we can adopt $\boldsymbol{Z}(\theta(\tau) - 0)$ as the phase sensitivity function. When the input is added immediately after the reset of the discrete state, which can also

be interpreted as a perturbation to the transition function as $\boldsymbol{\Phi}_{I_0(\theta(\tau))}(\boldsymbol{X}_0(\theta(\tau))) + \boldsymbol{c}$, we can adopt $\boldsymbol{Z}(\theta(\tau) + 0)$ as the phase sensitivity function.

Appendix F

Adjoint equation for the phase sensitivity function of hybrid limit cycles

An adjoint linear system to Eqs. (B.3) and (B.4) can also be introduced as

$$\dot{\mathbf{\Psi}}(t) = -\mathbf{A}^{\dagger}(k,t)\ \mathbf{\Psi}(t) \quad \text{for} \quad t \ (\text{mod}\ T) \in (\tau_{k-1}(\boldsymbol{s}^*), \tau_k(\boldsymbol{s}^*)), \tag{F.1}$$

$$\mathbf{\Psi}(t) = \mathbf{C}_k^{\dagger}\ \mathbf{\Psi}(t+0) \quad \text{at} \quad t \ (\text{mod}\ T) = \tau_k(\boldsymbol{s}^*), \tag{F.2}$$

with the initial condition

$$\mathbf{\Psi}(0) = \mathbf{I}. \tag{F.3}$$

Note that the above adjoint system can be integrated only backward in time because $\mathbf{C}_k$ can be singular. The state transition matrix $\mathbf{H}_k(t,s)$ of the variational equation (see Eqs. (B.9) and (B.10) for the definition) can always be inverted when $t, s \in [\tau_{k-1}(\boldsymbol{s}^*) + nT, \tau_k(\boldsymbol{s}^*) + nT]$ for each $k = 1, ..., m_0$. In each time domain, we can obtain

$$(\dot{\mathbf{H}}_k^{-1})^{\dagger}(t,s) = -\mathbf{A}^{\dagger}(k,t)\ (\mathbf{H}_k^{-1})^{\dagger}(t,s) \quad \text{for} \quad t, s \in [\tau_{k-1}(\boldsymbol{s}^*) + nT, \tau_k(\boldsymbol{s}^*) + nT] \tag{F.4}$$

by differentiating the identity

$$\mathbf{H}_k^{-1}(t,s) \cdot \mathbf{H}_k(t,s) = \mathbf{I} \tag{F.5}$$

with t. Using the periodicity $\mathbf{H}_k(t,s) = \mathbf{H}_k(t+nT, s+nT)$, we can formally consider that Eq. (F.4) holds in the negative time domain. Thus, the matrix $(\mathbf{H}_k^{-1})^{\dagger}(t,s)$

satisfies the adjoint system (F.1) within each time interval with the initial condition $(\mathbf{H}_k^{-1})^\dagger(s,s) = \mathbf{I}$. Thus, $(\mathbf{H}_k^{-1})^\dagger(t,s)$ is a state transition matrix of the adjoint Eqs. (F.1) satisfying

$$\begin{aligned}
&\boldsymbol{\Psi}(t) = (\mathbf{H}_k^{-1})^\dagger(t,s)\boldsymbol{\Psi}(s) \\
&\quad \text{for } t,s \in (\tau_{k-1}(\boldsymbol{s}^*)-(n+1)T, \tau_k(\boldsymbol{s}^*)-(n+1)T], k \in \mathcal{M}_0 \\
&\quad \text{and for } \ t,s \in (\tau_{m_0}(\boldsymbol{s}^*) - (n+1)T, -nT]
\end{aligned} \tag{F.6}$$

We define a monodromy matrix of the adjoint system as $\mathbf{M}_{adj} = \boldsymbol{\Psi}(-T)$. It is easy to see that $\mathbf{M}_{adj}$ can be expressed as

$$\begin{aligned}
\mathbf{M}_{adj} &= \left(\prod_{k=1}^{m_0}{}^{+} (\mathbf{H}_{m_0+1-k}^{-1})^\dagger(\tau_{m_0-k}(\boldsymbol{s}^*), \tau_{m_0+1-k}(\boldsymbol{s}^*))\mathbf{C}_{m_0+1-k}^\dagger \right) (\mathbf{H}_1^{-1})^\dagger(\tau_{m_0}(\boldsymbol{s}^*), T) \\
&= \left(\prod_{k=1}^{m_0}{}^{+} \mathbf{H}_{m_0+1-k}^\dagger(\tau_{m_0+1-k}(\boldsymbol{s}^*), \tau_{m_0-k}(\boldsymbol{s}^*))\mathbf{C}_{m_0+1-k}^\dagger \right) \mathbf{H}_1^\dagger(T, \tau_{m_0}(\boldsymbol{s}^*)) = \mathbf{M}^\dagger.
\end{aligned} \tag{F.7}$$

In the second equality, we used the relation $\mathbf{H}_k(t,s) = \mathbf{H}_k^{-1}(s,t)$. Similarly, we consider adjoint linear systems corresponding to the systems with initial variations Eq. (B.1), whose solutions are $\boldsymbol{\Psi}(\cdot\,;\theta)$, which satisfies

$$\dot{\boldsymbol{\Psi}}(t;\theta) = -\mathbf{A}^\dagger(k, t+\theta)\ \boldsymbol{\Psi}(t;\theta) \ \text{ for } \ t+\theta \ (\text{mod } T) \in (\tau_{k-1}(\boldsymbol{s}^*), \tau_k(\boldsymbol{s}^*)), \tag{F.8}$$

$$\boldsymbol{\Psi}(t) = \mathbf{C}_k^\dagger\ \boldsymbol{\Psi}(t+0) \ \text{ at } \ t+\theta \ (\text{mod } T) = \tau_k(\boldsymbol{s}^*), \tag{F.9}$$

$$\boldsymbol{\Psi}(0;\theta) = \mathbf{I}. \tag{F.10}$$

It can be easily shown that $\mathbf{M}_{adj}(\theta) = \mathbf{M}^\dagger(\theta)$, where $\mathbf{M}_{adj}(\theta) \equiv \boldsymbol{\Psi}(-T;\theta)$.

Since we assume that the hybrid limit cycle χ is linearly stable, the monodromy matrix $\mathbf{M}(\theta)$ has a single eigenvalue 1 and all other eigenvalues are strictly inside the unit circle on the complex plane. We denote the eigenvalues as λ_i $(i = 1, 2, ..., N)$ and the corresponding right eigenvectors as $\boldsymbol{u}_i(\theta)$, where $\lambda_1 = 1$ and $|\lambda_i| < 1$ $(i = 2, ..., N)$. For simplicity, we hereafter consider the case where all eigenvalues are real and semisimple. A similar argument holds for the case of complex conjugates and eigenvalues with the generalized eigenspaces. It can be shown that $\boldsymbol{u}_i(\theta)$ corresponding to the eigenvalue λ_i with $|\lambda_i| < 1$ $(i = 2, ..., N)$ is tangent to the conditional isochron $W_{I_0(\theta)}(\theta)$ at $\boldsymbol{X}_0(\theta)$, and that the right eigenvector corresponding to $\lambda_1 = 1$ is tangent to the limit cycle χ at $\boldsymbol{s}_0(\theta)$.

Let $\boldsymbol{\eta}(t)$ be a variation vector from the unperturbed limit-cycle orbit $\boldsymbol{X}_0(t+\theta)$. If the initial value $\boldsymbol{\eta}(0) = \epsilon \boldsymbol{h}$, where $|\epsilon| \ll 1$, given to the initial state $\boldsymbol{X}_0(\theta)$ is parallel to the eigenvector $\boldsymbol{u}_i(\theta)$ corresponding to $|\lambda_i| < 1 (i = 2, \cdots, N)$, i.e., $\boldsymbol{\eta}(0) \propto \boldsymbol{u}_i(\theta)$, the linear response to the initial perturbation $\boldsymbol{\eta}(0)$ eventually vanishes, i.e.,

$$\begin{aligned} \lim_{n\to\infty} \boldsymbol{\eta}(nT) &= \lim_{n\to\infty} \epsilon \boldsymbol{\Xi}(nT;\theta)\boldsymbol{h} \\ &= \lim_{n\to\infty} \epsilon \mathbf{M}(\theta)^n \boldsymbol{h} = \lim_{n\to\infty} \epsilon \lambda_i^n \boldsymbol{h} = \mathbf{0}, \end{aligned} \tag{F.11}$$

as the system state revolves around χ. Hence, the state $\lim_{n\to\infty}[\boldsymbol{X}_0(nT+\theta) + \boldsymbol{\eta}(nT)]$ can be approximated by $\boldsymbol{X}_0(\theta) + O(\epsilon^2)$, and it shares the same phase with $\boldsymbol{X}_0(\theta) + \boldsymbol{\eta}(0)$. Using the total differentiability of the phase function $\boldsymbol{\Theta}$ with respect to the continuous state, the directional derivative of the phase in the direction $\boldsymbol{h}$ is obtained as

$$\begin{aligned} &\nabla \boldsymbol{\Theta}(I_0(\theta), \boldsymbol{X}_0(\theta)) \cdot \boldsymbol{h} \\ &= \lim_{\epsilon\to 0} \frac{\boldsymbol{\Theta}(I_0(\theta), \boldsymbol{X}_0(\theta) + \boldsymbol{\eta}(0)) - \boldsymbol{\Theta}(I_0(\theta), \boldsymbol{X}_0(\theta))}{\epsilon} \\ &= \lim_{\epsilon\to 0} \frac{\boldsymbol{\Theta}(I_0(\theta), \boldsymbol{X}_0(\theta) + O(\epsilon^2)) - \boldsymbol{\Theta}(I_0(\theta), \boldsymbol{X}_0(\theta))}{\epsilon} \\ &= \lim_{\epsilon\to 0} O(\epsilon) = 0. \end{aligned} \tag{F.12}$$

Therefore, $\boldsymbol{u}_i(\theta) (i = 2, \cdots, N)$ is tangent to $W_{I_0(\theta)}(\theta)$ at $\boldsymbol{X}_0(\theta)$. In contrast, if $\boldsymbol{\eta}(0)$ is parallel to $\boldsymbol{u}_1$, $\boldsymbol{\eta}(t)$ does not decay since $\mathbf{M}(\theta)^n \boldsymbol{\eta}(0) = \boldsymbol{\eta}(0)$. In Ref. [95, Th. 4.2.], it is shown that $\boldsymbol{F}(I_0(\theta), \boldsymbol{X}_0(\theta))$ is a right eigenvector of $\mathbf{M}(\theta)$ associated with the eigenvalue of unity. Hence $\boldsymbol{u}_1(\theta)$ is parallel to $\boldsymbol{F}(I_0(\theta), \boldsymbol{X}_0(\theta))$, which means that it is tangent to the limit cycle χ at $\boldsymbol{s}_0(\theta)$.

We denote the left eigenvector corresponding to eigenvalue $\lambda_1 = 1$ of $\mathbf{M}(\theta)$ as $\boldsymbol{Z}(\theta)$. Then, $\boldsymbol{Z}(\theta)$ is orthogonal to all right eigenvectors $\boldsymbol{u}_i(\theta)$ $(i = 2, ..., N)$ with eigenvalues $|\lambda_i| < 1$, namely, $\boldsymbol{Z}(\theta)$ is normal to the submanifold $W_{I_0(\theta)}(\theta)$ at $\boldsymbol{s}_0(\theta)$ and is parallel to the gradient vector $\nabla \boldsymbol{\Theta}|_{\boldsymbol{s}_0(\theta)}$. Thus, when $\boldsymbol{Z}(\theta)$ is normalized so that $\boldsymbol{Z}(\theta) = \nabla \boldsymbol{\Theta}|_{\boldsymbol{s}_0(\theta)}$ holds, it gives the linear response of the phase variable to an applied perturbation, hence we call it a phase sensitivity function.

In the following, we describe why one can obtain the phase sensitivity function from the adjoint equation. Since the system given by (F.1) and (F.2) is linear, the solution of the adjoint linear system

$$\dot{\boldsymbol{\psi}}(t) = -\mathbf{A}^\dagger(k,t)\boldsymbol{\psi}(t) \quad \text{for} \quad t \ (\mathrm{mod}\ T) \in (\tau_{k-1}(\boldsymbol{s}^*), \tau_k(\boldsymbol{s}^*)), \tag{F.13}$$

$$\boldsymbol{\psi}(t) = \mathbf{C}_k^\dagger \boldsymbol{\psi}(t+0) \quad \text{at} \quad t \ (\mathrm{mod}\ T) = \tau_k(\boldsymbol{s}^*), \tag{F.14}$$

where $\boldsymbol{\psi}(t) \in \mathbb{R}^N$, is given as $\boldsymbol{\psi}(t) = \boldsymbol{\Psi}(t)\boldsymbol{\psi}(0)$. If we write $\boldsymbol{\psi}(0)$ as $\boldsymbol{Z}_1 + \boldsymbol{Z}_2$, where $\boldsymbol{Z}_1$ is the projection of $\boldsymbol{\psi}(0)$ onto the space spanned by $\boldsymbol{Z}(0)$ and $\boldsymbol{Z}_2$ is the remainder, the backward-in-time asymptotic solution is

$$\lim_{n\to\infty} \boldsymbol{\psi}(-nT) = \lim_{n\to\infty} \mathbf{M}_{adj}(0)^n(\boldsymbol{Z}_1 + \boldsymbol{Z}_2) = \lim_{n\to\infty} \mathbf{M}^{\dagger}(0)^n(\boldsymbol{Z}_1 + \boldsymbol{Z}_2) = \boldsymbol{Z}_1, \tag{F.15}$$

because $\boldsymbol{Z}(0)$ is a right eigenvector of $\mathbf{M}^{\dagger}(0)$ corresponding to the eigenvalue $\lambda_1 = 1$. From Eq. (F.15), one can see that the backward-in-time asymptotic solution is periodic, hence we write it as $\boldsymbol{\psi}_0(\theta)$ with the initial value $\boldsymbol{\psi}_0(0) = \boldsymbol{Z}_1$. The vector $\boldsymbol{\psi}_0(\theta)$ is parallel to $\boldsymbol{Z}(\theta)$ because the equalities $\mathbf{M}_{adj}(\theta)\boldsymbol{\psi}_0(\theta) = \mathbf{M}^{\dagger}(\theta)\boldsymbol{\psi}_0(\theta) = \boldsymbol{\psi}_0(\theta)$ hold, where the last equality means that $\boldsymbol{\psi}_0(\theta)$ is a left eigenvector of $\mathbf{M}(\theta)$ with a corresponding eigenvalue of unity. We normalize $\boldsymbol{\psi}(0)$ as follows:

$$\boldsymbol{\psi}(0) \cdot \boldsymbol{F}(I_0(0), \boldsymbol{X}_0(0)) = 1. \tag{F.16}$$

Since $\boldsymbol{F}(I_0(0), \boldsymbol{X}_0(0))$ is a right eigenvector of $\mathbf{M}(0)$ corresponding to the eigenvalue $\lambda_1 = 1$, $\boldsymbol{Z}_2 \cdot \boldsymbol{F}(I_0(0), \boldsymbol{X}_0(0)) = 0$ holds, and we obtain $\boldsymbol{\psi}_0(0) \cdot \boldsymbol{F}(I_0(0), \boldsymbol{X}_0(0)) = \boldsymbol{Z}_1 \cdot \boldsymbol{F}(I_0(0), \boldsymbol{X}_0(0)) = 1$. Therefore, under the condition (F.16), $\boldsymbol{\psi}_0(0)$ is equal to the phase sensitivity function $\boldsymbol{Z}(0)$ at $\theta = 0$ because it satisfies the relation (2.8).

It can be shown that the normalization condition is satisfied for all θ, i.e, $\boldsymbol{\psi}_0(\theta) \cdot \boldsymbol{F}(I_0(\theta), \boldsymbol{X}_0(\theta)) = 1$, if $\boldsymbol{\psi}(0)$ satisfies the above normalization condition at $t = 0$, as follows. Hereafter, we formally define $\boldsymbol{F}(I_0(t - nT), \boldsymbol{X}_0(t - nT)) = \boldsymbol{F}(I_0(t), \boldsymbol{X}_0(t))$, because $(I_0(t), \boldsymbol{X}_0(t))$ is a periodic solution. By differentiating $d\boldsymbol{X}_0(t)/dt = \boldsymbol{F}(I_0(t), \boldsymbol{X}_0(t))$ by t within the smooth interval, we obtain

$$\begin{aligned}
&\frac{d}{dt}\left(\frac{d\boldsymbol{X}_0(t)}{dt}\right) \\
&= \frac{d}{dt}\boldsymbol{F}(I_0(t), \boldsymbol{X}_0(t)) = \boldsymbol{A}(I_0(t), t)\left(\frac{d\boldsymbol{X}_0(t)}{dt}\right) \\
&= \boldsymbol{A}(I_0(t), t)\boldsymbol{F}(I_0(t), \boldsymbol{X}_0(t)).
\end{aligned} \tag{F.17}$$

Thus, $\boldsymbol{\xi}(t) = \boldsymbol{F}(I_0(t), \boldsymbol{X}_0(t))$ is a solution to the vector-valued version of the linearized system (B.3,B.4),

$$\frac{d}{dt}\boldsymbol{F}(I_0(t), \boldsymbol{X}_0(t)) = \boldsymbol{A}(I_0(t), t)\boldsymbol{F}(I_0(t), \boldsymbol{X}_0(t)), \tag{F.18}$$

from which we can derive

$$\begin{aligned}
&\frac{d}{dt}(\boldsymbol{\psi}(t)\cdot\boldsymbol{F}(I_0(t),\boldsymbol{X}_0(t)))\\
&=\frac{d}{dt}\boldsymbol{\psi}(t)\cdot\boldsymbol{F}(I_0(t),\boldsymbol{X}_0(t))+\boldsymbol{\psi}(t)\cdot\frac{d}{dt}\boldsymbol{F}(I_0(t),\boldsymbol{X}_0(t))\\
&=-\mathbf{A}(I_0(t),t)^{\dagger}\boldsymbol{\psi}(t)\cdot\boldsymbol{F}(I_0(t),\boldsymbol{X}_0(t)))+\boldsymbol{\psi}(t)\cdot\mathbf{A}(I_0(t),t)\boldsymbol{F}(I_0(t),\boldsymbol{X}_0(t)))\\
&=0. \qquad \text{(F.19)}
\end{aligned}$$

At the moment of switching ($t \pmod T = \tau_k(\boldsymbol{s}^*)$), the variation $\boldsymbol{\xi}(t) = \boldsymbol{F}(I_0(t), \boldsymbol{X}_0(t))$ changes as

$$\boldsymbol{F}(k+1,\boldsymbol{X}_0(t)) = \mathbf{C}_k\boldsymbol{F}(k,\boldsymbol{X}_0(t)). \qquad \text{(F.20)}$$

Thus,

$$\begin{aligned}
&\boldsymbol{\psi}(t+0)\cdot\boldsymbol{F}(k+1,\boldsymbol{X}_0(t))\\
&=\boldsymbol{\psi}(t+0)\cdot\mathbf{C}_k\boldsymbol{F}(k,\boldsymbol{X}_0(t))=\mathbf{C}_k^{\dagger}\boldsymbol{\psi}(t+0)\cdot\boldsymbol{F}(k,\boldsymbol{X}_0(t))\\
&=\boldsymbol{\psi}(t)\cdot\boldsymbol{F}(k,\boldsymbol{X}_0(t)). \qquad \text{(F.21)}
\end{aligned}$$

Therefore, the quantity $\boldsymbol{\psi}(t)\cdot\boldsymbol{F}(I_0(t),\boldsymbol{X}_0(t))$ is invariant under the backward time evolution of the system given by (F.13) and (F.14).

Summarizing, we can obtain $\boldsymbol{Z}(\theta)$ by integrating the adjoint system (F.13,F.14) backward in time from a initial condition that satisfies the normalization condition (F.16) until a periodic solution is obtained. In conventional smooth systems, this procedure is called the *adjoint method* [8].

Appendix G

Averaging approximation and analysis of the synchronization dynamics of hybrid limit cycles

By differentiating both sides of Eq. (2.16) with respect to time and substituting the phase equation Eq. (E.2), we obtain a non-autonomous system

$$\dot{\psi} = \epsilon[\Delta + \boldsymbol{Z}((T/T_{ext})t + \psi) \cdot \boldsymbol{p}(t)]. \tag{G.1}$$

The averaging approximation for weakly perturbed oscillators [2, 8, 57] provides the following autonomous system:

$$\dot{\psi} = \epsilon[\Delta + \Gamma(\psi)] \equiv J(\psi), \tag{G.2}$$

where

$$\Gamma(\psi) = \frac{1}{T_{ext}} \int_0^{T_{ext}} \boldsymbol{Z}((T/T_{ext})t + \psi) \cdot \boldsymbol{p}(t)dt. \tag{G.3}$$

We here summarize some useful theorems for the analysis of the synchronization dynamics. Bogolyubov's second theorem [85, 103, 162, 163] affirms that the existence of a hyperbolic fixed point ψ^*, i.e., $J(\psi^*) = 0$ and $J'(\psi^*) \neq 0$, of the averaged system Eq. (G.2) assures its corresponding unique hyperbolic periodic solution of the original system Eq. (G.1) evolving in the neighborhood of ψ^* whose radius tends to zero together with ϵ. The Eckhaus/Sanchez-Palencia theorem [139] says that if ψ^* is a stable hyperbolic fixed point of the averaged system, the solution of the non-averaged system starting from the basin of attraction is estimated up to $O(\epsilon)$ by the averaged

one with the same initial condition, which is uniformly valid over a semi-infinite time interval. Samoilenko and Stanzhitskii [164] have given similar results under a less restrictive condition, where the hyperbolicity assumption in the Eckhaus/Sanchez-Palencia theorem is replaced by the asymptotic stability. These theorems mean that in each basin of attraction, the precise behavior of the original system can be captured by the averaged system. Moreover, if the averaged system undergoes a saddle-node bifurcation at $\Delta = \Delta_c$ and $|\epsilon|$ is sufficiently small, the original system (in fact, its Poincaré map) also undergoes a saddle-node bifurcation at $\tilde{\Delta}_c$ near Δ_c [103]. Finally, from Bogolyubov's first theorem [85, 103, 162, 163], even when the averaged system has no asymptotically stable fixed points, the solution of the non-averaged system is estimated up to $O(\epsilon)$ on a time scale of order $O(1/\epsilon)$.

Using the above theorems, synchronization dynamics of the oscillator can be easily understood from the T-periodic function $\Gamma(\psi)$ as follows: if the condition $\Delta \in [-\max\Gamma(\psi), -\min\Gamma(\psi)]$ is satisfied, Eq. (G.2) has at least one fixed point ψ^* that satisfies $\Delta + \Gamma(\psi^*) = 0$. When it is asymptotically stable, the oscillator is locked to the external forcing and the stable phase difference between the oscillator and the forcing is approximated by ψ^*. If there are two or more stable fixed points, the oscillator can synchronize with the periodic forcing at multiple phase differences depending on the initial condition. Each basin of attraction and convergence rate toward the stable phase differences can be estimated from $\Gamma(\psi)$. Appearances and disappearances of stable phase differences, depending on the parameter of the frequency mismatch Δ, can also be predicted from $\Gamma(\psi)$. When there are no stable phase differences, the phase slipping behavior occurs. The mean period of the phase slipping can also be estimated from $\Gamma(\psi)$.

When one considers Eq. (G.1) as a regularized multivalued system as explained in Appendix E, the integral in Eq. (G.3) should be interpreted in a suitable sense such as Aumann's [165], and the differential equation Eq. (G.2) should be replaced by a differential inclusion. See [100–102] for the theories including analogues of the theorems mentioned above on the averaging approximation in systems with jumps and multivalued righthand sides. Note that the jumps in the solution in [**?** 101, 102] are assumed to occur when the solution collides with a switching surface described by $t = \tau(\psi)$ in the extended phase space, which is suitable to the case where one considers the injection locking to a periodic impulsive signal.

Finally, when the mutual entrainment of pulse-coupled oscillators is analyzed [105, 106], which we do not consider in this study, averaging approaches of the above kind should be generalized to the autonomous case. The averaging theory for au-

tonomous systems with jumps has so far been limited to a specific cases [166, 167], and establishment of a general theory is desirable.

Appendix H

Direct method for measuring the phase sensitivity function

In the direct method, the βth element $Z^\beta(\theta)$ of $\boldsymbol{Z}(\theta)$ is computed as follows: first, we kick the system state $(I_0(\theta), \boldsymbol{X}_0(\theta))$ on the limit cycle χ by applying a weak impulsive perturbation $(0, \epsilon \boldsymbol{e}^\beta)$. We then evolve the orbit $(I(t), \boldsymbol{X}(t))$ from the perturbed initial condition $(I_0(\theta), \boldsymbol{X}_0(\theta) + \epsilon \boldsymbol{e}^\beta)$. After a long time, the perturbed orbit $(I(t), \boldsymbol{X}(t))$ returns sufficiently close to the limit cycle χ and the phase $\theta(I(t), \boldsymbol{X}(t))$ can be measured. Because the phase difference between two unperturbed systems is time-invariant, $\theta(I(t), \boldsymbol{X}(t)) - t_r$, where $t_r = t \bmod T$, is equal to the initial phase difference $\theta(I_0(\theta), \boldsymbol{X}_0(\theta) + \epsilon \boldsymbol{e}^\beta) - \theta$. Thus, for sufficiently small ϵ, we can calculate $Z^\beta(\theta)$ according to:

$$Z^\beta(\theta) = \boldsymbol{Z}(\theta) \cdot \boldsymbol{e}^\beta \approx \frac{[\theta(I_0(\theta), \boldsymbol{X}_0(\theta) + \epsilon \boldsymbol{e}^\beta) - \theta]}{\epsilon} = \frac{[\theta(I(t), \boldsymbol{X}(t)) - t_r]}{\epsilon}. \tag{H.1}$$

In the direct method, the perturbation needs to be sufficiently small, as strong perturbations induce nonlinearity in the phase response. However, too weak perturbations result in tiny phase responses, which are difficult to measure accurately. Thus, the direct method is vulnerable to incorrect estimation of the phase response. Moreover, the direct method requires much longer computation times than those for the adjoint method. To calculate $\boldsymbol{Z}(\theta)$ at m points on the limit cycle in hybrid dynamical systems with N-dimensional continuous states, it is necessary to repeat the above long-time evolution $m \times N$ times if we use the direct method. In contrast, we need only a single long-time evolution in the adjoint method. Therefore, the adjoint method has a significant advantage in computing $\boldsymbol{Z}(\theta)$.

Appendix I

Derivation of the negative logarithmic scaling law

From Eq. (G.2), the period of phase slipping is estimated as

$$T_{\text{slip}} = \left| \int_0^T \frac{d\psi}{\epsilon[\Delta + \Gamma(\psi)]} \right|. \tag{I.1}$$

We suppose $\Gamma(\psi)$ has a maximum $-\Delta_c$ (the argument of the same kind holds for the minimum) at $\psi = \psi^*$, and suppose the semiderivatives $\Gamma'(\psi^* - 0) = \beta_1, \Gamma'(\psi^* + 0) = \beta_2$ are nonzero. When Δ is sufficiently close to the critical value Δ_c, T_{slip} is evaluated as

$$\begin{aligned} T_{\text{slip}} &\simeq -\frac{1}{\epsilon} \left(\int_0^{\psi^*} \frac{d\psi}{\Delta - \Delta_c + \beta_1(\psi - \psi^*)} + \int_{\psi^*}^T \frac{d\psi}{\Delta - \Delta_c + \beta_2(\psi - \psi^*)} \right) \\ &\simeq -\frac{1}{\epsilon} \left(\int_{-\infty}^{\psi^*} \frac{d\psi}{\Delta - \Delta_c + \beta_1(\psi - \psi^*)} + \int_{\psi^*}^{\infty} \frac{d\psi}{\Delta - \Delta_c + \beta_2(\psi - \psi^*)} \right) \\ &= -\frac{1}{\epsilon} \left(\frac{1}{\beta_1} - \frac{1}{\beta_2} \right) \ln |\Delta - \Delta_c|. \end{aligned} \tag{I.2}$$

Hence, T_{slip} increases as $-\ln |\Delta - \Delta_c|$ when $\Delta \to \Delta_c$.

Appendix J

The Fourier averages and the generalized Laplace averages

In this section, we introduce methods to obtain the phase and amplitudes by direct numerical simulation of the dynamics.

The phase variable $\theta(\boldsymbol{X})$ is evaluated as $\theta(\boldsymbol{X}) = \arg(f^*_{\lambda_1}(\boldsymbol{X}))$, where the Fourier average [91] $f^*_{\lambda_1}(\boldsymbol{X})$ of an observable f is given by

$$f^*_{\lambda_1}(\boldsymbol{X}) = \lim_{s\to\infty} \frac{1}{s} \int_0^s f \circ \phi(t, \boldsymbol{X}) e^{-\lambda_1 t} \mathrm{d}t. \tag{J.1}$$

The amplitude variable $r_i(\boldsymbol{X})$ is obtained by $r_i(\boldsymbol{X}) = \mathrm{Re}(f^*_{\lambda_i}(\boldsymbol{X}))$, where the generalized Laplace average [134] $f^*_{\lambda_i}(\boldsymbol{X})$ of f is given by

$$f^*_{\lambda_i}(\boldsymbol{X}) = \lim_{s\to\infty} \frac{1}{s} \int_0^s \left[f \circ \phi(t, \boldsymbol{X}) - \bar{f} - \sum_{k=1}^{i-1} f^*_{\lambda_k}(\boldsymbol{X}) e^{\lambda_k t} \right] e^{-\lambda_i t} \mathrm{d}t, \tag{J.2}$$

where $\bar{f}$ is an averaged observable along the periodic orbit
χ: $\bar{f} = (1/T) \int_0^T f \circ \phi(t, \boldsymbol{X}_0(t_*)) \mathrm{d}t$.

We can simplify the generalized Laplace averages using convenient observables g_i $(i = 2, \cdots, N)$ defined as

$$g_i(\boldsymbol{X}) = \nabla r_i(\boldsymbol{X}_0(\theta_*)) \cdot (\boldsymbol{X} - \boldsymbol{X}_0(\theta_*)), \tag{J.3}$$

where $\theta_* = \theta(\boldsymbol{X})$. Here, the adjoint covariant Lyapunov vectors $\nabla r_i(\boldsymbol{X}_0(\theta_*))$ are normalized so that they are dual to the unitized covariant Lyapunov vectors $\boldsymbol{\gamma}_i(\boldsymbol{X}_0(\theta_*))$. Each of these observables evolves with its corresponding characteristic exponent asymptotically, because, in the close-enough neighborhood of the periodic orbit χ, g_i co-

incides with the ith amplitude variable r_i. Hence, we can show that $\bar{g}_i = 0$ and $(g_i)^*_{\lambda_k}(\boldsymbol{X}) = 0$ $(k = 1, \cdots, i-1)$ for any $\boldsymbol{X}$ in the basin of attraction $\mathcal{B}$. Thus, we can replace the generalized Laplace average with the Laplace average:

$$(g_i)^*_{\lambda_i}(\boldsymbol{X}) = \lim_{s\to\infty} \frac{1}{s} \int_0^s g_i \circ \phi(t, \boldsymbol{X}) e^{-\lambda_i t} \mathrm{d}t. \tag{J.4}$$